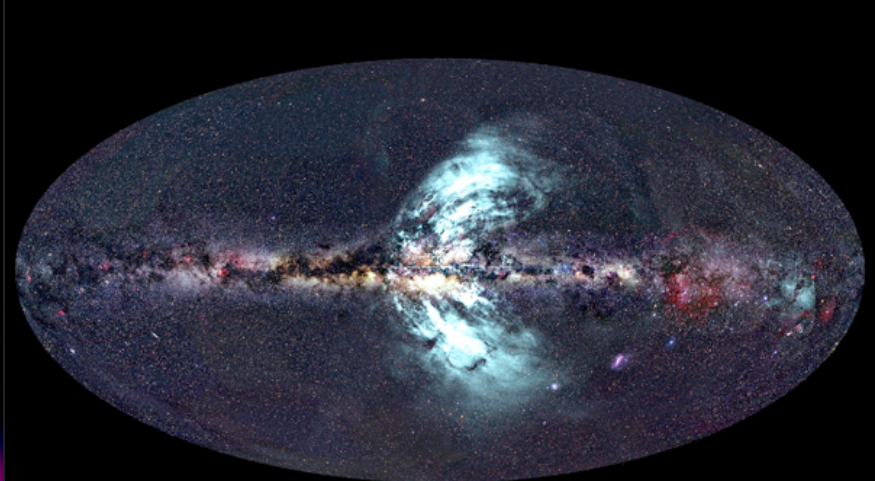
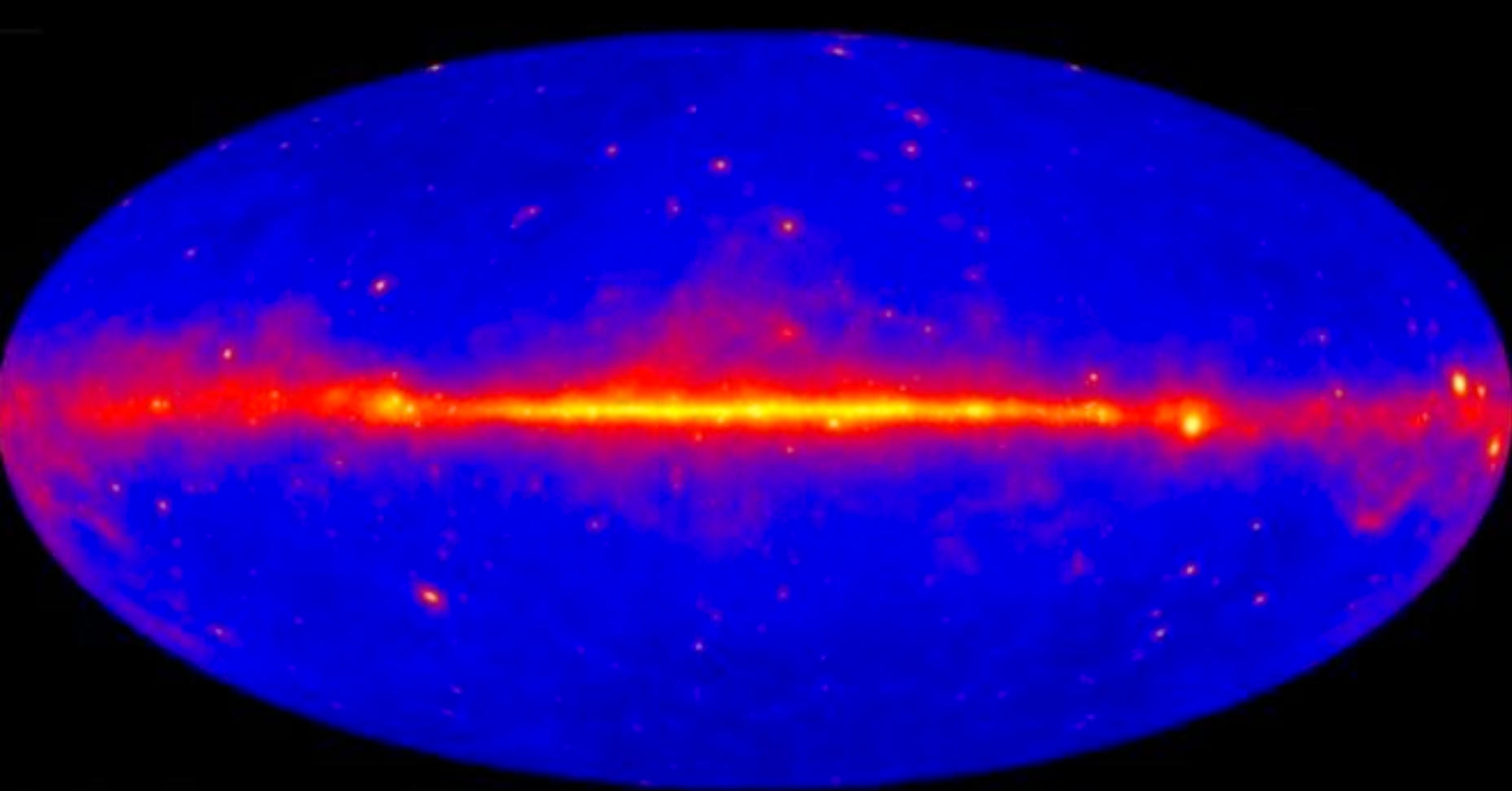


DARK MATTER IN THE MILKY WAY

THE INDIRECT DETECTION OF DARK MATTER

Francesca Calore and Tim Linden



DARK MATTER IN THE MILKY WAY

THE INDIRECT DETECTION OF **WIMP** DARK MATTER

Francesca Calore and Tim Linden

- **DARK MATTER PARTICLE PHYSICS**
- **DARK MATTER INDIRECT DETECTION**
- **SEARCHES WITH GAMMA RAYS**
- **SEARCHES WITH CHARGED COSMIC RAYS AND OTHER WAVELENGTHS**

DARK MATTER INDIRECT DETECTION

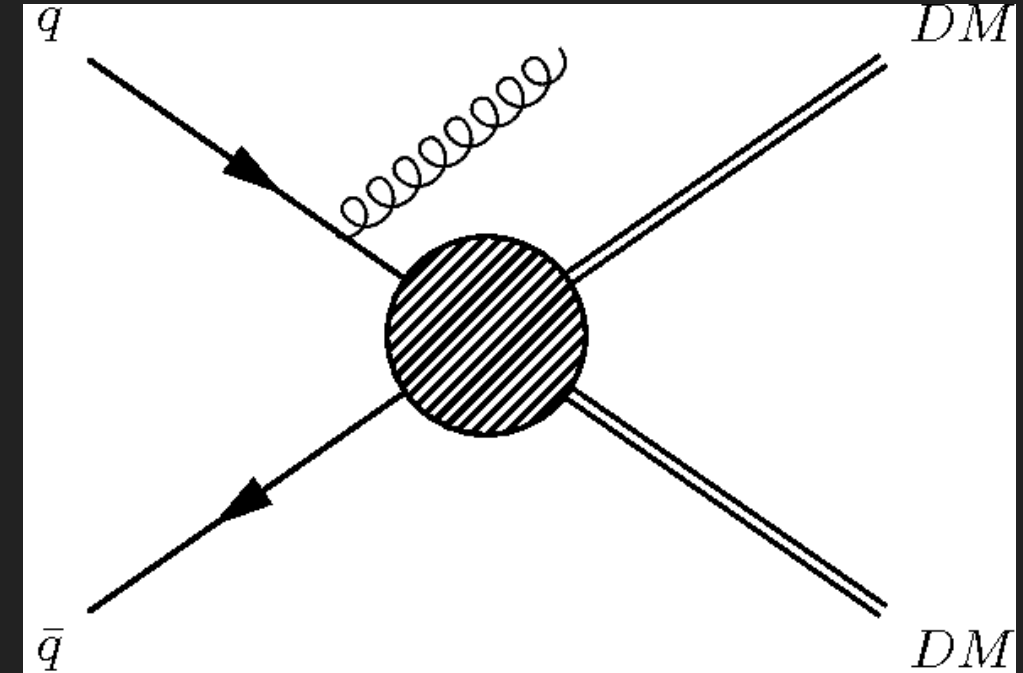
We want to investigate an interaction where dark matter annihilates to produce final states containing standard model particles.

Will make one assumption at this point:

1.) Dark Matter is stable because it is protected by a conserved symmetry (e.g. r -parity). This only needs to be approximately true.

In this case, we can generically write down an interaction rate:

$$\Gamma_{\text{SM, ann}} = \left(\int \frac{\rho_{\text{DM}}^2}{m_{\chi}^2} dV \right) \times (\sigma v) \times (N_{\text{SM, ann}})$$



DARK MATTER INDIRECT DETECTION

Will make three more assumptions:

1.) *This interaction is CP-symmetric, i.e. at high temperatures:*

$$\Gamma_{\chi\chi \rightarrow q\bar{q}} = \Gamma_{q\bar{q} \rightarrow \chi\chi}$$

2.) *The interaction rate is sufficiently large such that the number of dark matter and standard model particles equilibrates in the early universe (alternative is freeze-in dark matter).*

$$\begin{aligned} \Gamma &\gtrsim H && \Rightarrow \text{thermal equilibrium} \\ \Gamma &\lesssim H && \Rightarrow \text{decoupled evolution} \end{aligned}$$

DARK MATTER INDIRECT DETECTION

Will make three more assumptions:

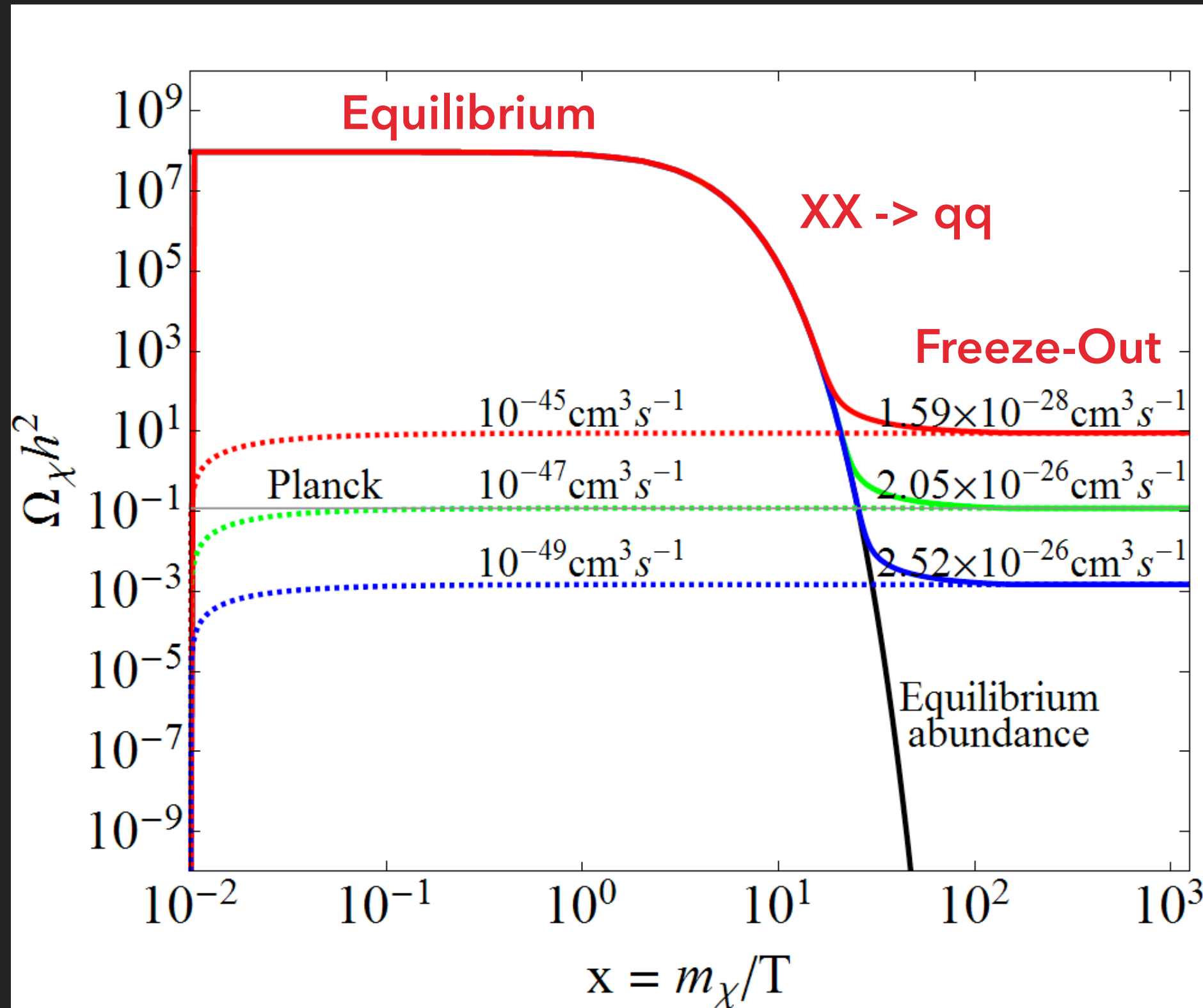
3.) Freeze out occurs when the dark matter particle is non-relativistic (alternative is hot dark matter).

$$m \geq T$$

In that case, statistical mechanics tells us that the number density of dark matter is given by

$$n_{\text{non-rel}} \sim (mT)^{3/2} \exp\left(-\frac{m}{T}\right) \quad \text{for } m \gg T.$$

DARK MATTER INDIRECT DETECTION



DARK MATTER INDIRECT DETECTION

We can set the interaction strength $\Gamma = n\sigma$, the number density of dark matter times its interaction cross-section. And we want to find the time of freeze-out by setting this to equal the Hubble Constant.

$$H^2 = \frac{8\pi G_N}{3} \rho$$

Assuming a radiation dominated universe, we get:

$$\rho \simeq \rho_{\text{rad}} = \frac{\pi^2}{30} \cdot g \cdot T^4$$

Setting $n\sigma = H$ and noting that $H \cong T^2 / m^{\text{P}}$ we get that:

$$n_{\text{f.o.}} \sim \frac{T_{\text{f.o.}}^2}{M_P \cdot \sigma}$$

DARK MATTER INDIRECT DETECTION

Intriguingly, we note that if we put in values for the weak nuclear force (i.e. $\sigma = G_F^2 m_\chi^2$) we get:

note $n_0 \sim 1/m_\chi$ at constant density of the universe!

$$\Omega_\chi = \frac{m_\chi \cdot n_\chi(T = T_0)}{\rho_c} = \frac{m_\chi T_0^3 n_0}{\rho_c T_0^3}$$

Noting that in an iso-entropic universe n_0 / T_0^3 is constant:

$$\Omega_\chi = \frac{m_\chi T_0^3 n_{f.o.}}{\rho_c T_{f.o.}^3} = \frac{T_0^3}{\rho_c} x_{f.o.} \left(\frac{n_{f.o.}}{T_{f.o.}^2} \right) = \left(\frac{T_0^3}{\rho_c M_P} \right) \frac{x_{f.o.}}{\sigma}$$

And simplifying (by substituting in known constants) we obtain:

$$\left(\frac{\Omega_\chi}{0.2} \right) \simeq \frac{x_{f.o.}}{20} \left(\frac{10^{-8} \text{ GeV}^{-2}}{\sigma} \right)$$

This derivation closely follows 1301.0952

DARK MATTER INDIRECT DETECTION

And simplifying (by substituting in known constants) we obtain:

$$\left(\frac{\Omega_\chi}{0.2}\right) \simeq \frac{x_{\text{f.o.}}}{20} \left(\frac{10^{-8} \text{ GeV}^{-2}}{\sigma}\right)$$

Which can be written in more familiar units as:

$$\langle\sigma v\rangle \sim 10^{-8} \text{ GeV}^{-2} (3 \times 10^{-28} \text{ GeV}^2 \text{ cm}^2) 10^{10} \frac{\text{cm}}{\text{s}} = 3 \times 10^{-26} \frac{\text{cm}^3}{\text{s}}$$

DARK MATTER INDIRECT DETECTION

So besides very quickly going over some math, what do we learn?

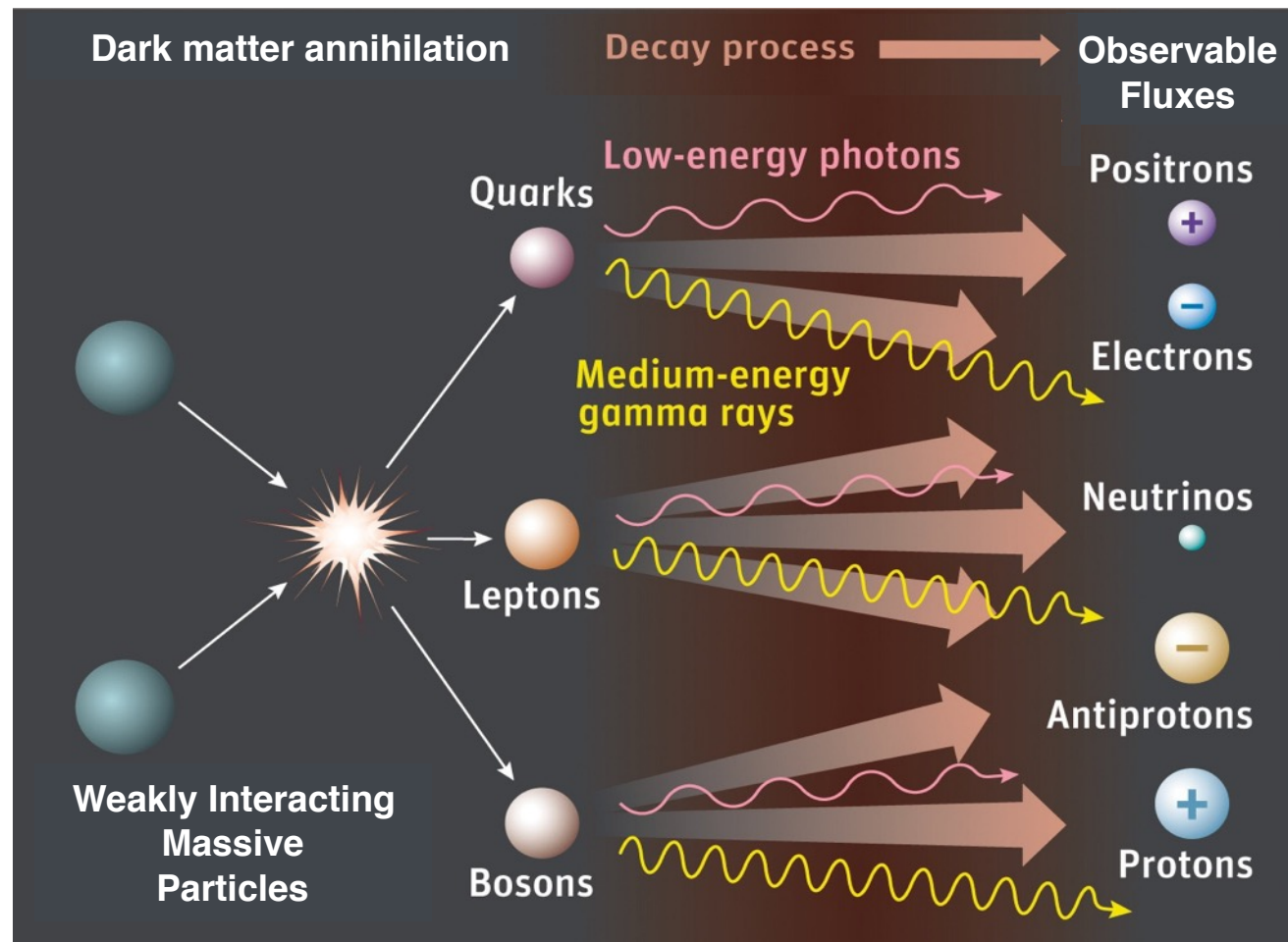
1.) Dark Matter annihilations at the present day are directly linked to annihilations in the early universe.

2.) The Weak nuclear force provides the correct interaction strength to produce the observed dark matter density.

2.) Under a very reasonable (though not certain) set of assumptions, the annihilation cross-section is fixed by the observed relic density.

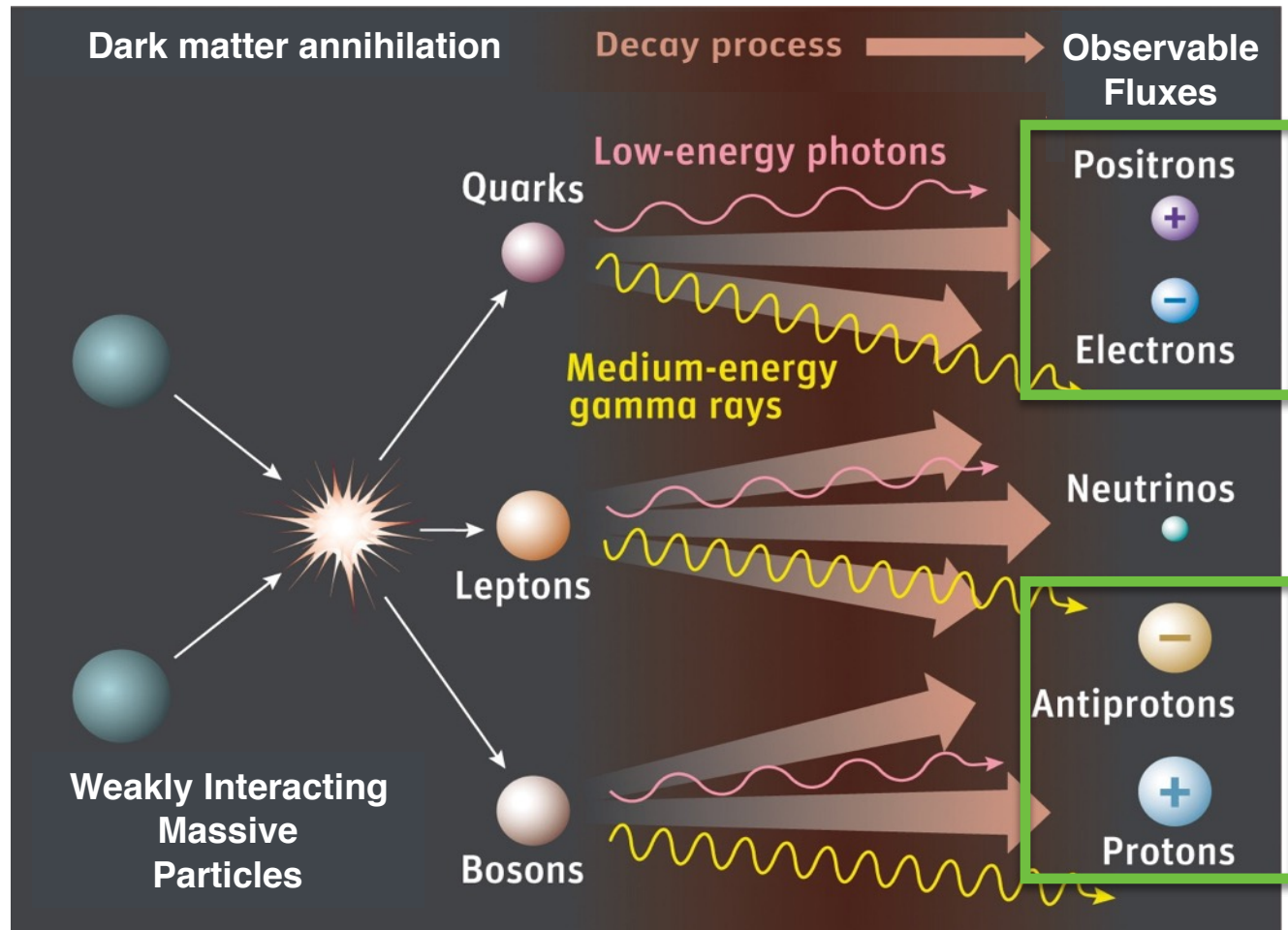
This is unique among WIMP detection strategies (direct/collider detection)

Indirect dark matter detection



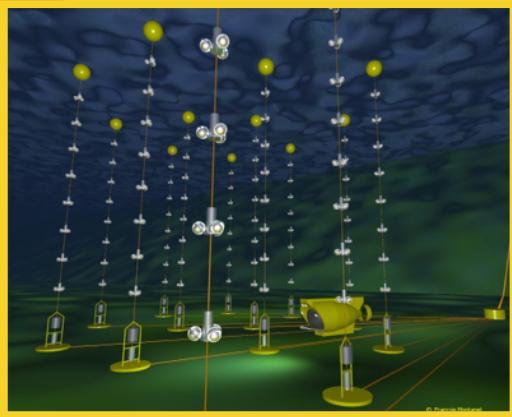
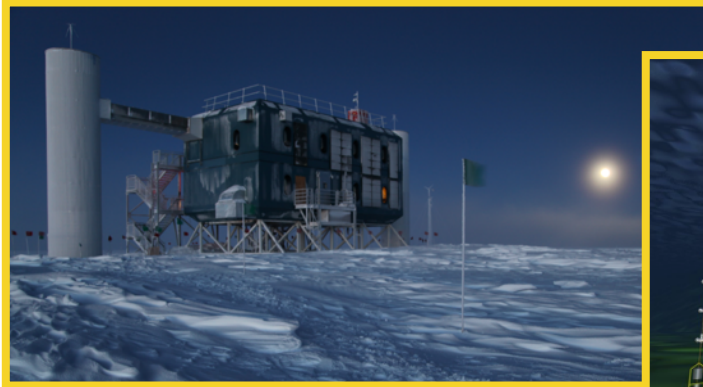
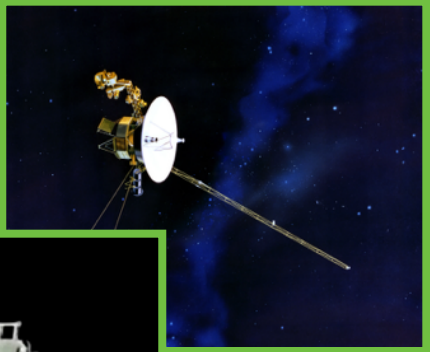
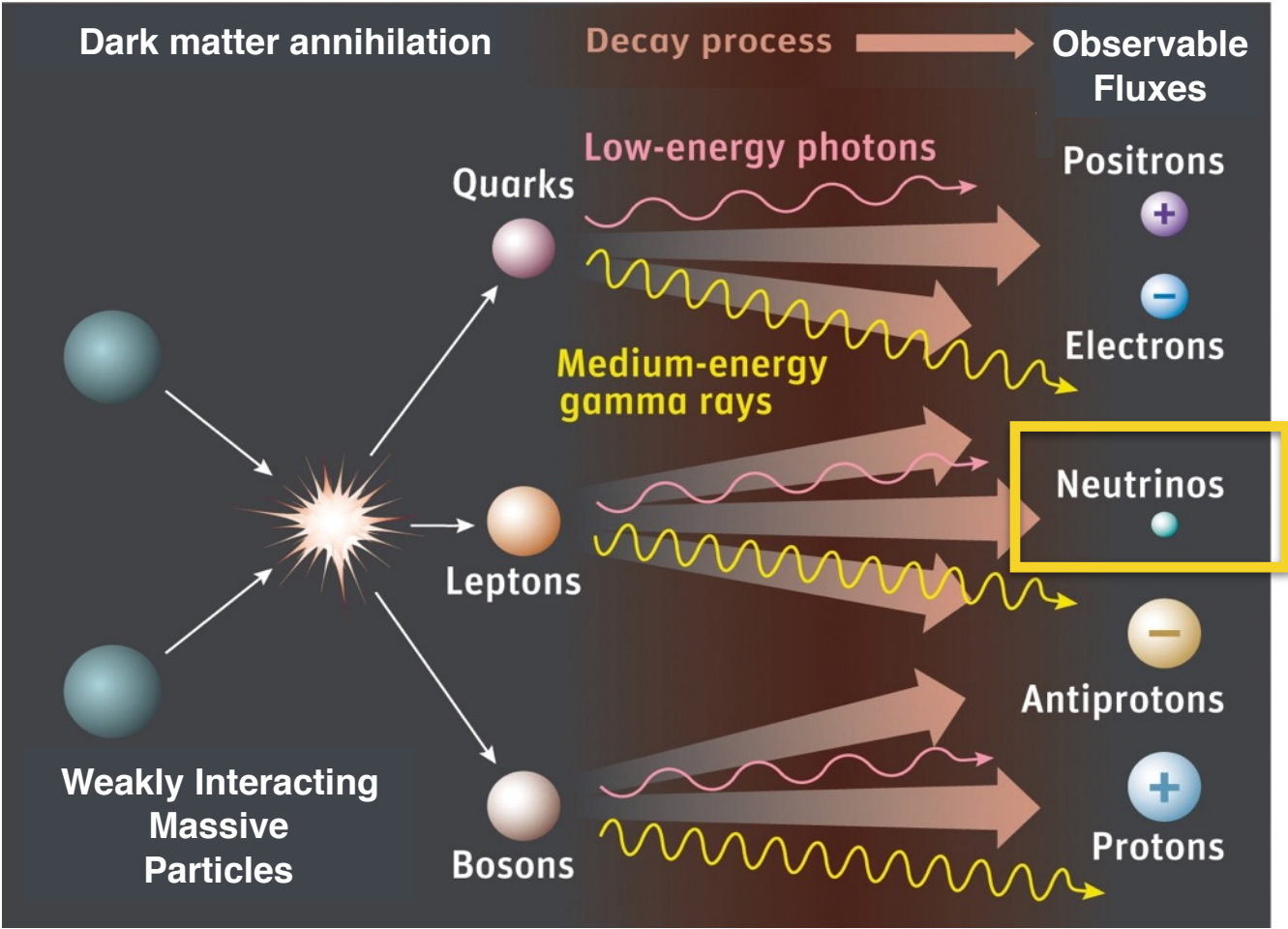
Indirect searches
for stable dark matter annihilation
(or decay) products.

Indirect dark matter detection



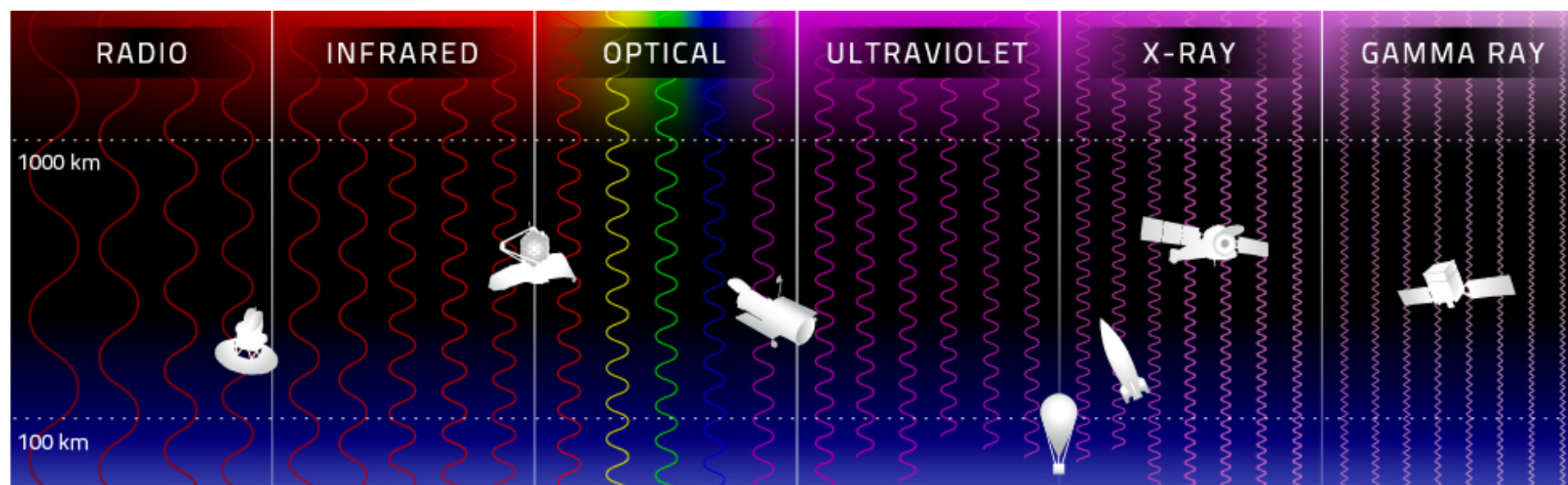
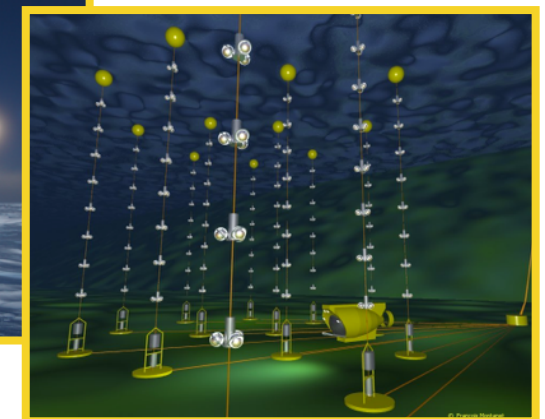
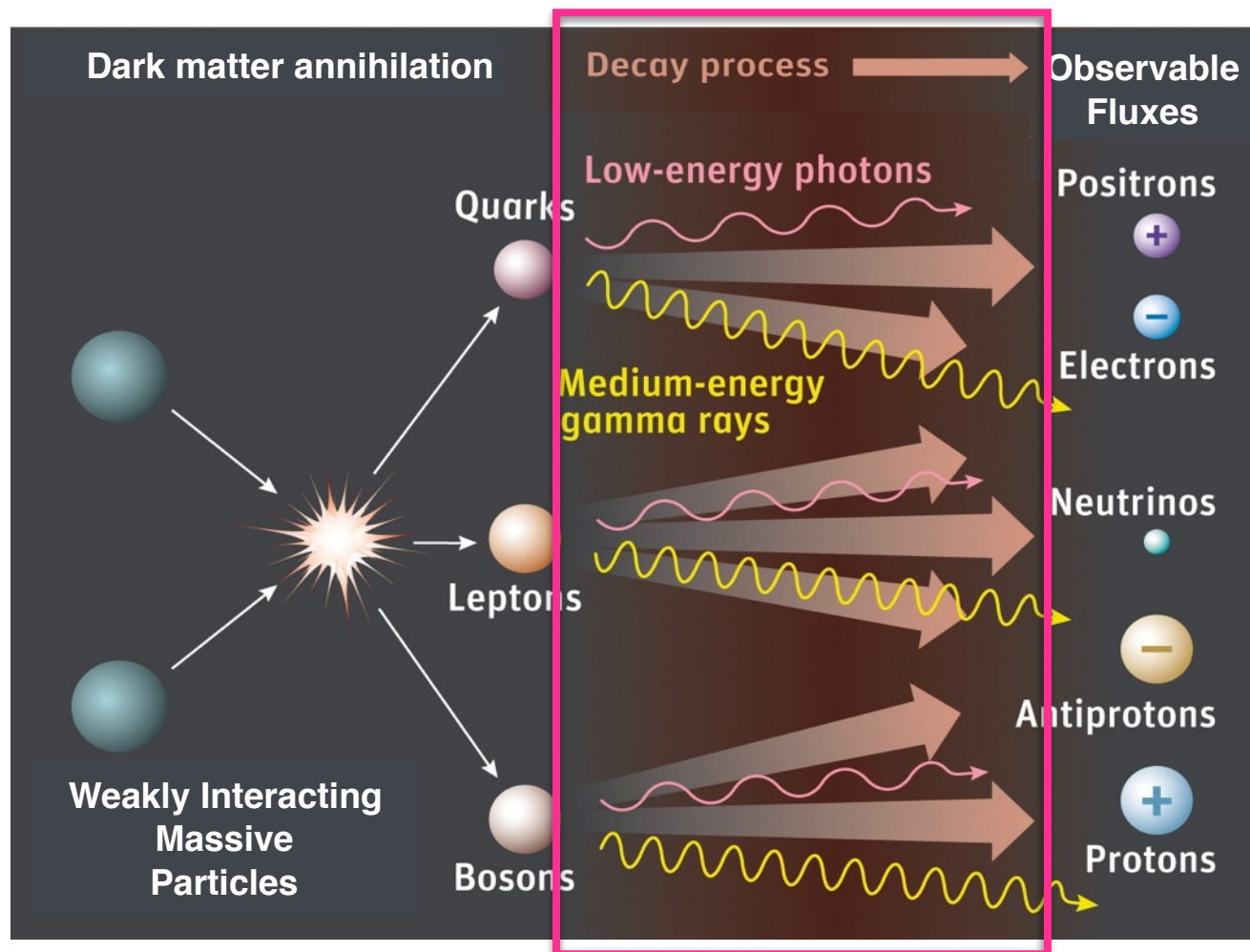
Indirect searches
for stable dark matter annihilation
(or decay) products.

Indirect dark matter detection

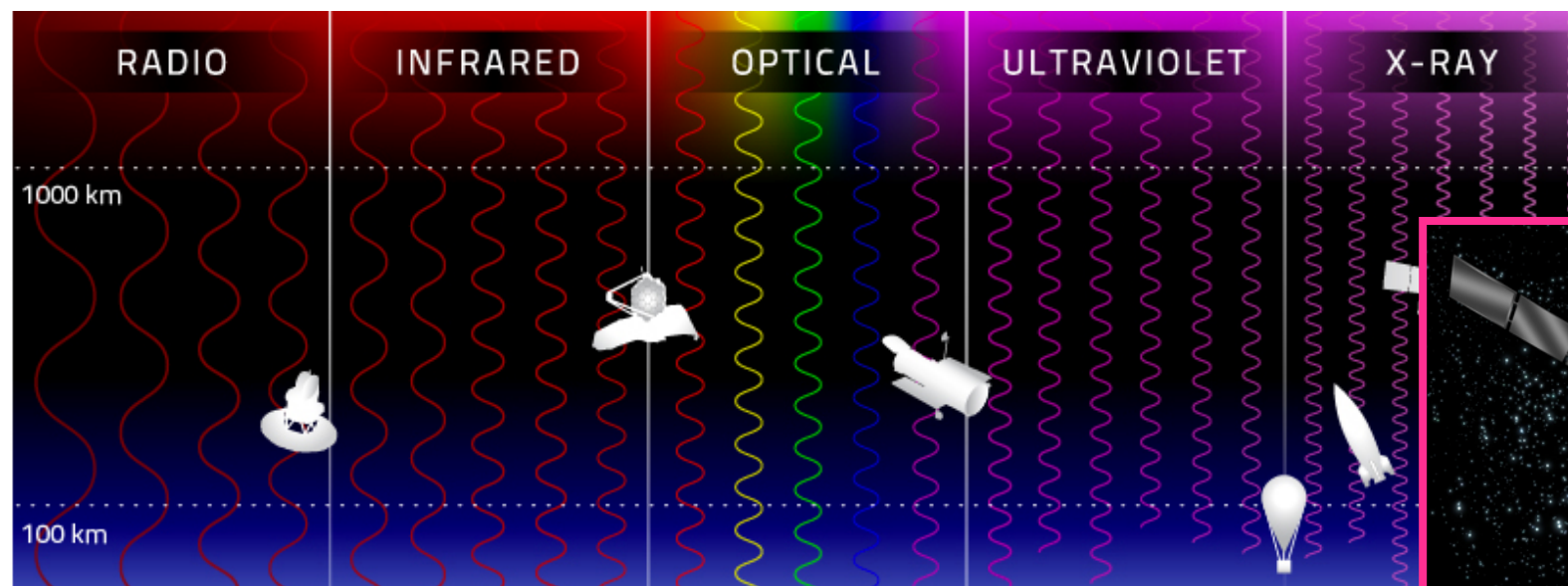
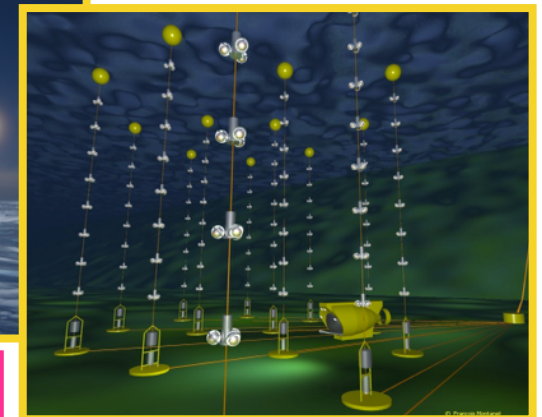
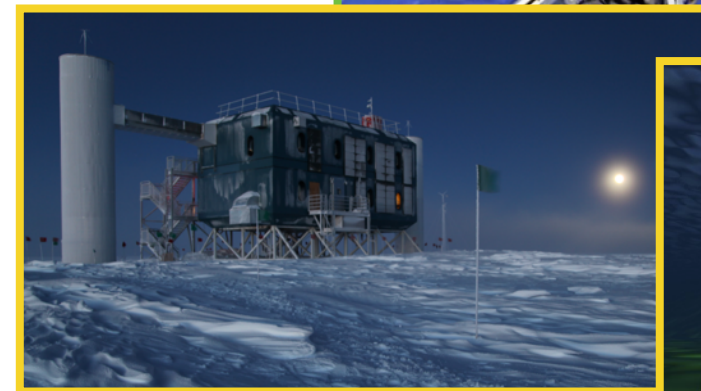
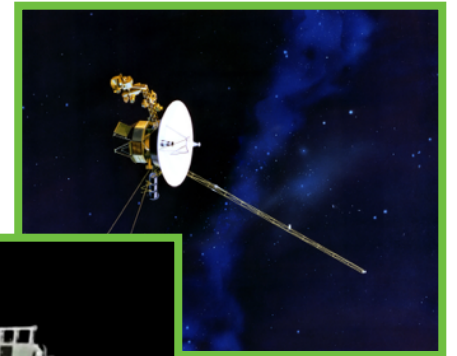
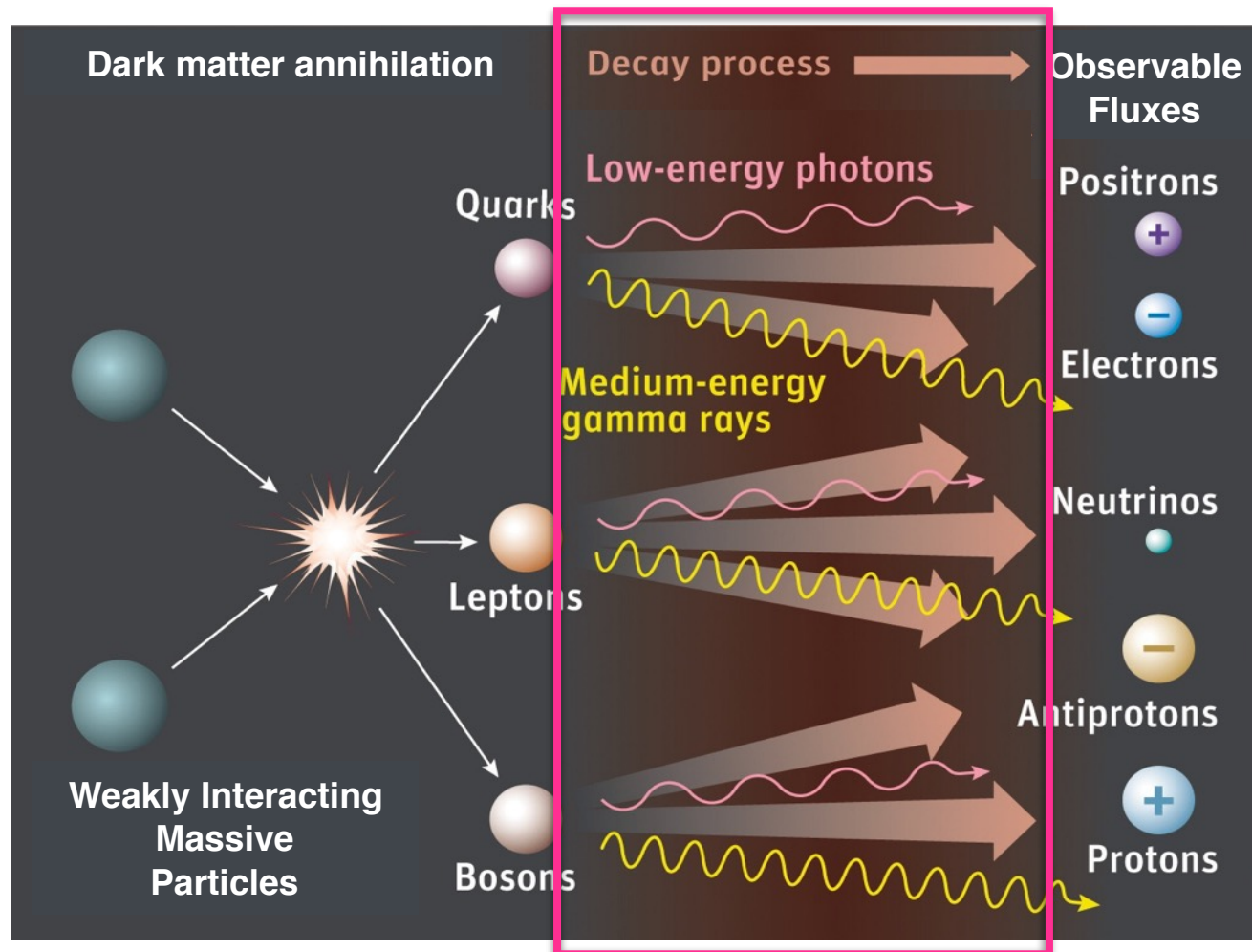


Indirect searches
for stable dark matter annihilation
(or decay) products.

Indirect dark matter detection



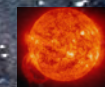
Indirect dark matter detection



Indirect dark matter detection messengers in the Galaxy



$$\frac{d^3 N_X}{dV dt dE} = \frac{\langle \sigma v \rangle \rho_{\text{DM}}^2}{2m_{\text{DM}}^2} \frac{dN_X}{dE}$$



Sun

Indirect dark matter detection messengers in the Galaxy



$$\frac{d^3 N_X}{dV dt dE} = \frac{\langle \sigma v \rangle \rho_{\text{DM}}^2}{2m_{\text{DM}}^2} \frac{dN_X}{dE}$$



Charged cosmic rays

- ✓ Diffusive propagation in Galactic magnetic field
- ✓ Lost directionality
- ➔ Spectral signatures

Indirect dark matter detection messengers in the Galaxy



$$\frac{d^3 N_X}{dV dt dE} = \frac{\langle \sigma v \rangle \rho_{\text{DM}}^2}{2m_{\text{DM}}^2} \frac{dN_X}{dE}$$

Charged cosmic rays

- ✓ Diffusive propagation in Galactic magnetic field
- ✓ Lost directionality
- ➔ Spectral signatures

Photons & neutrinos

- ✓ Unperturbed path
- ✓ Point to the source
- ➔ Spectral and spatial signatures

Gamma rays from dark matter annihilation

Gamma-ray differential flux from dark matter annihilation with spatial distribution ρ_{DM}

$$\frac{d\Phi_\gamma}{dE_\gamma}(E_\gamma, s, \Delta\Omega) = \frac{\langle\sigma v\rangle}{2m_{\text{DM}}^2} \sum_i B_i \frac{dN_\gamma^i}{dE_\gamma} \frac{1}{4\pi} \int_0^{\Delta\Omega} d\Omega \int_{\text{l.o.s}} \rho_{\text{DM}}^2(s) ds$$

Gamma rays from dark matter annihilation

Gamma-ray differential flux from dark matter annihilation with spatial distribution ρ_{DM}

$$\frac{d\Phi_\gamma}{dE_\gamma}(E_\gamma, s, \Delta\Omega) = \frac{\langle\sigma v\rangle}{2m_{\text{DM}}^2} \sum_i B_i \frac{dN_\gamma^i}{dE_\gamma} \frac{1}{4\pi} \int_0^{\Delta\Omega} d\Omega \int_{\text{l.o.s}} \rho_{\text{DM}}^2(s) ds$$

Particle Physics factor

→ Spectral information

Gamma rays from dark matter annihilation

Gamma-ray differential flux from dark matter annihilation with spatial distribution ρ_{DM}

$$\frac{d\Phi_\gamma}{dE_\gamma}(E_\gamma, s, \Delta\Omega) = \frac{\langle\sigma v\rangle}{2m_{\text{DM}}^2} \sum_i B_i \frac{dN_\gamma^i}{dE_\gamma} \frac{1}{4\pi} \int_0^{\Delta\Omega} d\Omega \int_{\text{l.o.s}} \rho_{\text{DM}}^2(s) ds$$

Particle Physics factor

→ Spectral information

Astrophysics factor

→ Spatial information

The particle physics factor

Gamma-ray differential flux from dark matter annihilation with spatial distribution ρ_{DM}

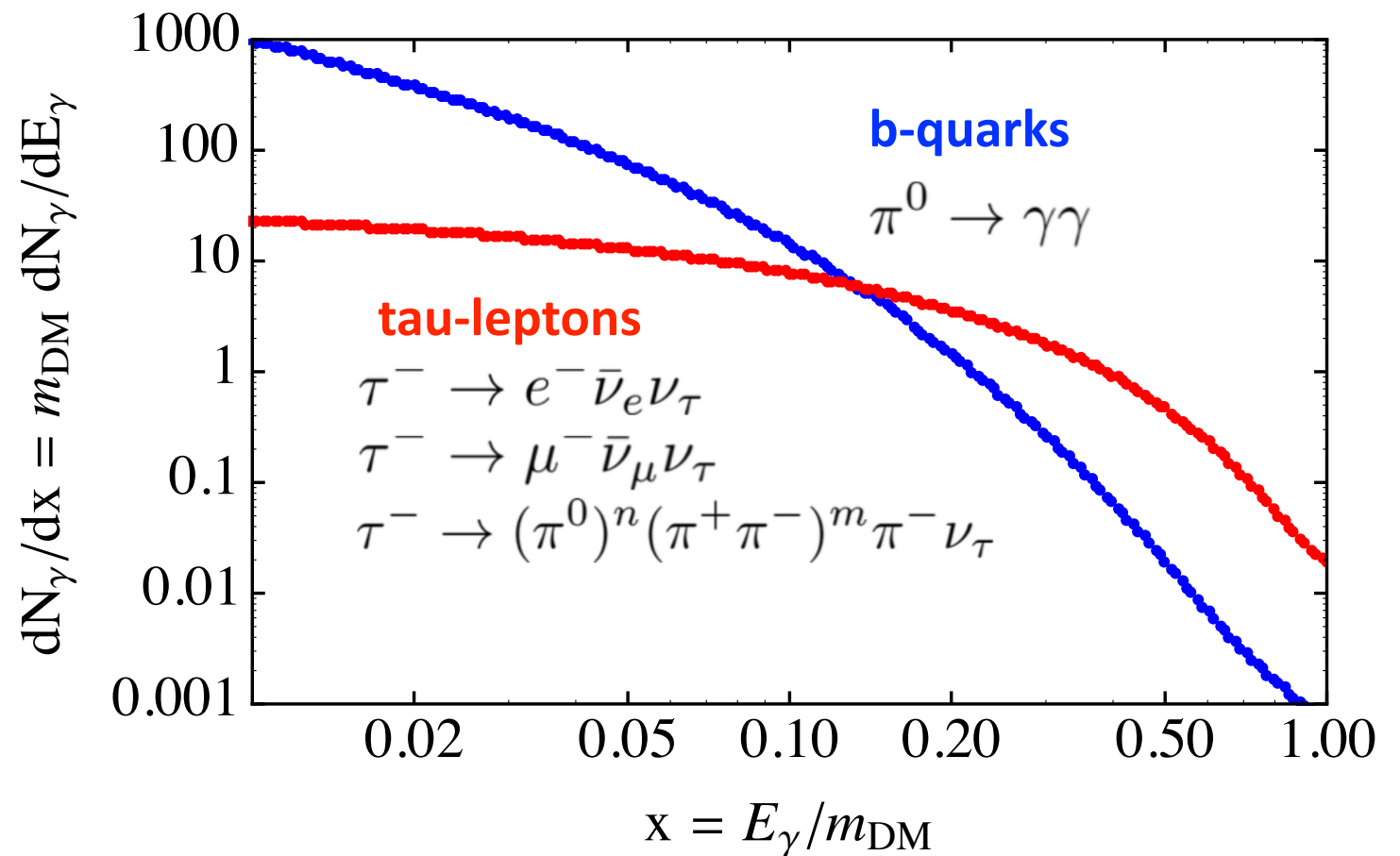
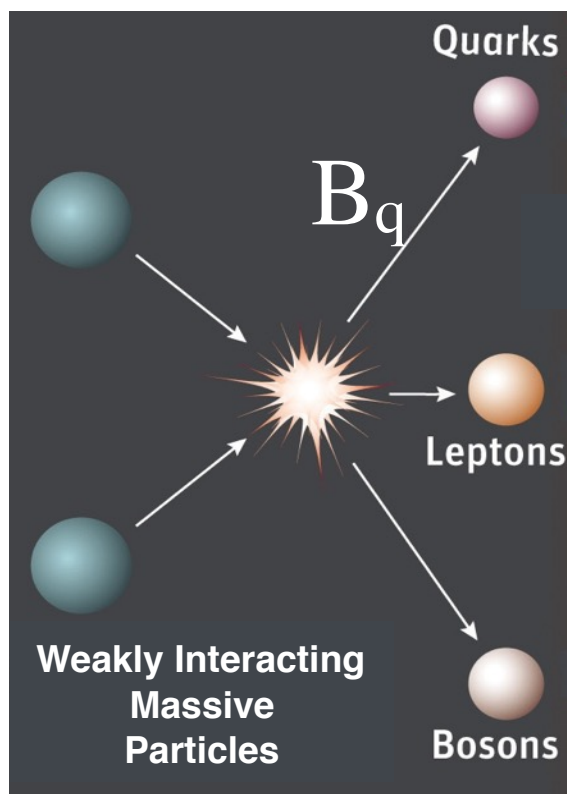
$$\frac{d\Phi_\gamma}{dE_\gamma}(E_\gamma, s, \Delta\Omega) = \frac{\langle\sigma v\rangle}{2m_{\text{DM}}^2} \sum_i B_i \frac{dN_\gamma^i}{dE_\gamma} \frac{1}{4\pi} \int_0^{\Delta\Omega} d\Omega \int_{\text{l.o.s}} \rho_{\text{DM}}^2(s) ds$$

The particle physics factor

Gamma-ray differential flux from dark matter annihilation with spatial distribution ρ_{DM}

$$\frac{d\Phi_\gamma}{dE_\gamma}(E_\gamma, s, \Delta\Omega) = \frac{\langle\sigma v\rangle}{2m_{\text{DM}}^2} \sum_i B_i \frac{dN_\gamma^i}{dE_\gamma} \frac{1}{4\pi} \int_0^{\Delta\Omega} d\Omega \int_{\text{l.o.s}} \rho_{\text{DM}}^2(s) ds$$

DM DM \rightarrow SM SM

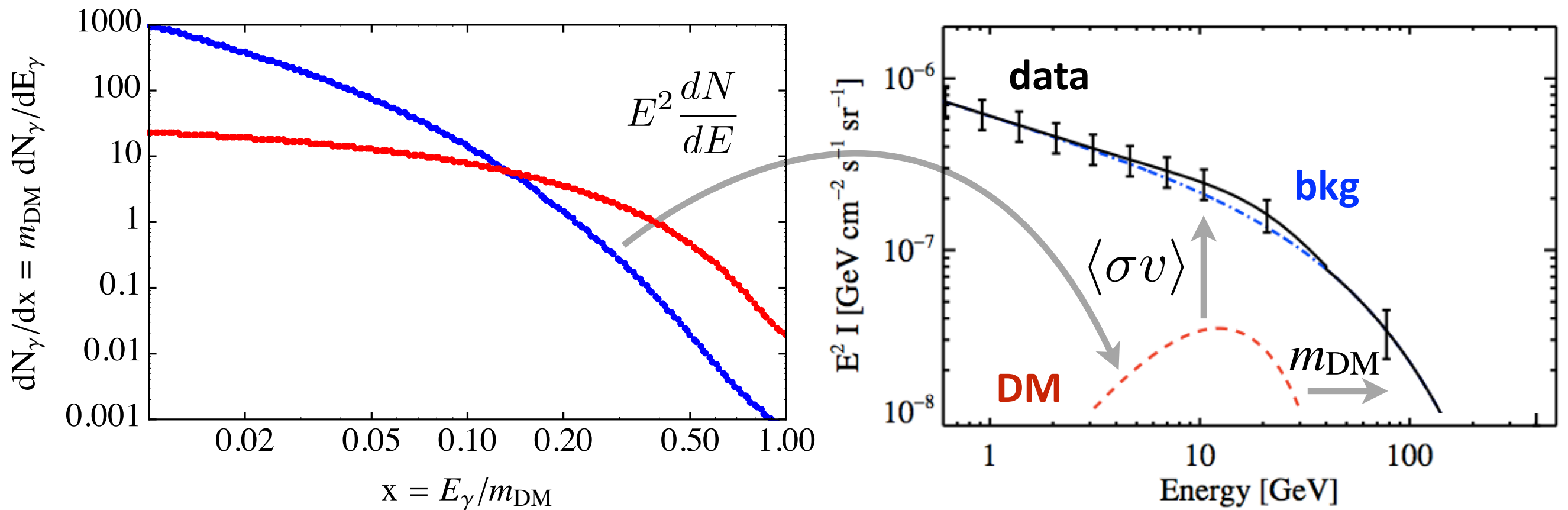


Typical gamma-ray emission from hadronic decays and cascades

The particle physics factor

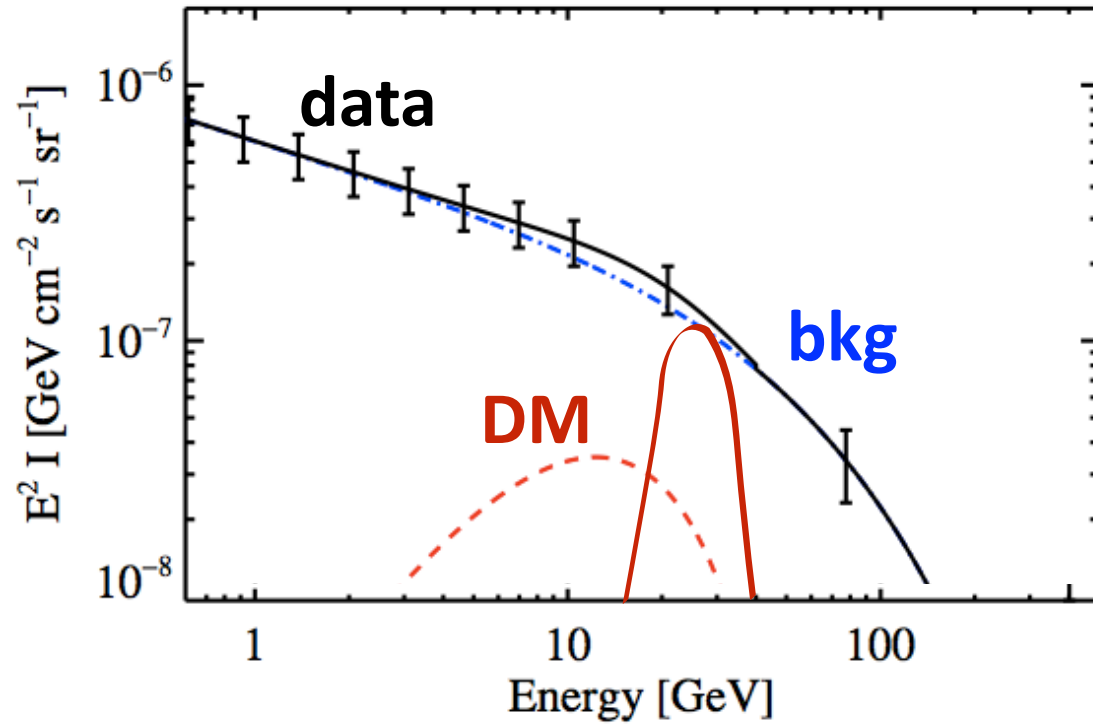
Gamma-ray differential flux from dark matter annihilation with spatial distribution ρ_{DM}

$$\frac{d\Phi_\gamma}{dE_\gamma}(E_\gamma, s, \Delta\Omega) = \frac{\langle\sigma v\rangle}{2m_{\text{DM}}^2} \sum_i B_i \frac{dN_\gamma^i}{dE_\gamma} \frac{1}{4\pi} \int_0^{\Delta\Omega} d\Omega \int_{\text{l.o.s}} \rho_{\text{DM}}^2(s) ds$$



Typical gamma-ray emission from hadronic decays and cascades

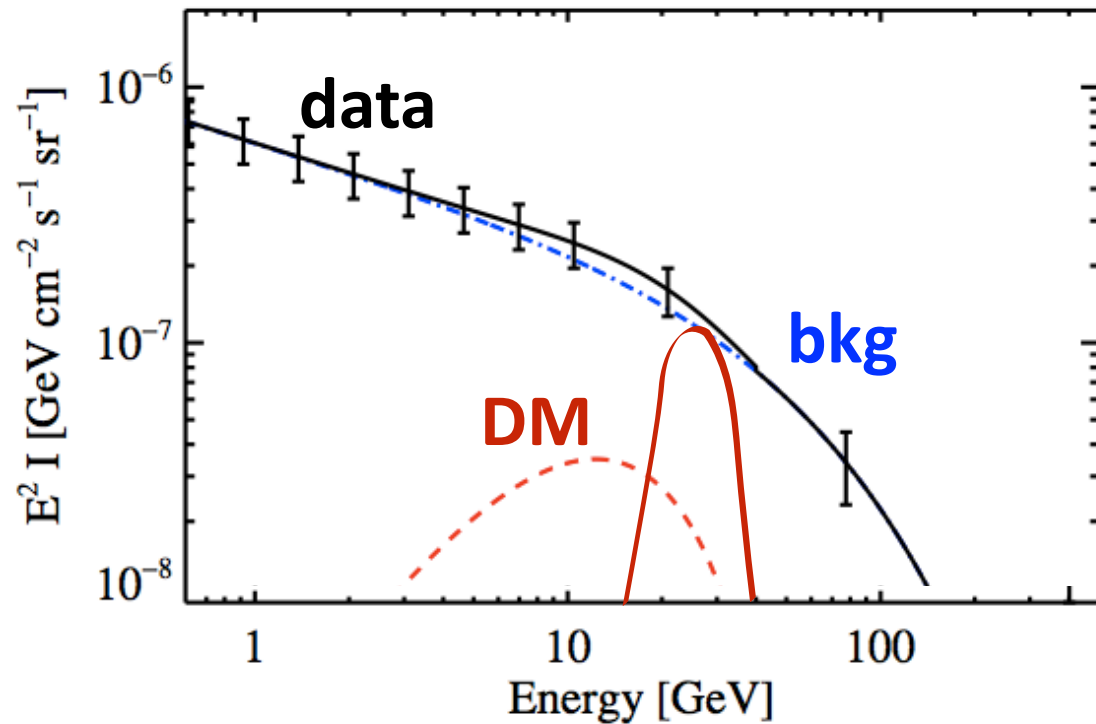
Spectral features in annihilation spectrum



SPECTRAL FEATURES

Smoking-gun dark matter signatures

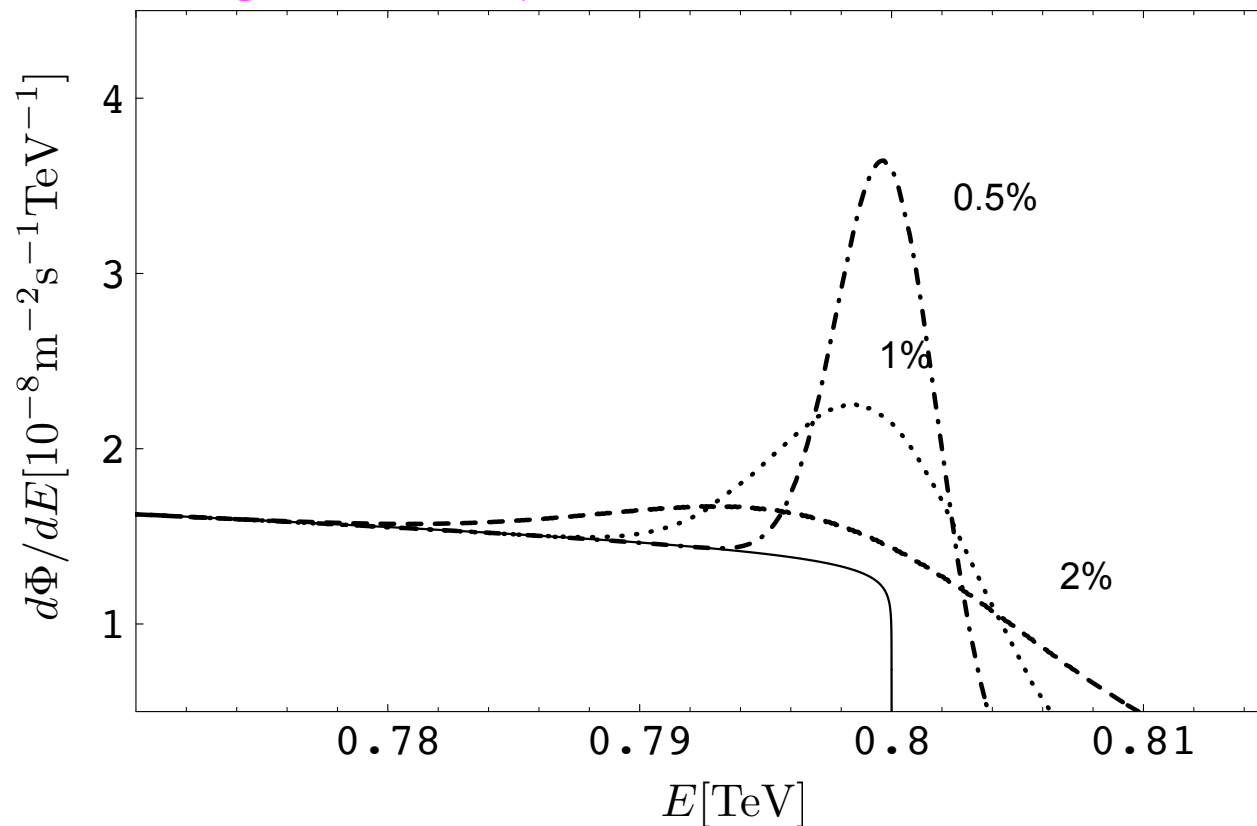
Spectral features in annihilation spectrum



SPECTRAL FEATURES

Smoking-gun dark matter signatures

Bergström et al., JCAP'05



Gamma-ray line from loop suppressed direct annihilation into

$$\gamma\gamma, Z\gamma, H\gamma$$

Looking for dark matter **spectral features** in gamma rays requires optimised search strategies.

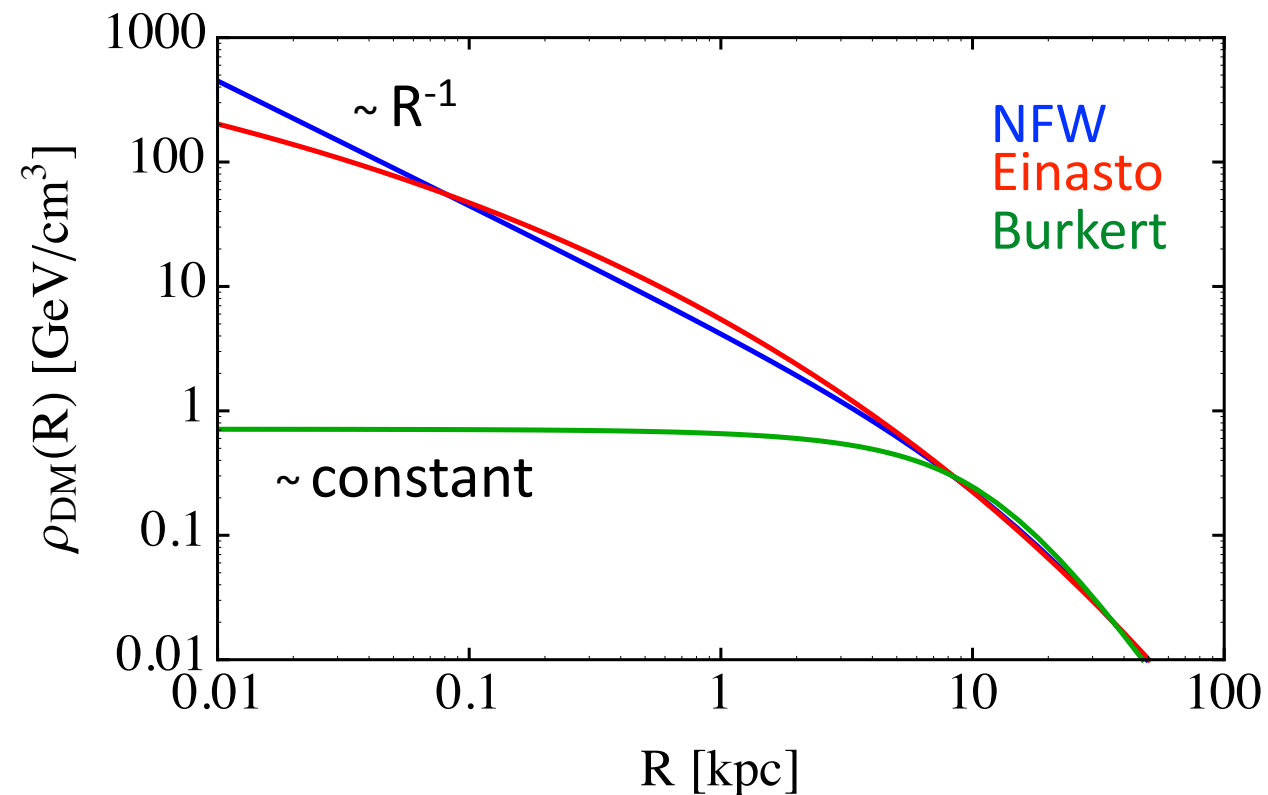
Bringmann, Calore+ PRD'11

The astrophysics factor

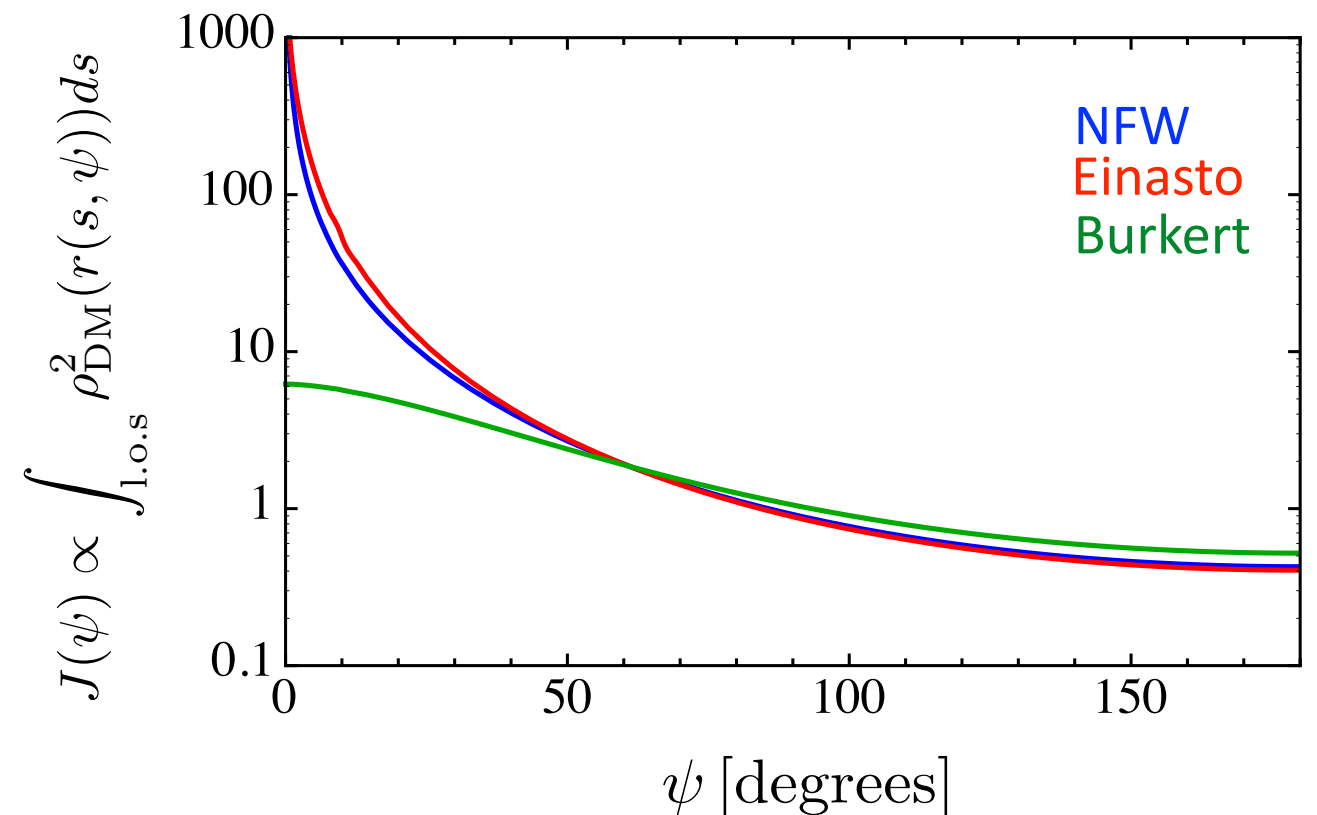
Gamma-ray differential flux from dark matter annihilation with spatial distribution ρ_{DM}

$$\frac{d\Phi_\gamma}{dE_\gamma}(E_\gamma, s, \Delta\Omega) = \frac{\langle\sigma v\rangle}{2m_{\text{DM}}^2} \sum_i B_i \frac{dN_\gamma^i}{dE_\gamma} \left[\frac{1}{4\pi} \int_0^{\Delta\Omega} d\Omega \int_{\text{l.o.s}} \rho_{\text{DM}}^2(s) ds \right]$$

Dark matter density profiles:



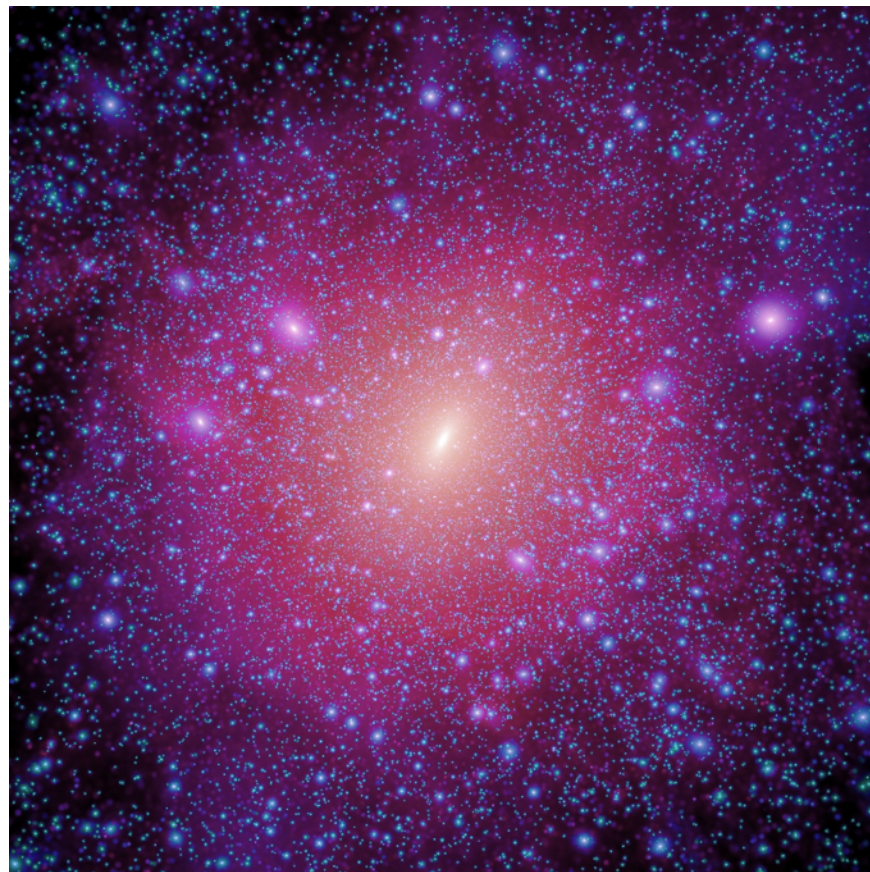
Spatial distribution of the signal:



The dark matter spatial distribution

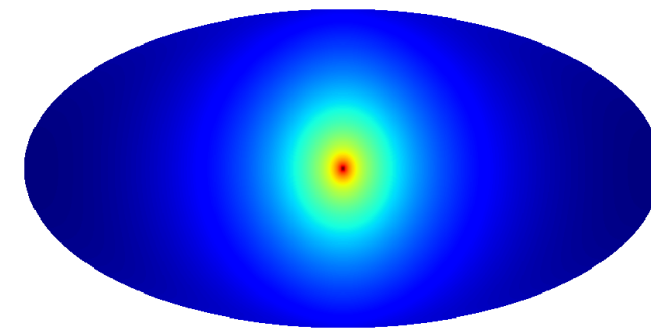
Simulations of structure formation allow to predict the distribution and size of haloes in cosmological volumes

Aquarius DM N-body simulation



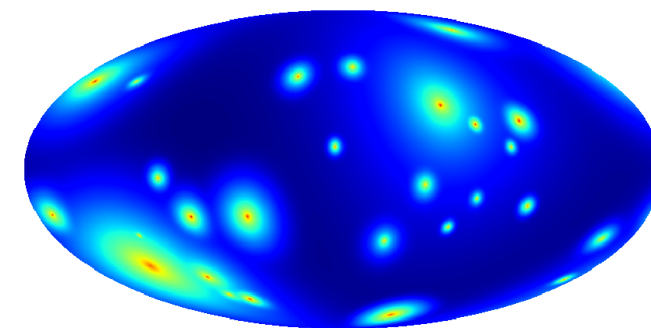
Springel+ MNRAS'08

Expected gamma-ray flux



Main halo

-10.1179 $\log(d\Phi/dE[\text{cm}^{-2} \text{s}^{-1} \text{sr}^{-1} \text{GeV}^{-1}])$ -6.31792



Sub-haloes

-20.0487 $\log(d\Phi/dE[\text{cm}^{-2} \text{s}^{-1} \text{sr}^{-1} \text{GeV}^{-1}])$ -6.56571

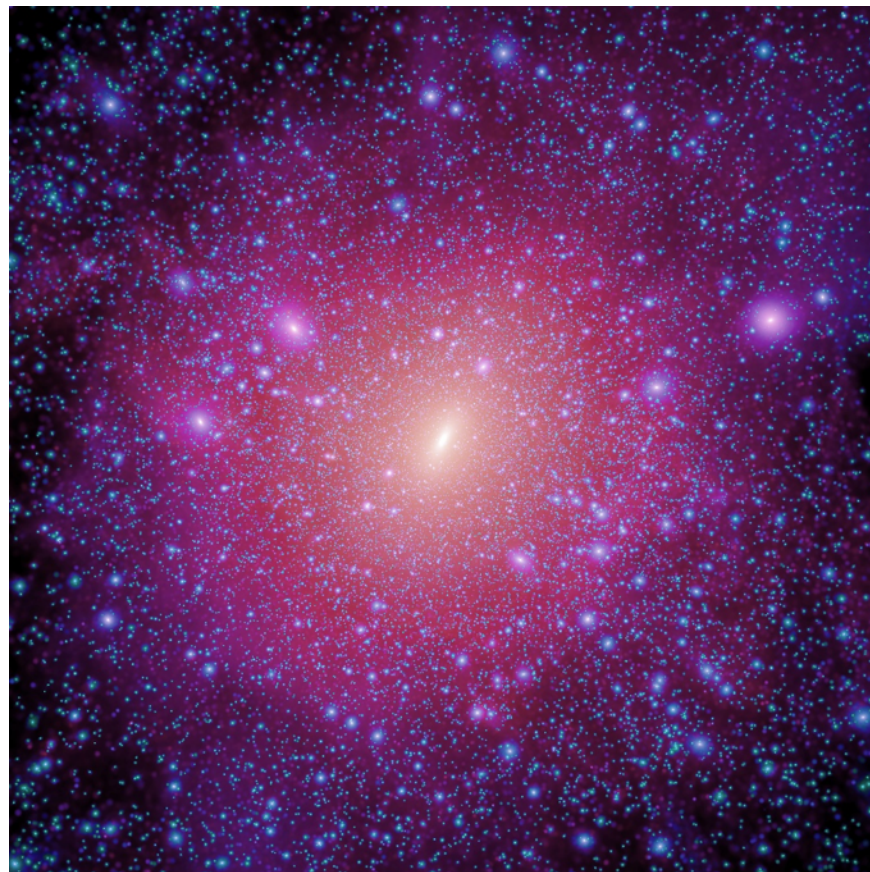
Calore, Donato, Macciò, Stinson+ MNRAS'14

SPATIAL (ANGULAR) FEATURES

The dark matter spatial distribution

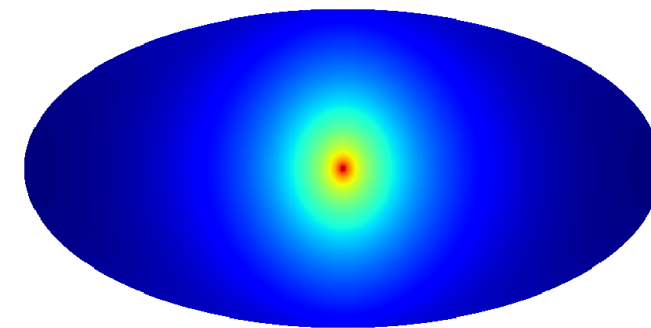
Simulations of structure formation allow to predict the distribution and size of haloes in cosmological volumes

Aquarius DM N-body simulation



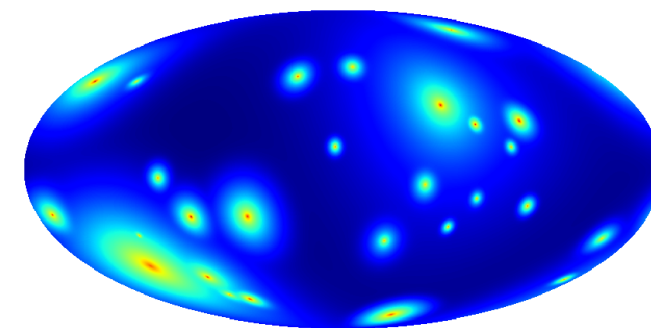
Springel+ MNRAS'08

Expected gamma-ray flux



Main halo

-10.1179 $\log(d\Phi/dE[\text{cm}^{-2} \text{s}^{-1} \text{sr}^{-1} \text{GeV}^{-1}])$ -6.31792



Sub-haloes

-20.0487 $\log(d\Phi/dE[\text{cm}^{-2} \text{s}^{-1} \text{sr}^{-1} \text{GeV}^{-1}])$ -6.56571

Calore, Donato, Macciò, Stinson+ MNRAS'14

SPATIAL (ANGULAR) FEATURES

Important effect of baryons during galaxy formation (highly debated)

Current gamma-ray telescopes

Space based:

(Pair conversion detector)



Fermi LAT
since 2008

$A_{\text{eff}} \sim 1\text{m}^2$
 $T \sim < 10\text{yr}$
 20 MeV – 300 GeV

Ground based:

(Atmospheric Cherenkov Telescopes)

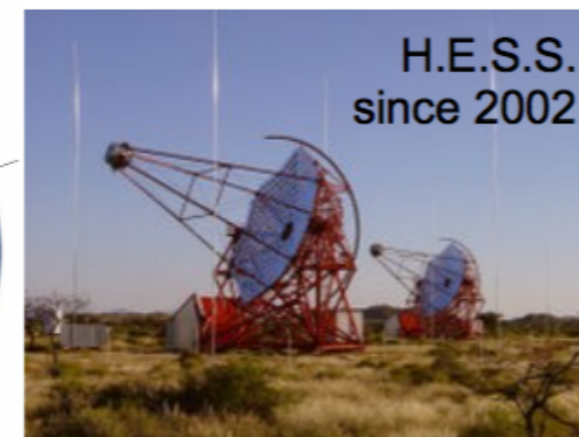
$A_{\text{eff}} \sim 1\text{km}^2$
 $T \sim < 100\text{h}$
 $> 10\text{ GeV}$



VERITAS
since 2007

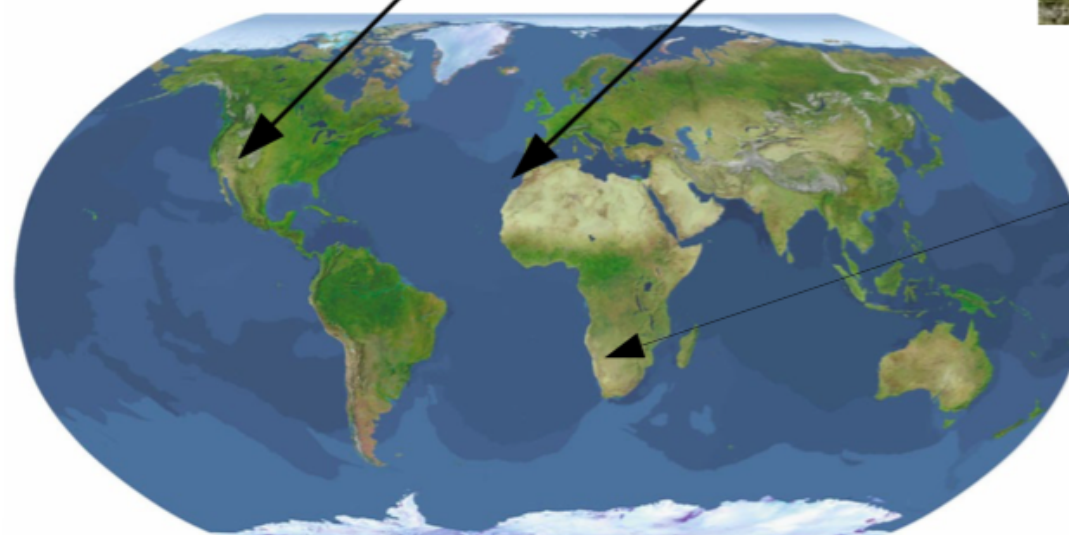
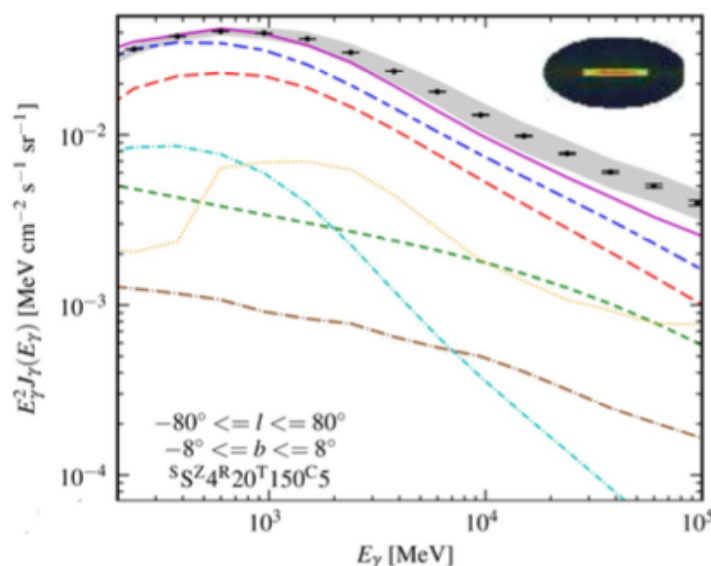


MAGIC
since 2004



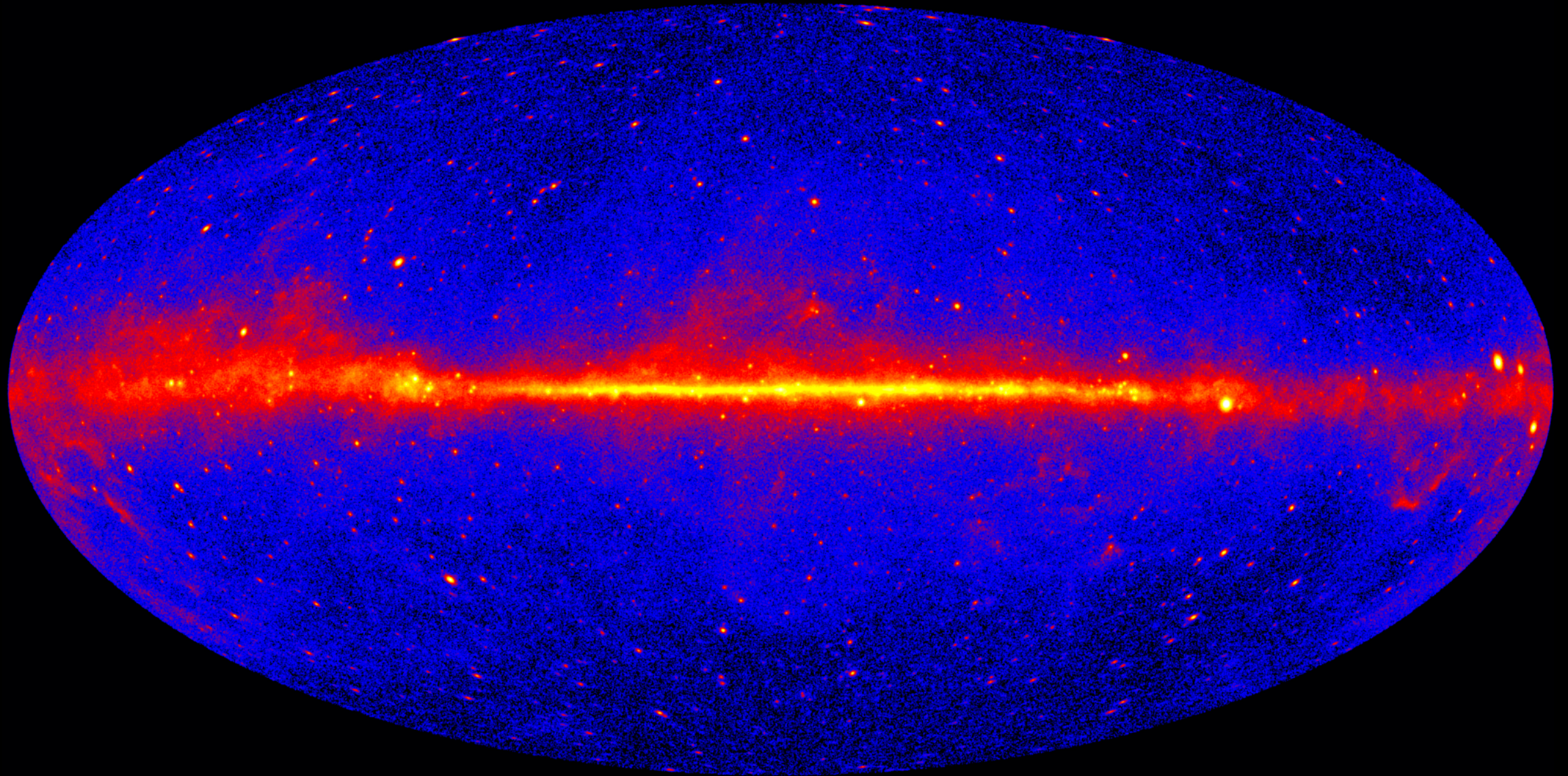
H.E.S.S.
since 2002

Fluxes are falling rapidly with increasing energy
 High energy measurements require huge collection areas



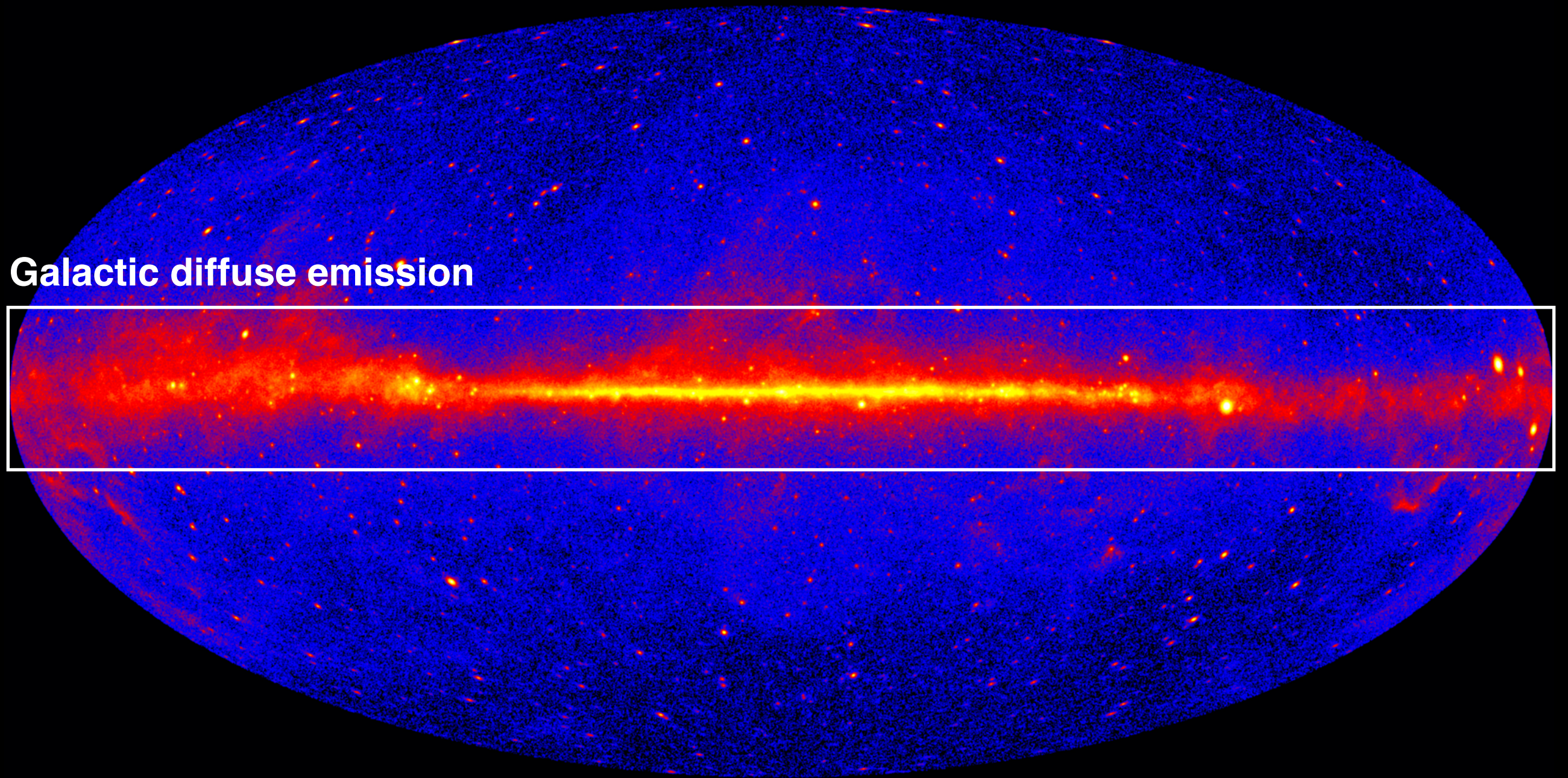


The Fermi-LAT gamma-ray sky



Astrophysical components: The Galactic diffuse emission

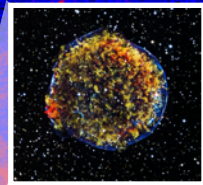
Galactic diffuse emission



Astrophysical components: The Galactic diffuse emission

★ CR interactions with gas and radiation field

CR sources



Tycho's SNR
(SN 1572)

Cassiopeia A

Cygnus Loop

W51C

W49B

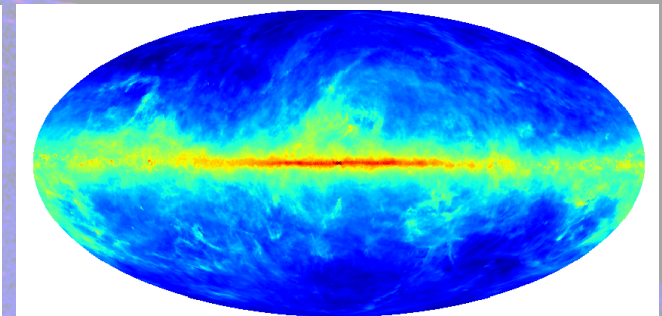
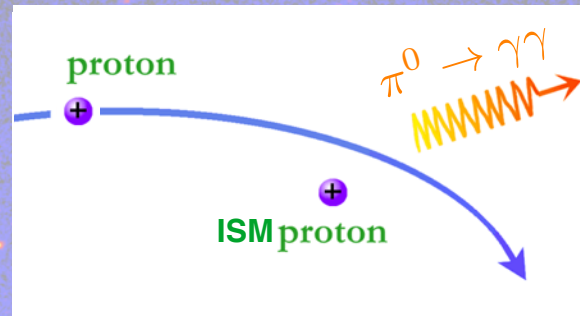
W44

CR propagation

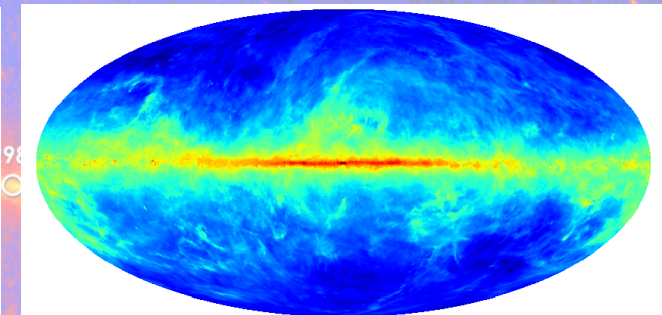
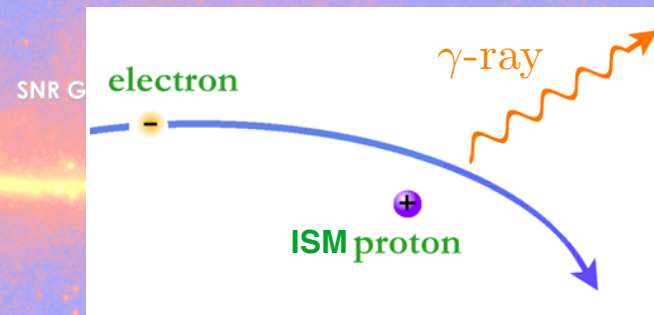
Source

Sun

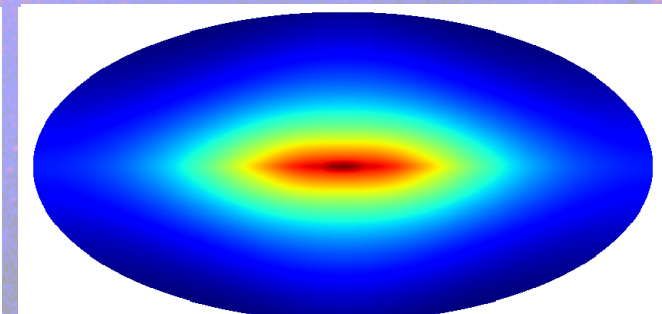
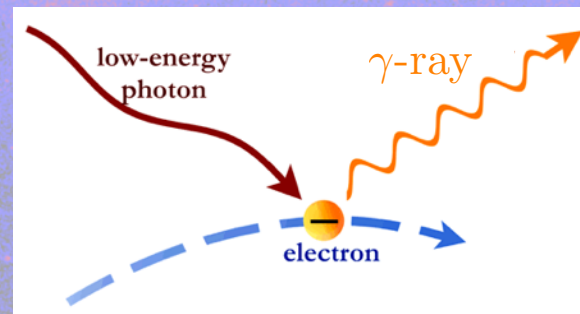
Pion decay



Bremsstrahlung



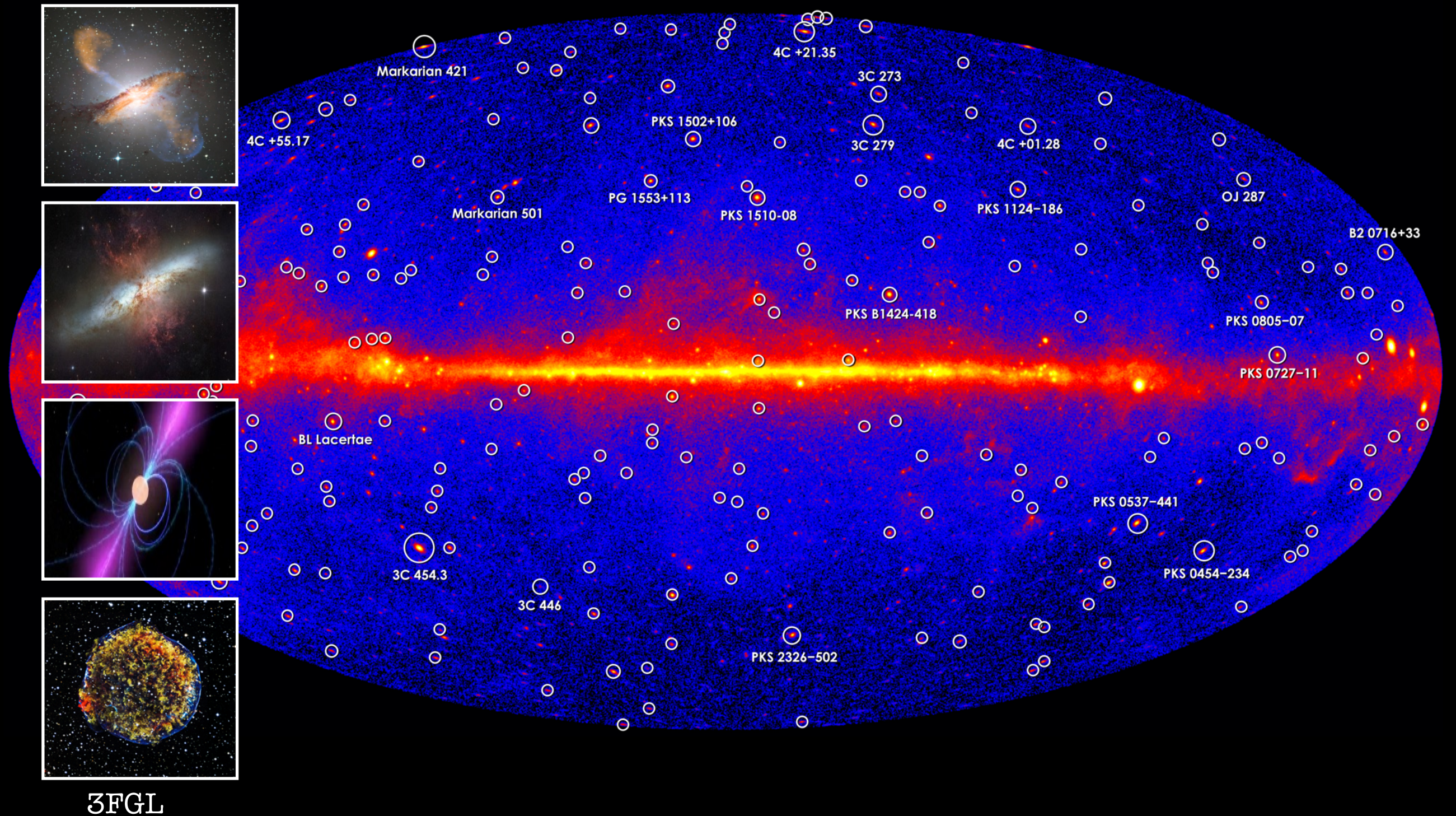
Inverse Compton



Galactic diffuse gamma-ray emission
(GDE)

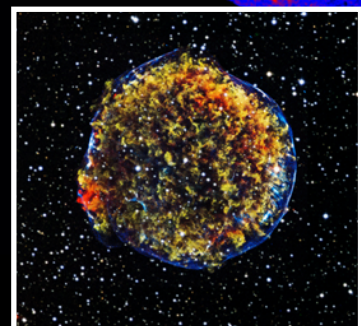
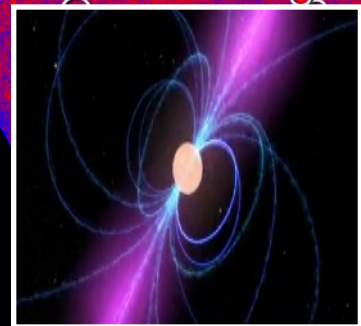
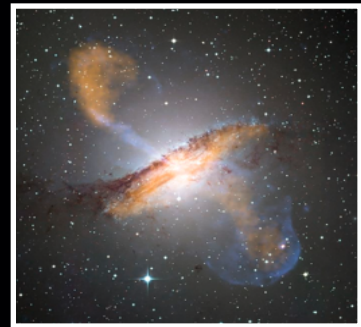
Astrophysical components: Detected sources and Fermi bubbles

Detected sources

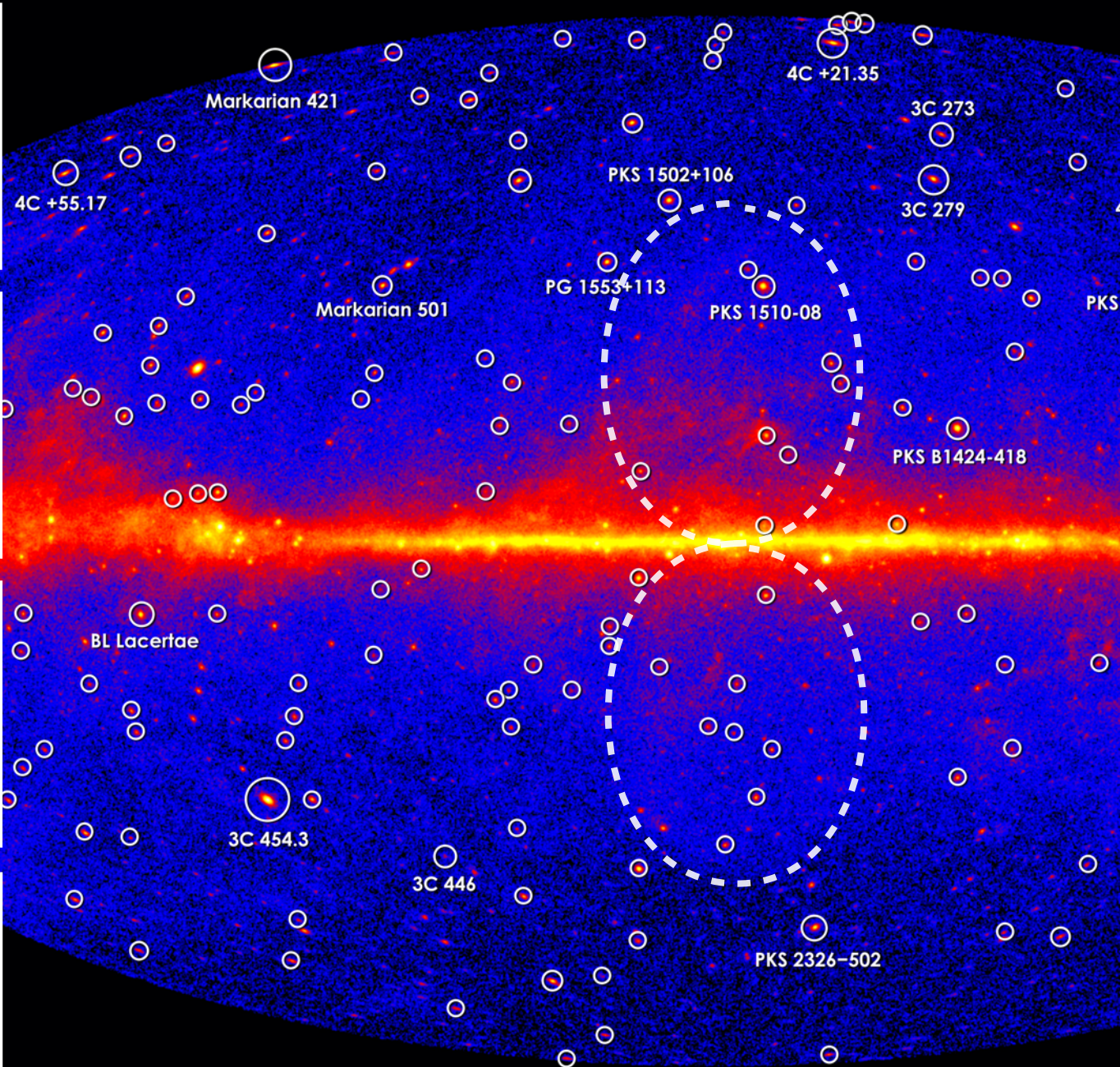


Astrophysical components: Detected sources and Fermi bubbles

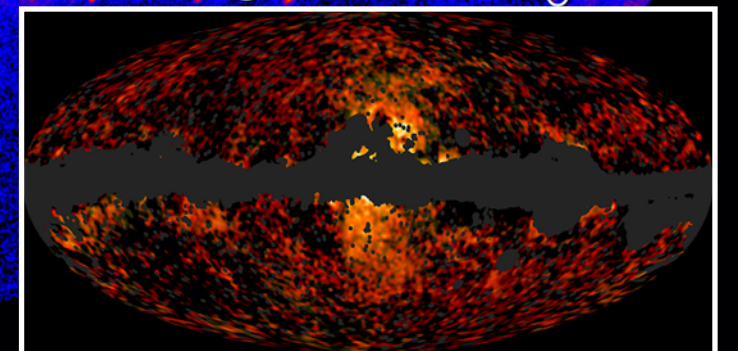
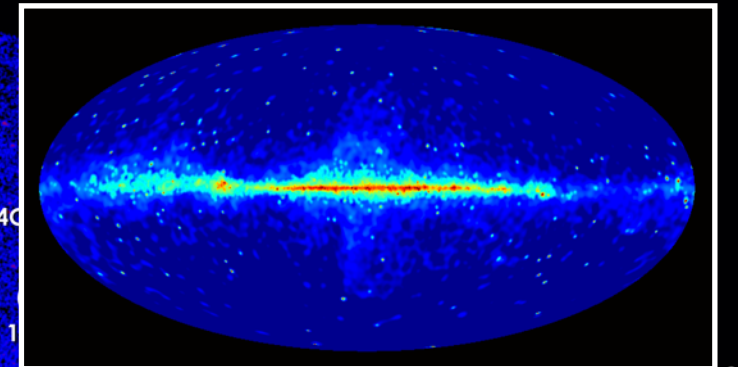
Detected sources



3FGL

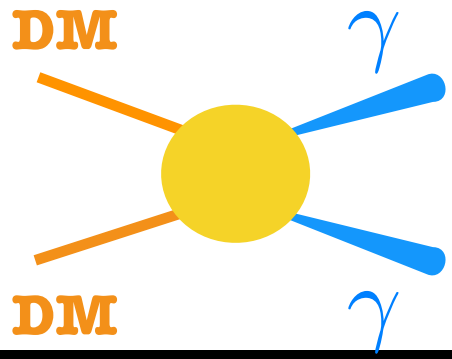


Fermi bubbles



Su+ ApJ'10;

Fermi-LAT Coll. ApJ'14



Targets for dark matter searches

Galactic Center

- high statistics
- brightest dark matter source but uncertain distribution
- large background

Galactic Halo at High Latitude

- good statistics
- (extra)galactic backgrounds
- spectral and anisotropy measurements

Galaxy Clusters

- dark matter substructures
- cosmic-ray induced background

Dwarf Spheroidal Galaxies

- dark matter dominated nearby objects
- almost background-free

Dark Halos

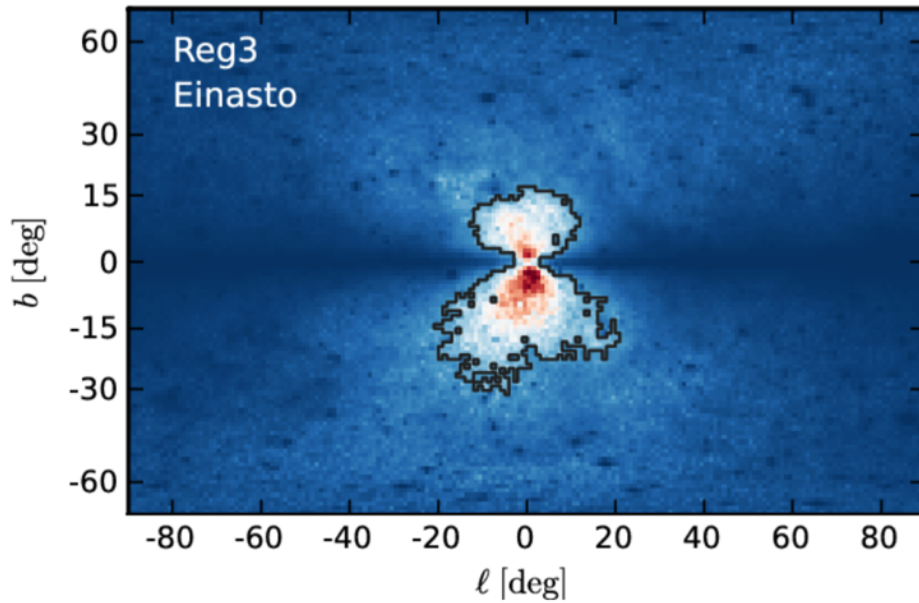
- pure dark matter objects
- unassociated gamma-ray sources

$$\propto \int_{\text{l.o.s.}} \rho_{\text{DM}}^2 ds$$

+ dedicated searches for gamma-ray lines

Searching for gamma-ray lines

Gamma-ray line searches

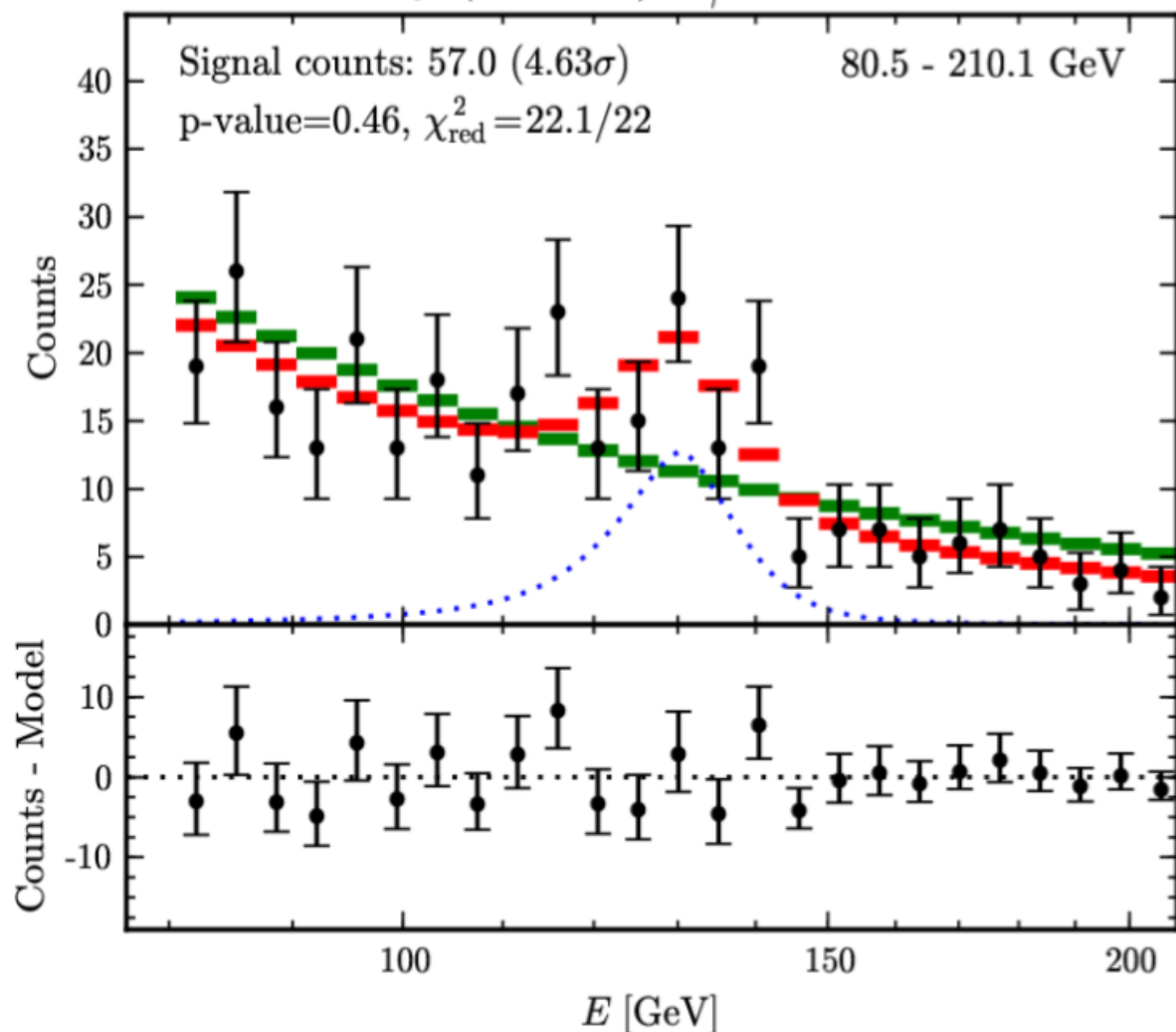


Optimised region of interest about the Galactic center, depends on the DM profile.

$$\frac{N_S}{\sqrt{N_B}}$$

Signal/Noise ratio

Reg4 (SOURCE), $E_\gamma = 129.8$ GeV



A gamma-ray line signal at 130 GeV?

Bringmann+ JCAP'12

Weniger JCAP'12

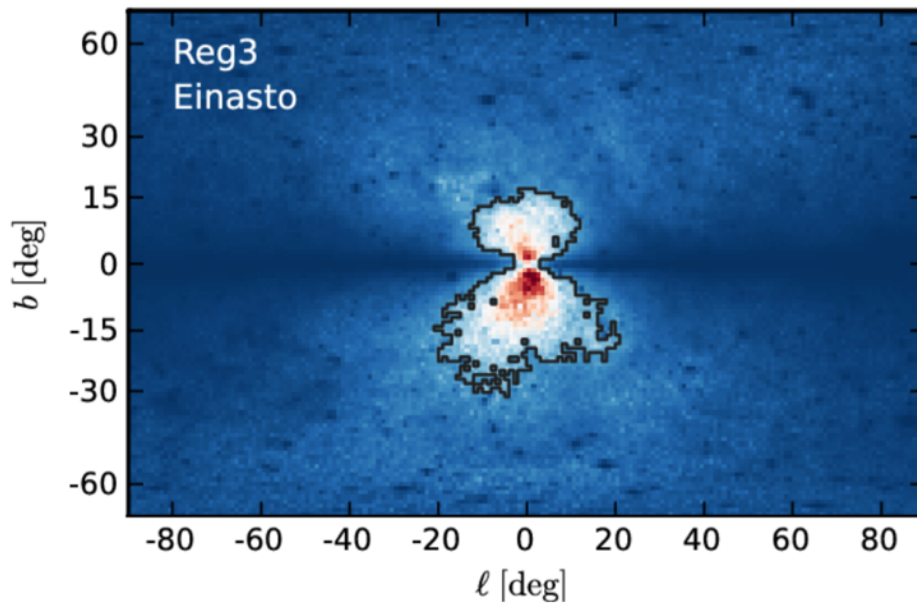
43 months of SOURCE data (P7V6)

Local significance: 4.6 sigma

Global significance: 3.2 sigma

Profumo&Linden, JCAP'12; Ibarra+ JCAP'12; Dudas+'12;
Cline PRD'12; Choi&Seto PRD'12; Buckley&Hooper PRD'12;
etc....

Gamma-ray line searches

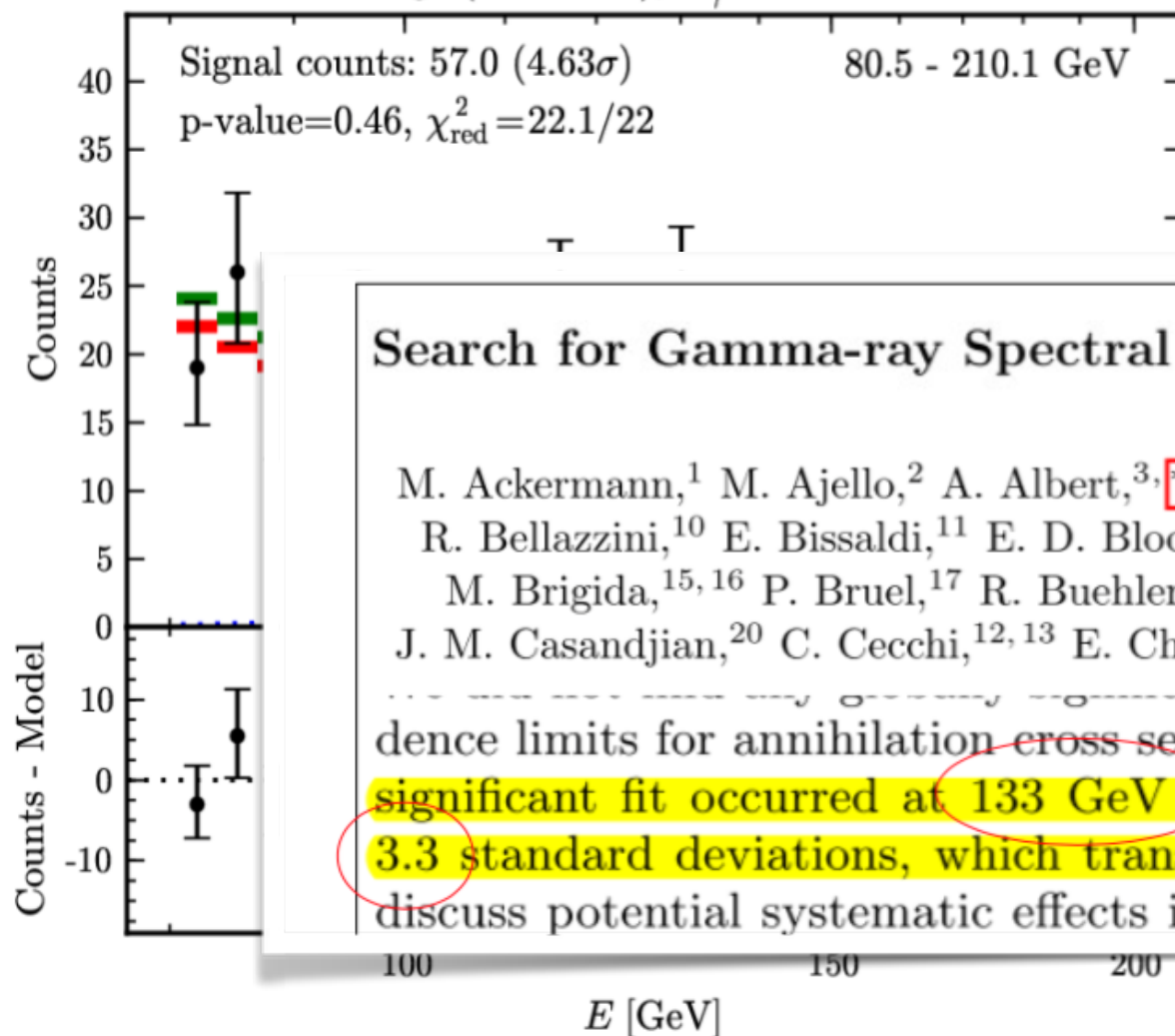


Optimised region of interest about the Galactic center, depends on the DM profile.

$$\frac{N_S}{\sqrt{N_B}}$$

Signal/Noise ratio

Reg4 (SOURCE), $E_\gamma = 129.8$ GeV



A gamma-ray line signal at 130 GeV?

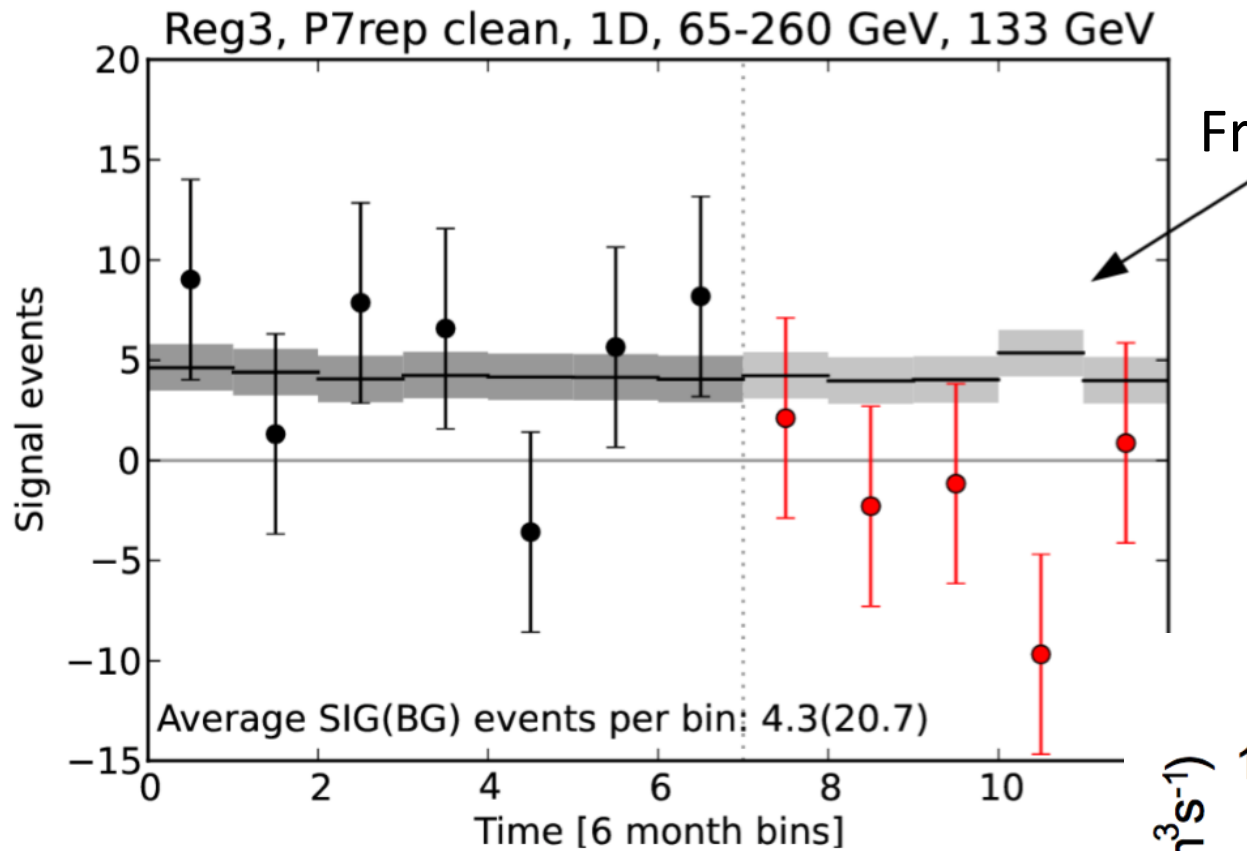
Bringmann+ JCAP'12
Weniger JCAP'12

Search for Gamma-ray Spectral Lines with the *Fermi* Large Area Telescope and Dark Matter Implications

M. Ackermann,¹ M. Ajello,² A. Albert,^{3,*} A. Allafort,⁴ L. Baldini,⁵ G. Barbiellini,^{6,7} D. Bastieri,^{8,9} K. Bechtol,⁴ R. Bellazzini,¹⁰ E. Bissaldi,¹¹ E. D. Bloom,^{4,†} E. Bonamente,^{12,13} E. Bottacini,⁴ T. J. Brandt,¹⁴ J. Bregeon,¹⁰ M. Brigida,^{15,16} P. Bruel,¹⁷ R. Buehler,¹ S. Buson,^{8,9} G. A. Caliandro,¹⁸ R. A. Cameron,⁴ P. A. Caraveo,¹⁹ J. M. Casandjian,²⁰ C. Cecchi,^{12,13} E. Charles,^{4,‡} R.C.G. Chaves,²⁰ A. Chekhtman,²¹ J. Chiang,⁴ S. Ciprini,^{22,23}

dence limits for annihilation cross sections of self-conjugate WIMPs and decay lifetimes. Our most significant fit occurred at 133 GeV in our smallest search region and had a local significance of 3.3 standard deviations, which translates to a global significance of 1.5 standard deviations. We discuss potential systematic effects in this search, and examine the feature at 133 GeV in detail.

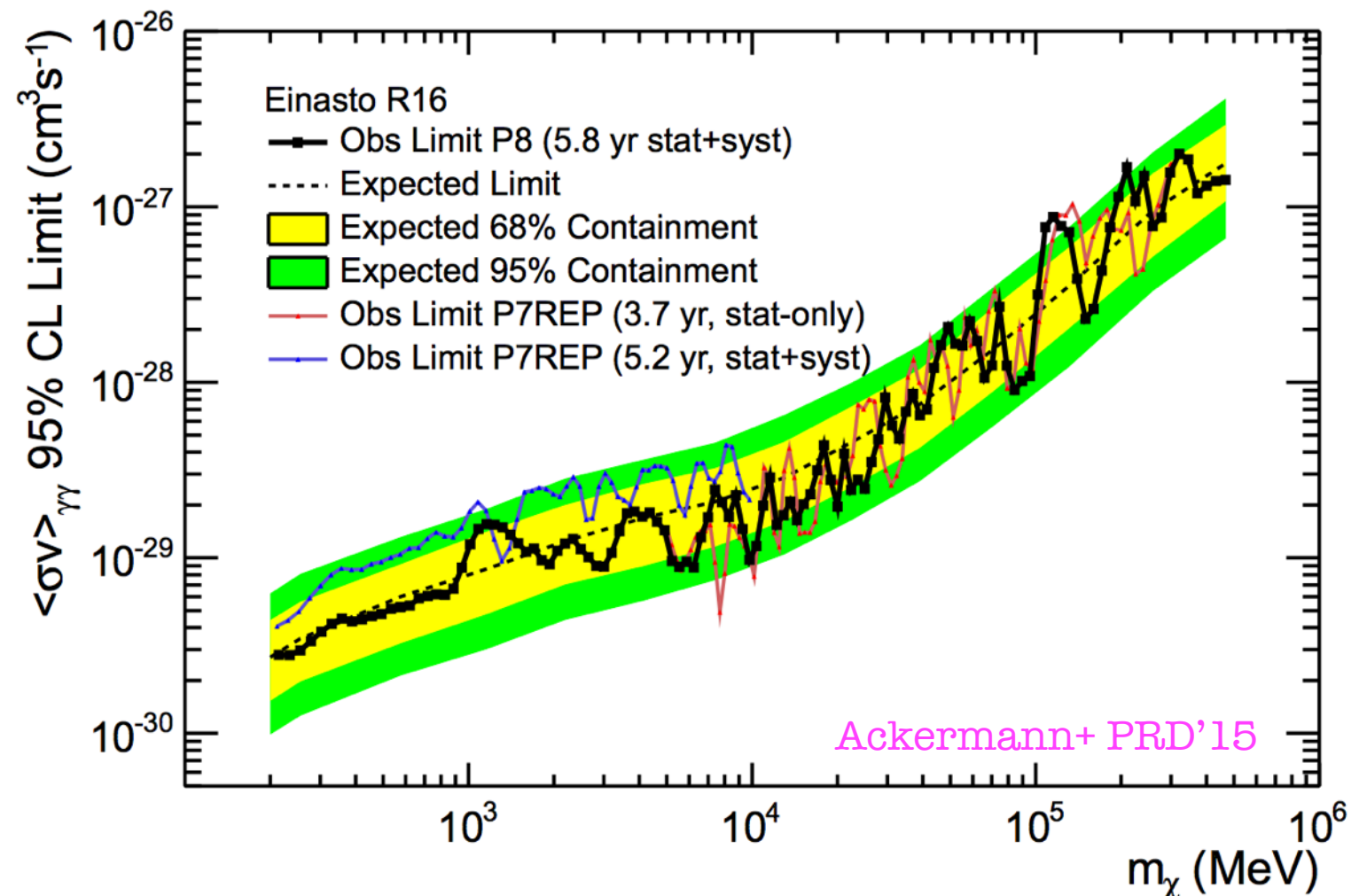
Gamma-ray line searches



But no signal since Summer 2012!

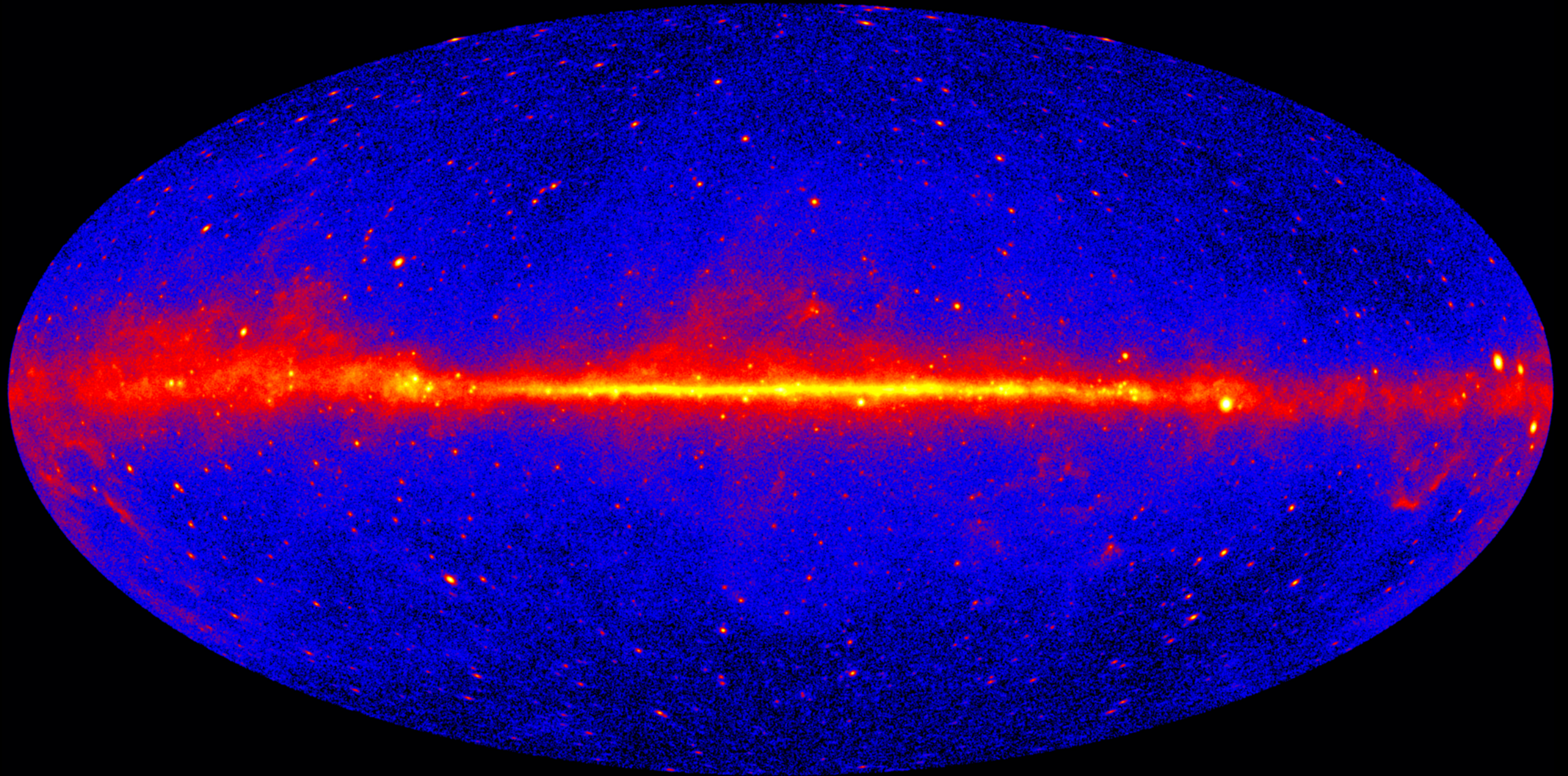
Using Fermi LAT data alone, the signal hypothesis can be excluded at more than 3 sigma.

- 200MeV - 500 GeV
 - 5.8 years of data
 - 5 optimised sky regions
- > Local significance: 0.72 sigma

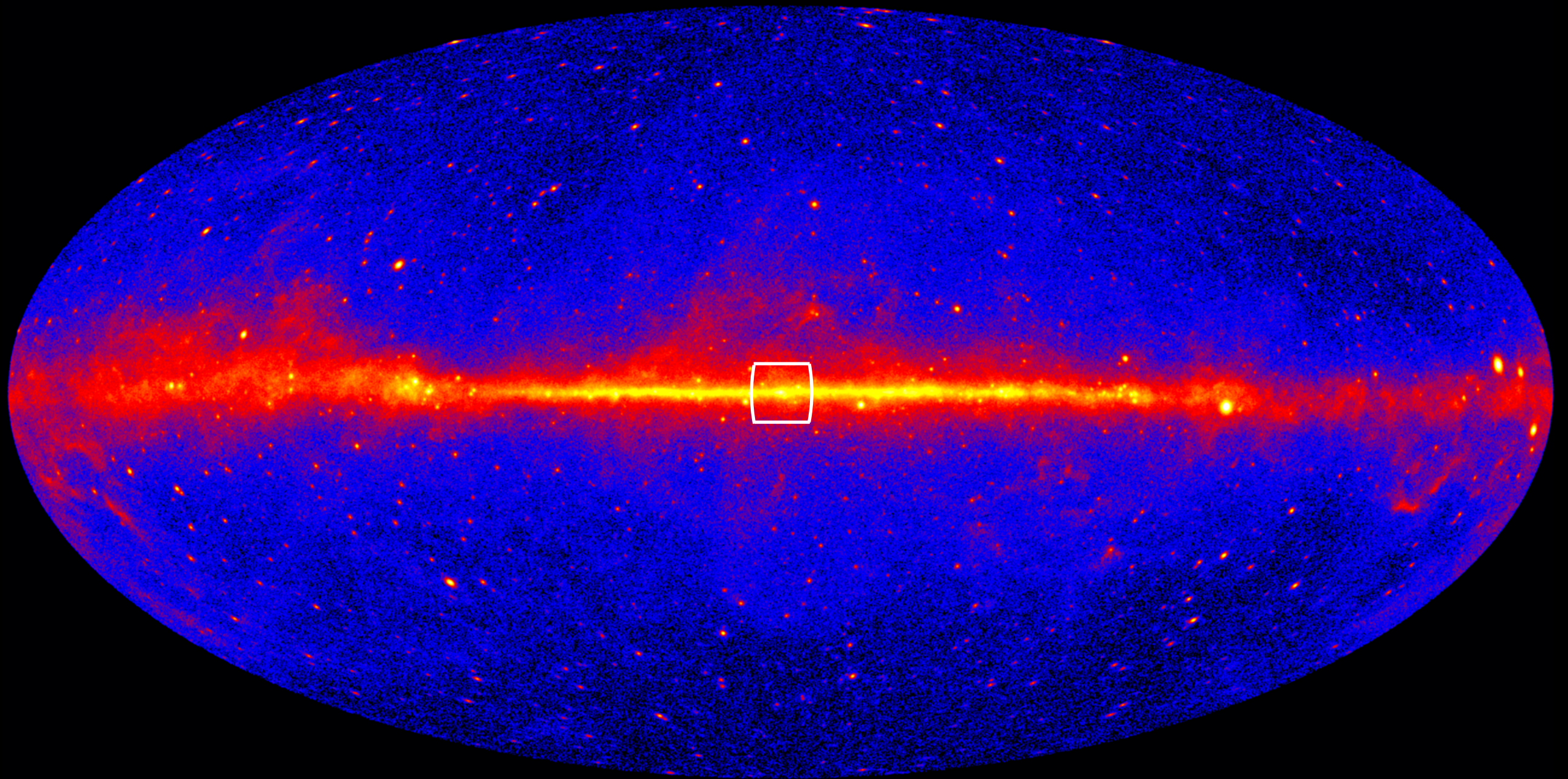


Searching for dark matter in the inner Galaxy

The low-latitude Fermi-LAT gamma-ray sky



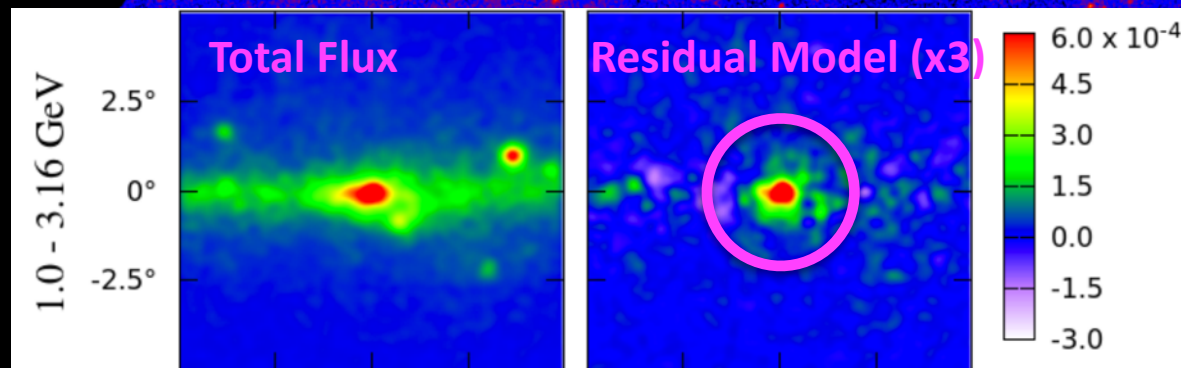
The low-latitude Fermi-LAT gamma-ray sky



The low-latitude Fermi-LAT gamma-ray sky

The Galactic centre GeV excess (at the Galactic centre)

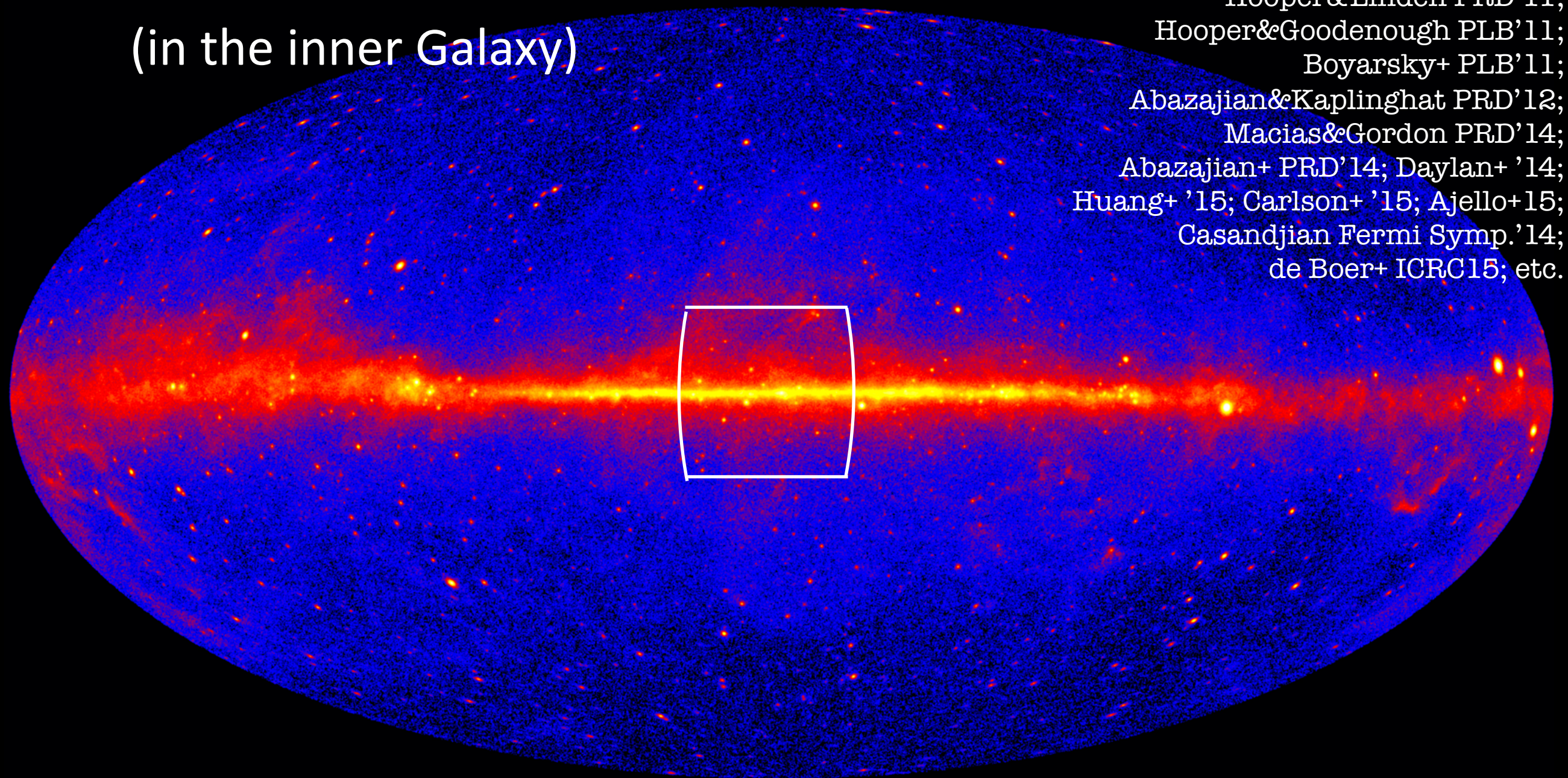
Hooper&Goodenough '09; Vitale&Morselli '09;
Hooper&Linden PRD'11;
Hooper&Goodenough PLB'11;
Boyarsky+ PLB'11;
Abazajian&Kaplinghat PRD'12;
Macias&Gordon PRD'14;
Abazajian+ PRD'14; Daylan+ '14;
Huang+ '15; Carlson+ '15; Ajello+15;
Casandjian Fermi Symp.'14;
de Boer+ ICRC15; etc.



Daylan+ '14

The low-latitude Fermi-LAT gamma-ray sky

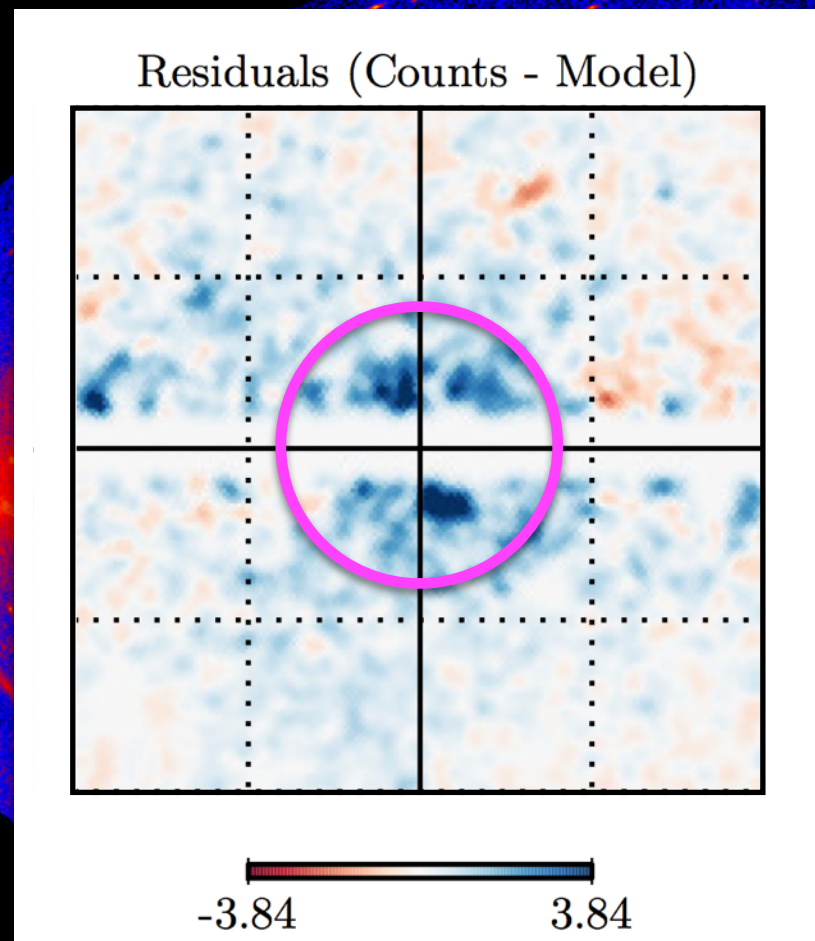
The Galactic centre GeV excess (in the inner Galaxy)



Hooper&Goodenough '09; Vitale&Morselli '09;
Hooper&Linden PRD'11;
Hooper&Goodenough PLB'11;
Boyarsky+ PLB'11;
Abazajian&Kaplinghat PRD'12;
Macias&Gordon PRD'14;
Abazajian+ PRD'14; Daylan+ '14;
Huang+ '15; Carlson+ '15; Ajello+15;
Casandjian Fermi Symp.'14;
de Boer+ ICRC15; etc.

The low-latitude Fermi-LAT gamma-ray sky

The Galactic centre GeV excess (in the inner Galaxy)



Calore+ JCAP'15

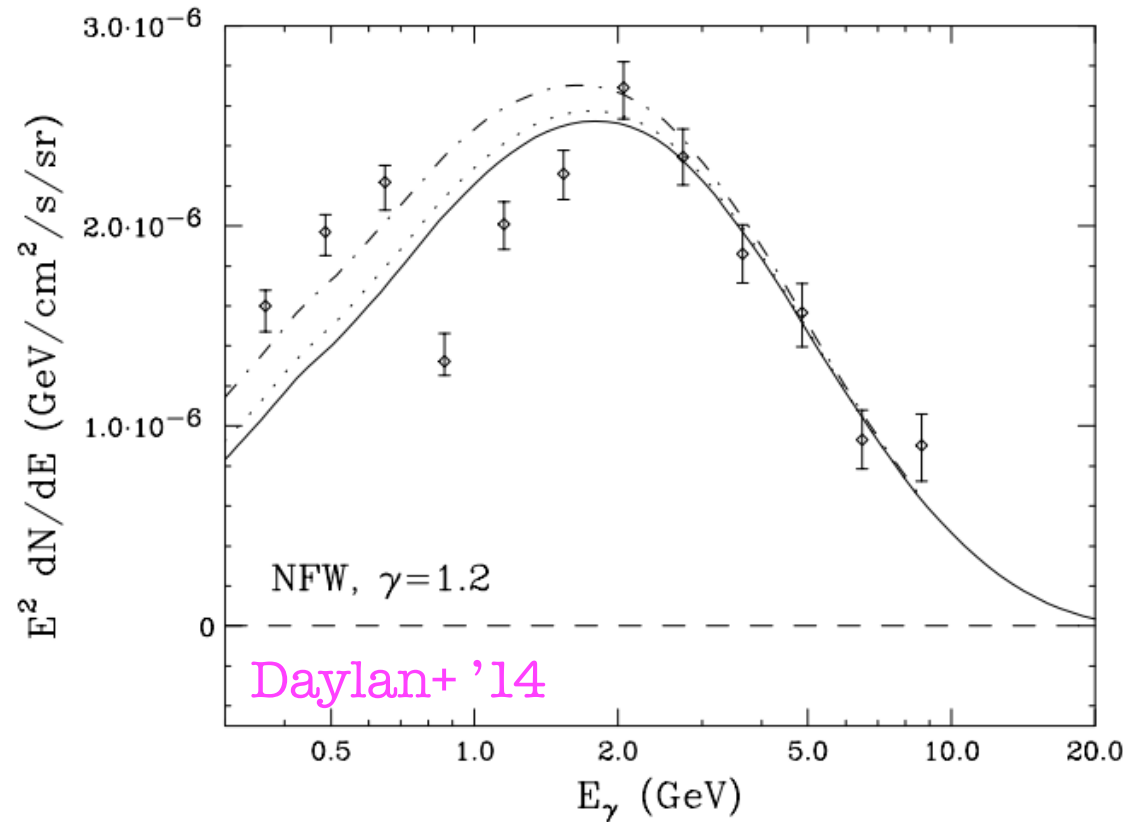
Hooper&Goodenough '09; Vitale&Morselli '09;
Hooper&Linden PRD'11;
Hooper&Goodenough PLB'11;
Boyarsky+ PLB'11;
Abazajian&Kaplinghat PRD'12;
Macias&Gordon PRD'14;
Abazajian+ PRD'14; Daylan+ '14;
Huang+ '15; Carlson+ '15; Ajello+15;
Casandjian Fermi Symp.'14;
de Boer+ ICRC15; etc.

Hooper&Slatyer PDU'13; Huang+ JCAP'13;
Zhou+ PRD'15; Daylan+ '14; Calore+ JCAP'15;
Gaggero+ 2015; Ajello+ 2015; Huang+ '15;
Linden+'16; Horiuchi+'16

The GeV excess at the Galactic centre

$$|\ell|, |b| \lesssim 2^\circ$$

Spectrum



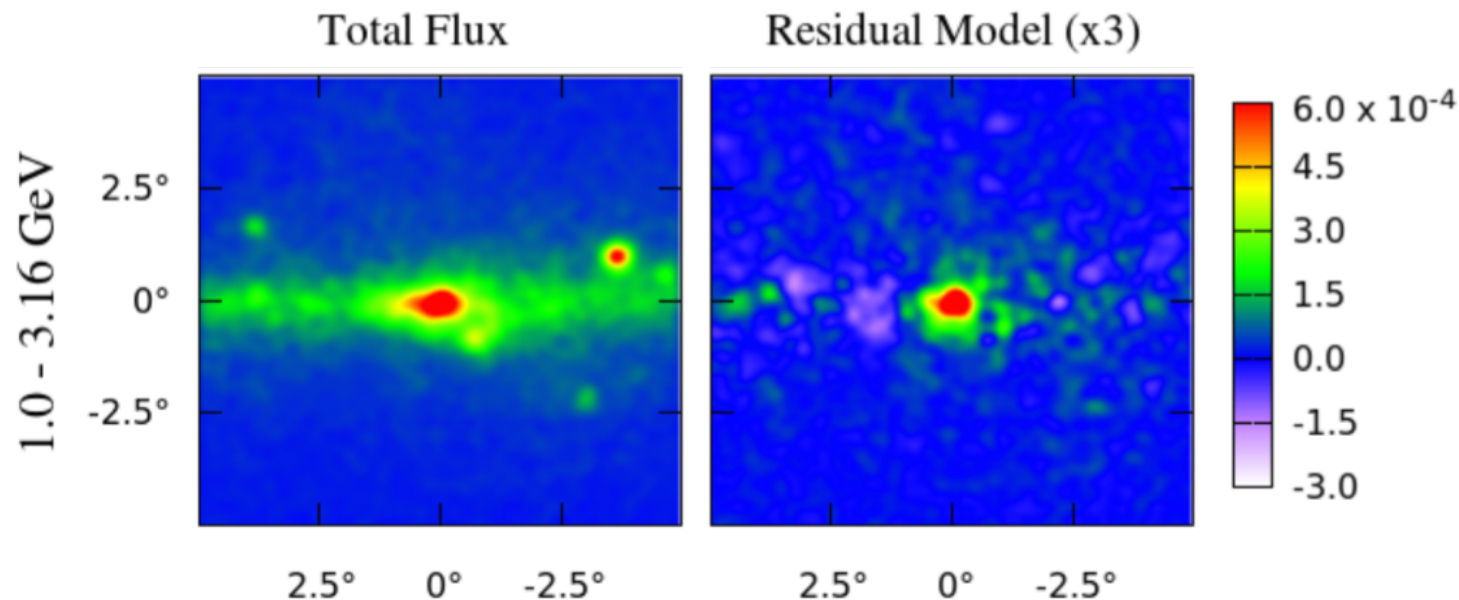
- ✓ **Extended excess emission** above: model for diffuse emission, Sgr A* and other point sources.
- ✓ The **spectrum** might strongly suffer from **background modeling**.

Abazjian+ PRD'14

- ✓ Compatible to be **spherically symmetric** about the Galactic centre.
- ✓ Emission profile:

$$\frac{dn}{dV} \sim r^{-\Gamma} \quad \Gamma \sim 2.6$$

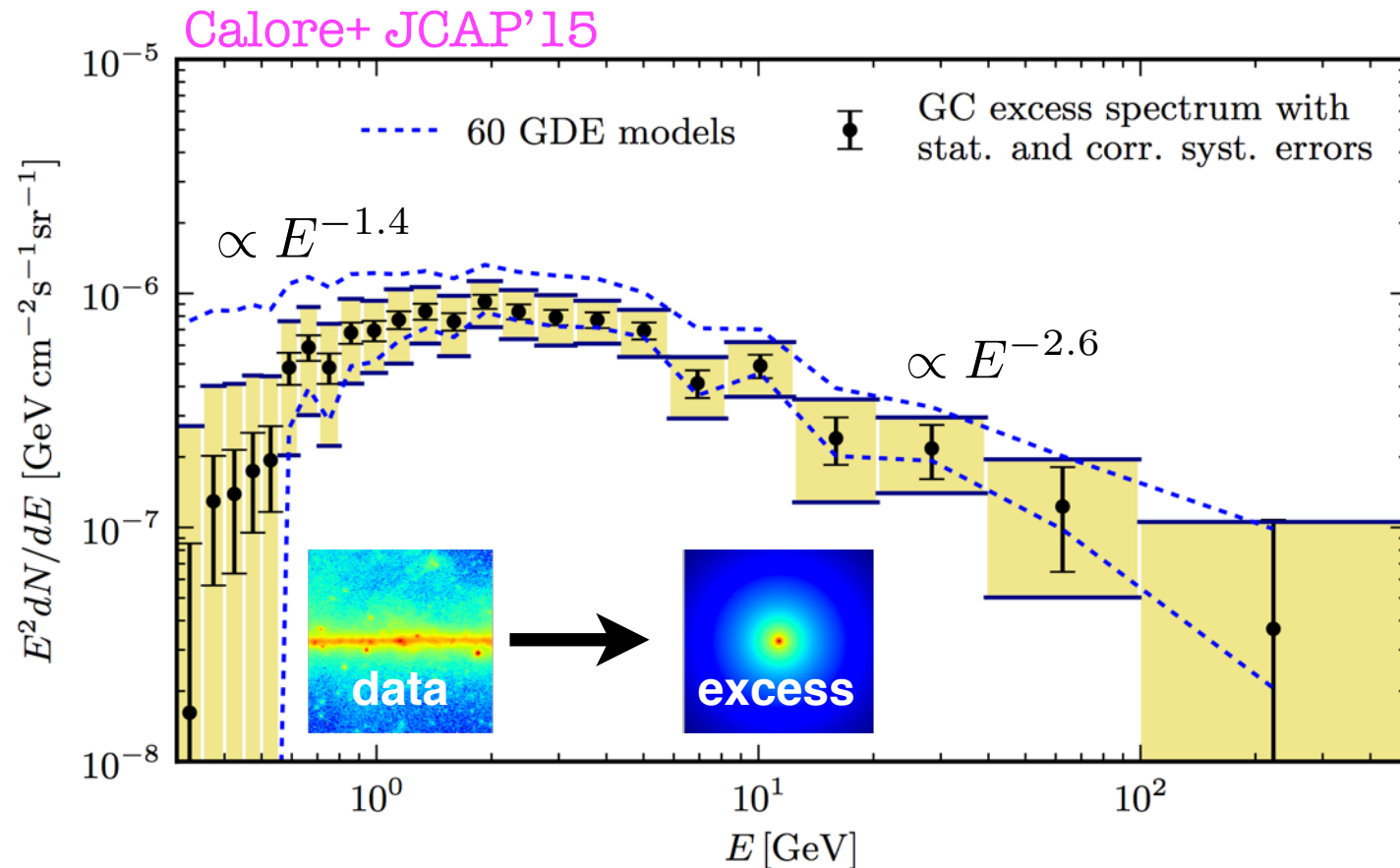
Morphology



The GeV excess in the inner Galaxy

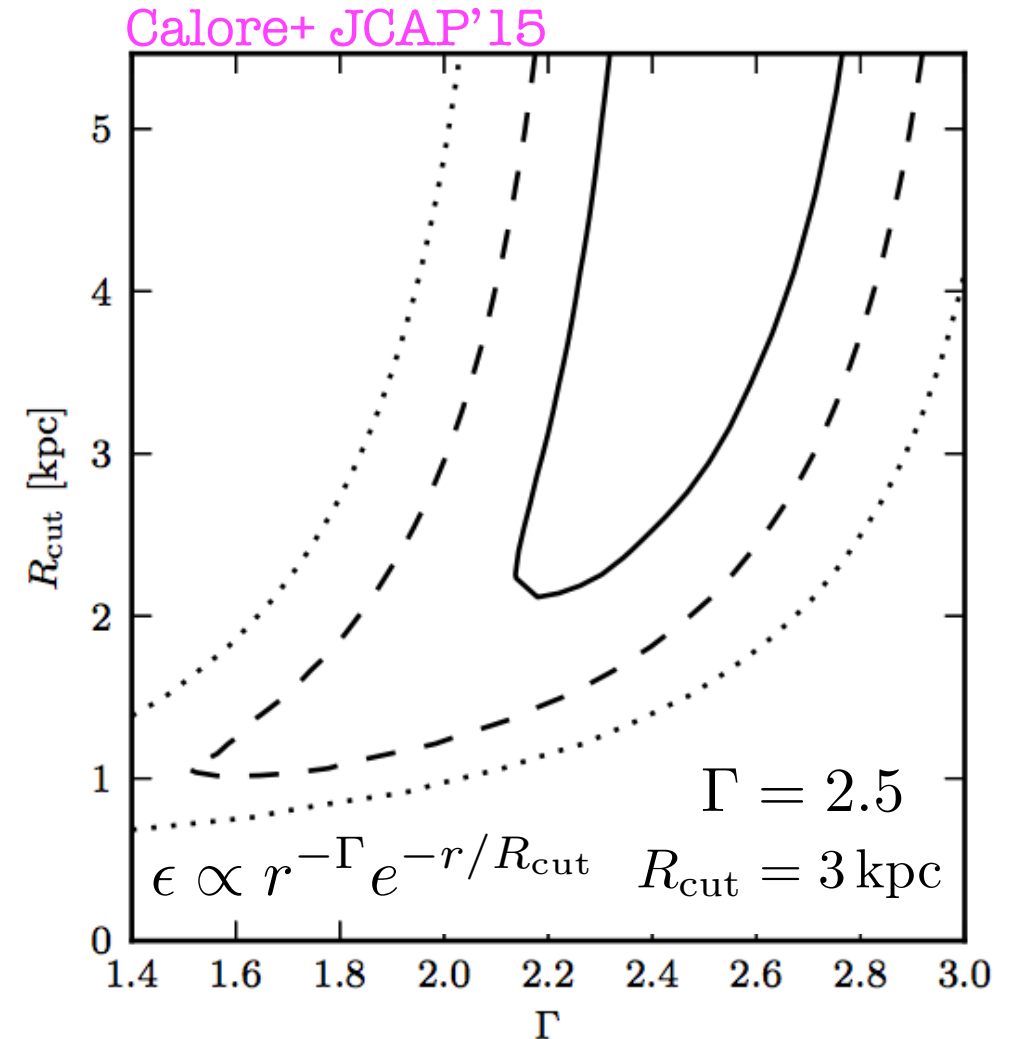
$$|\ell| \lesssim 20^\circ, \quad 2^\circ \lesssim |b| \lesssim 20^\circ$$

Spectrum



- ✓ **Stable spectrum** against background model systematics.
- ✓ Specific spectrum, **peak @ few GeV**.

Morphology

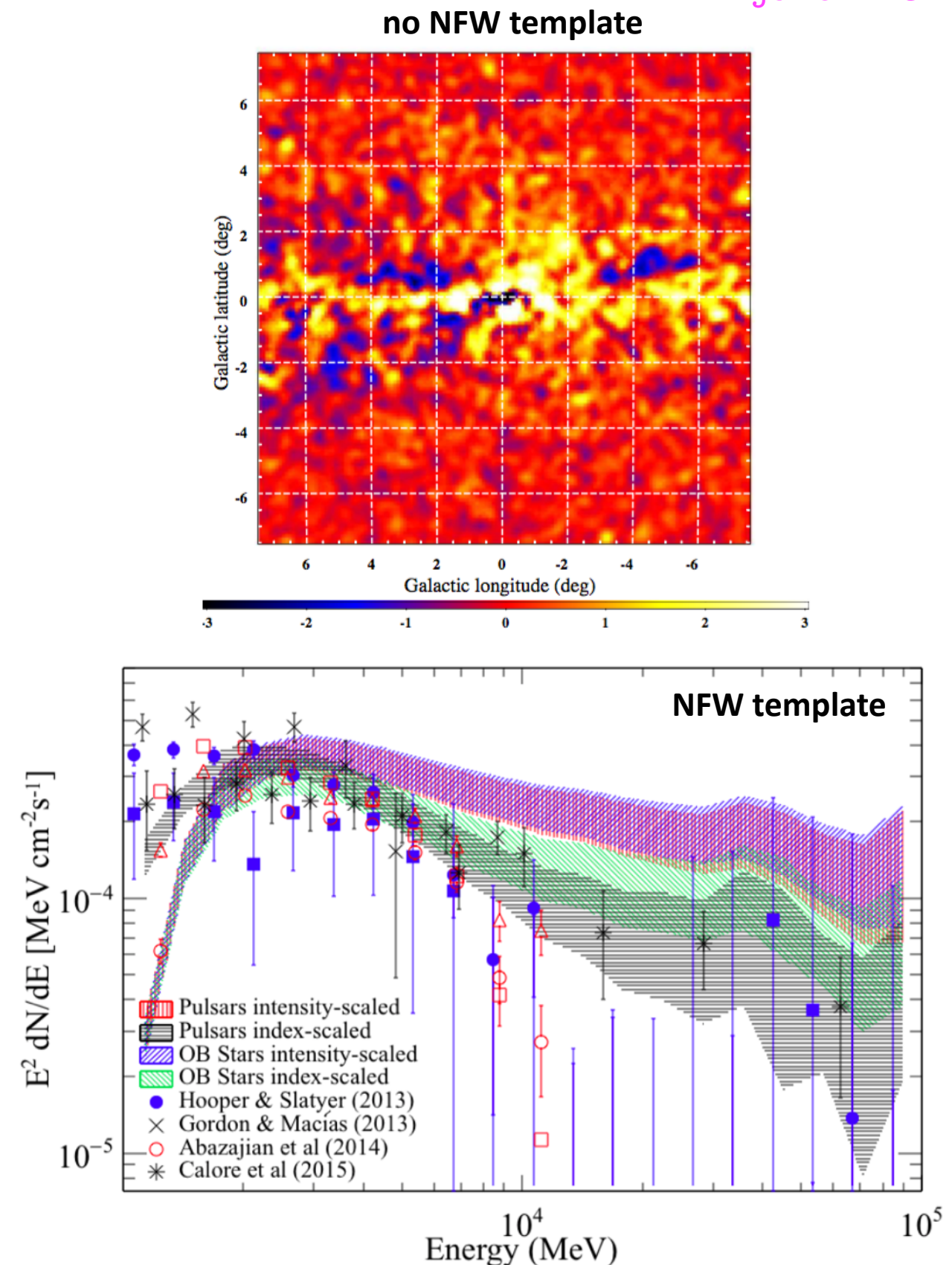


- ✓ Compatible with a spherically symmetric unique component.
- ✓ **Extended at least up to 10 degrees, 1.5 kpc**

The Fermi-LAT Collaboration analysis

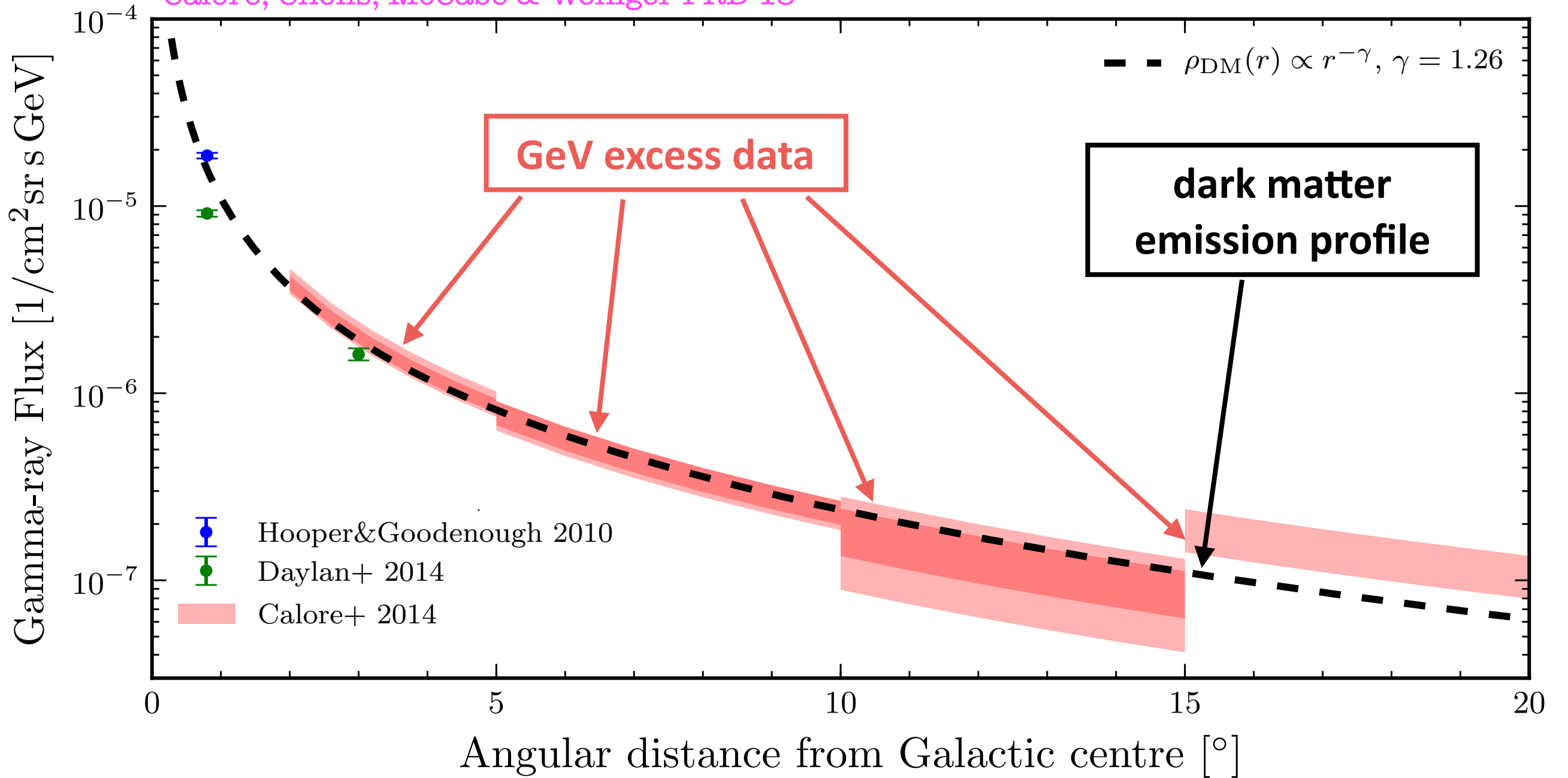
Ajello+ '15

- $15^\circ \times 15^\circ$ ROI; tuning of GDE outside \rightarrow specialised interstellar emission models.
- Wavelet transform for source identification (1FIG catalog).
- ✓ **IC emission in inner 1 kpc enhanced** w.r.to baseline prediction (20% of the total GDE emission).
- ✓ Positive residuals are left and can be partially absorbed by an **additional centrally peaked spatial template**.
- ✓ **Not all positive residuals are accounted for** by such a model.



Why is the GeV excess so exciting?

Calore, Cholis, McCabe & Weniger PRD'15

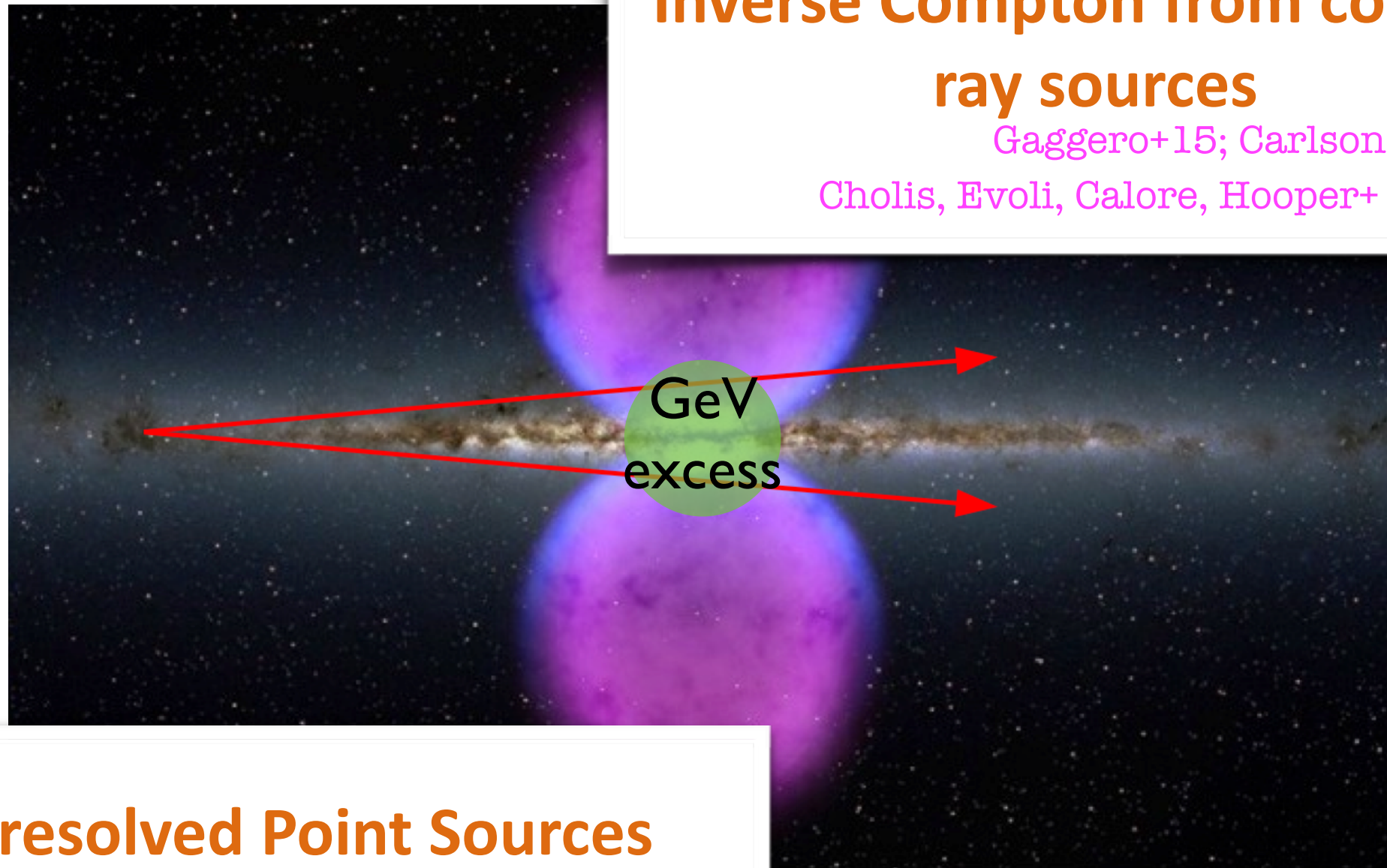


+ O(100) papers about DM interpretation

Possible astrophysical interpretations

Inverse Compton from cosmic-ray sources

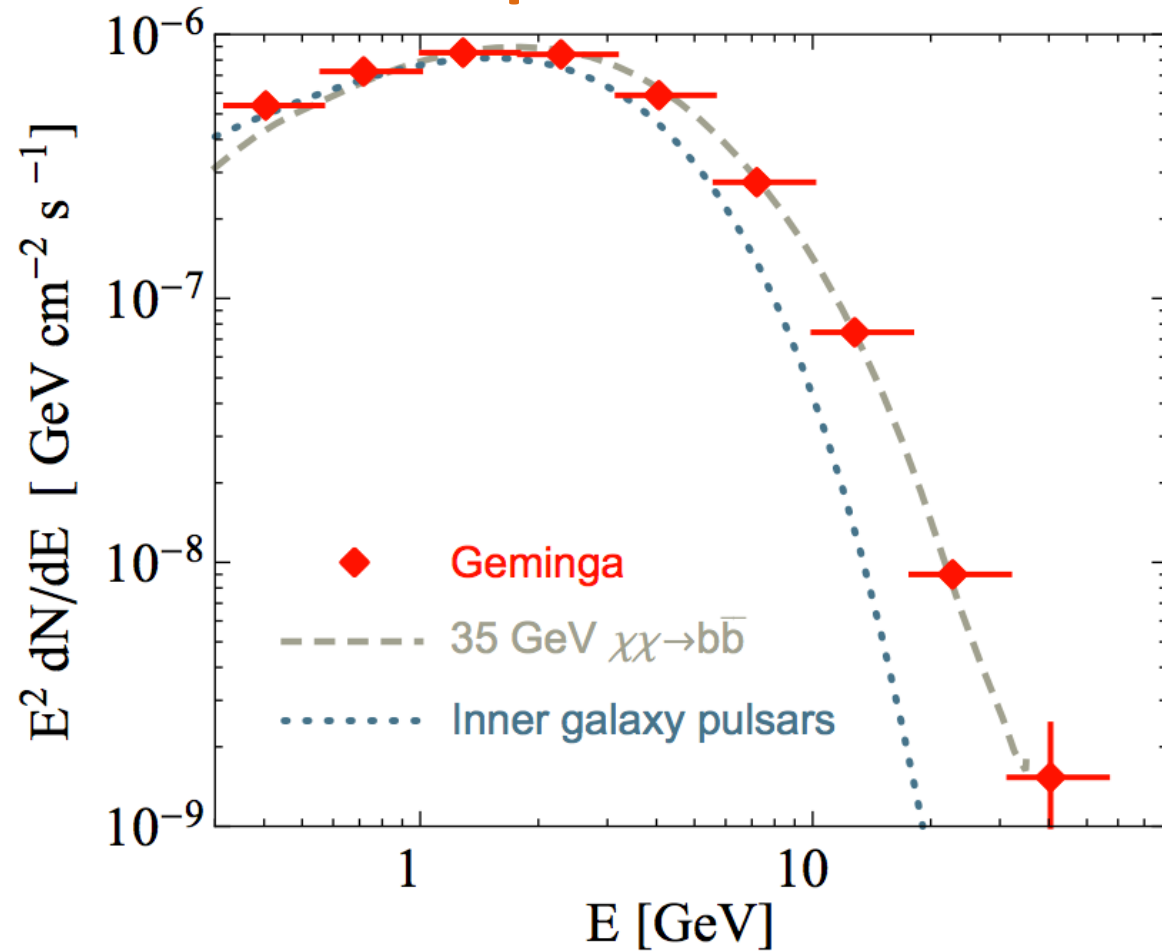
Gaggero+15; Carlson+ '15; etc
Cholis, Evoli, Calore, Hooper+ JCAP'15



Unresolved Point Sources

Unresolved pulsars and millisecond pulsars

Spectrum



- ✓ Spectrum compatible with Fermi-LAT observed **millisecond pulsars** (MSPs), and marginally **young pulsars**.

Morphology

$$\epsilon \propto r^{-\Gamma} e^{-r/R_{\text{cut}}}$$

$$\Gamma = 2.5 \quad R_{\text{cut}} = 3 \text{ kpc}$$

- ✓ Proposed population of MSPs in the bulge (vs disk).

Cholis+'14;

Petrovic+ JCAP'15; Yuang+ MNRAS'14;

- ✓ Young pulsars from SF in the CMZ.

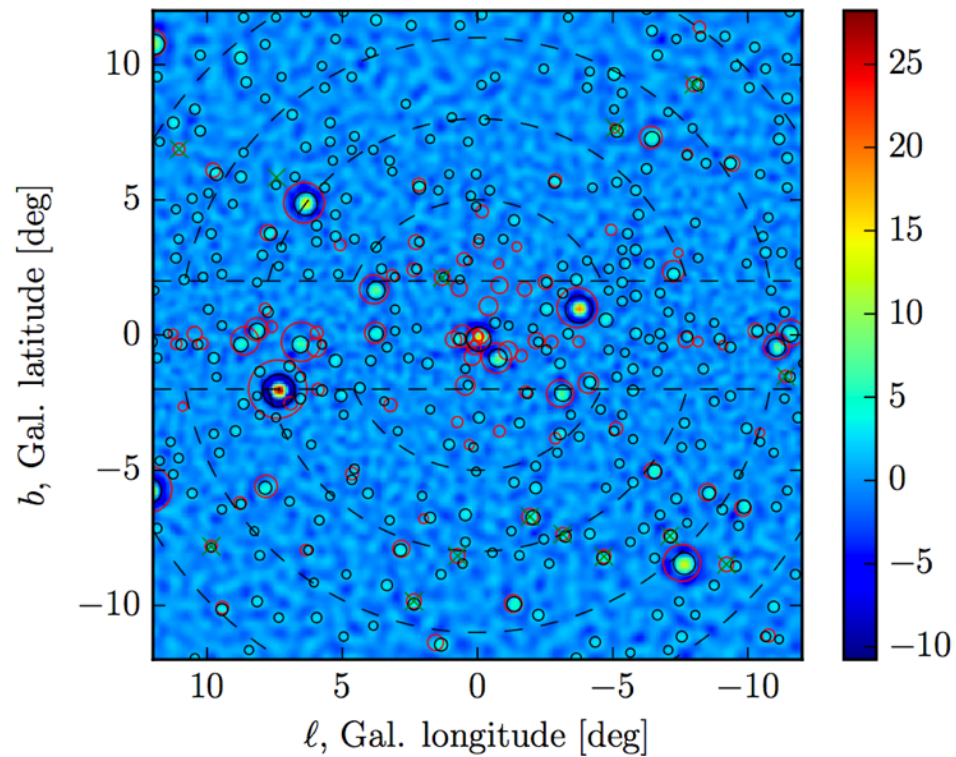
O'Leary+ '15

- ✓ Bulge MSPs: from tidally disrupted globular clusters.

Brandt&Kocsis'15

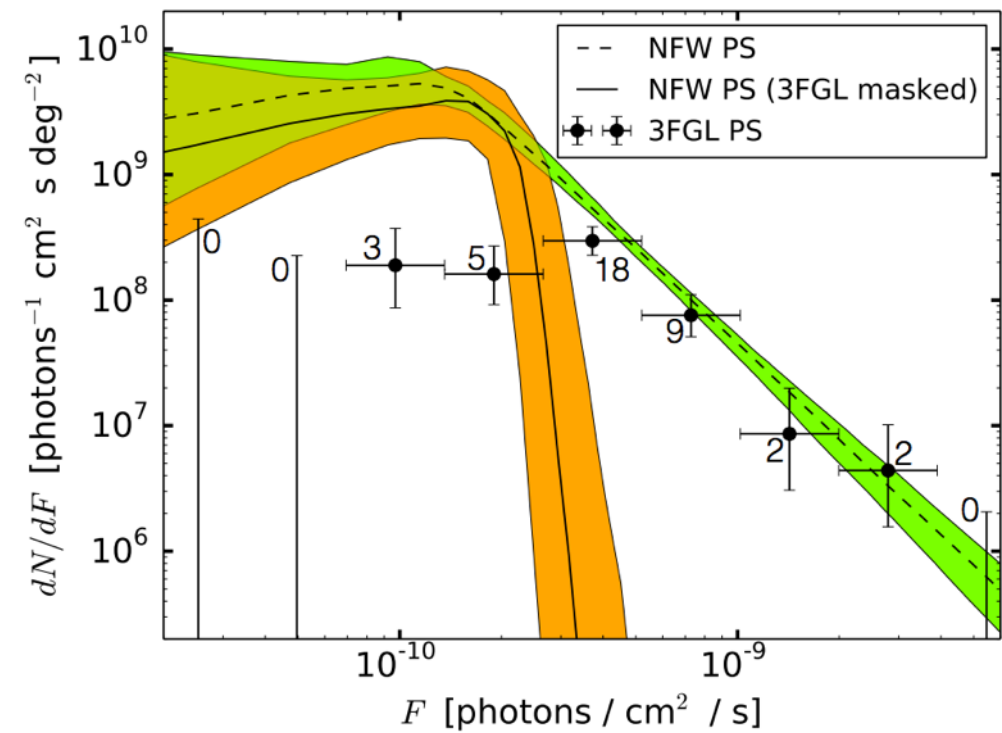
Support for MSPs interpretation

Bartels+ 15



Local maxima of normalised wavelet transform

Lee+'15



Non-Poissonian template fitting

Linden+'16

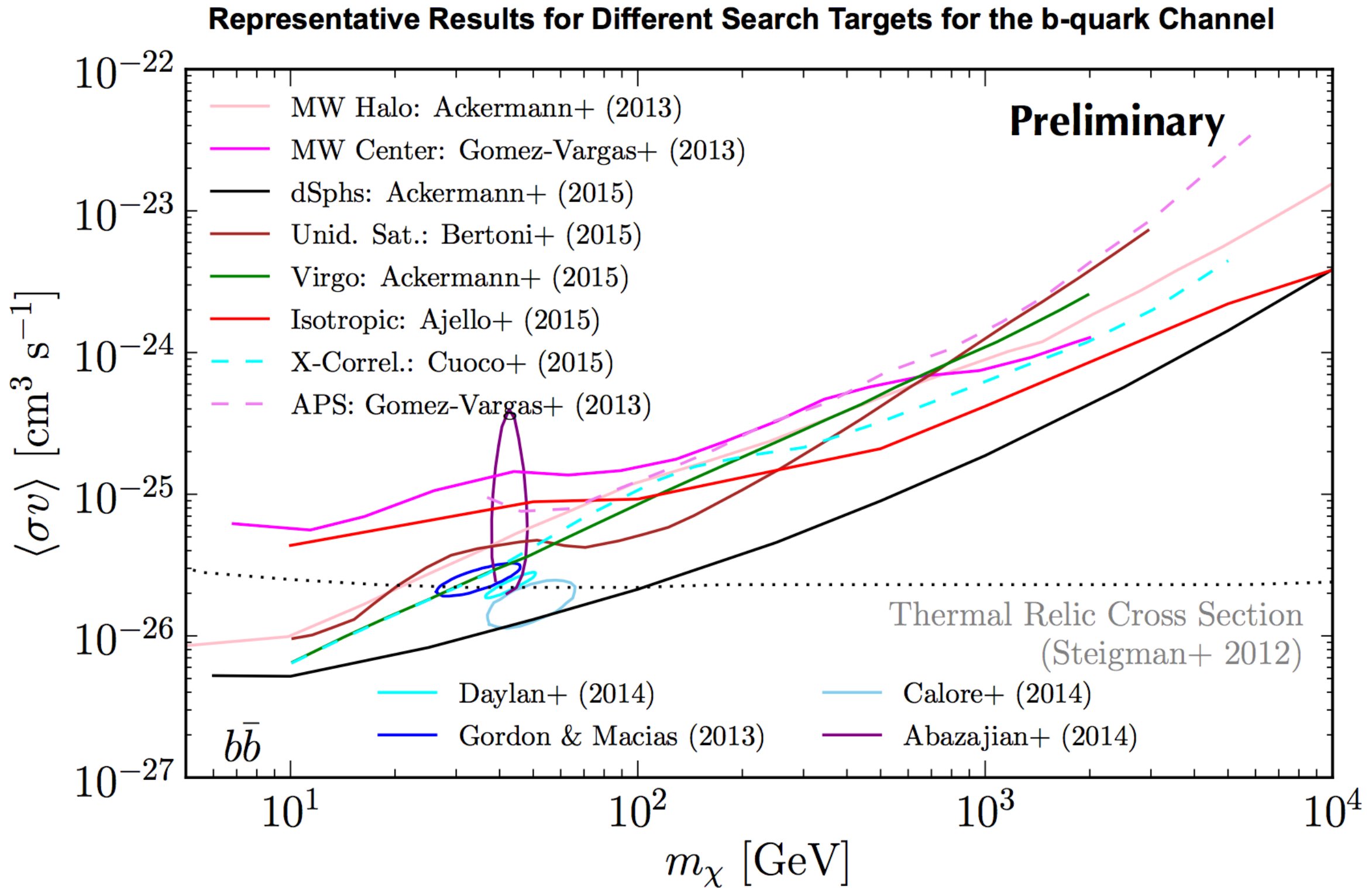
Sensitivity of future radio surveys (long-term)

Future dedicated observations can allow us to **discover the bulge MSP population.**

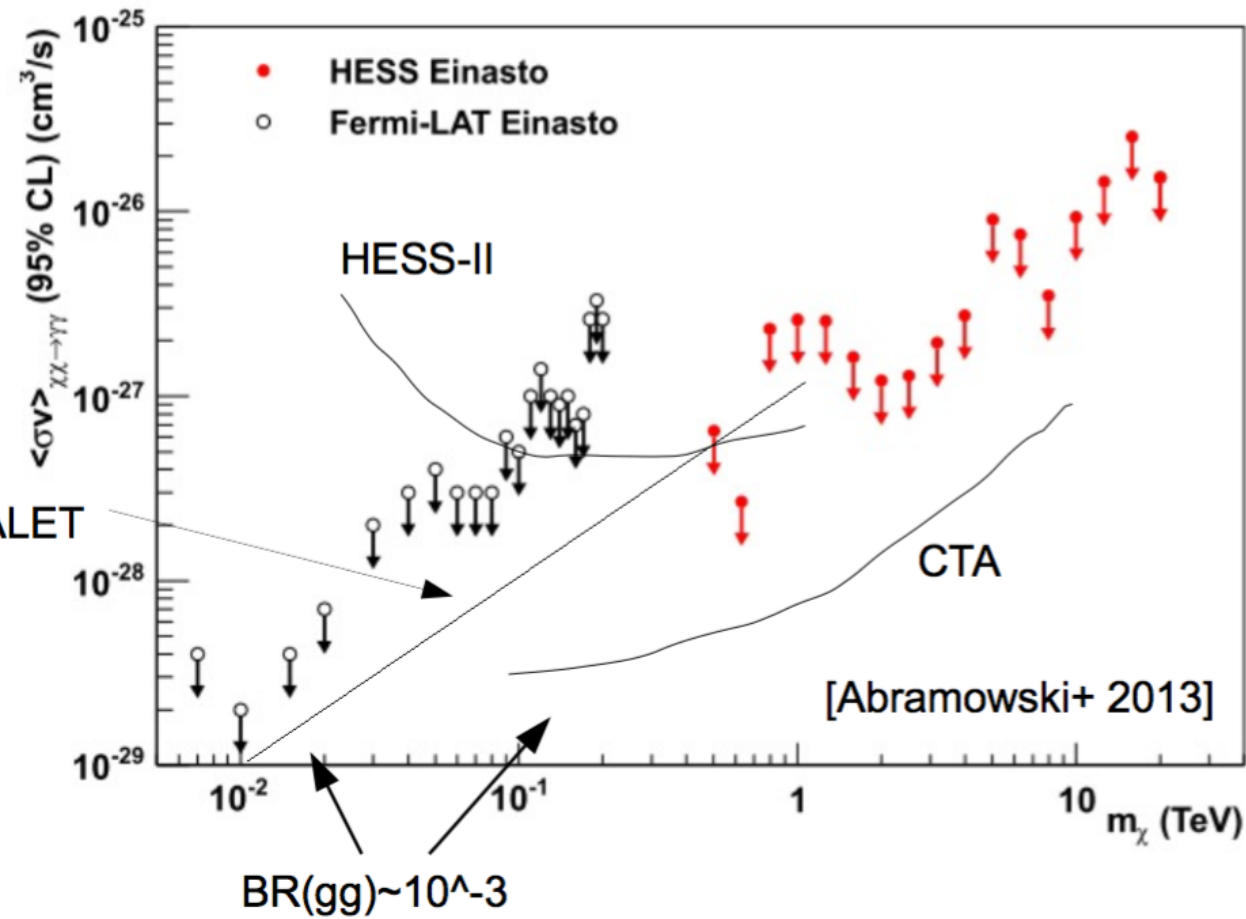


Calore, Di Mauro, Donato, Hessels & Weniger+'15
Fermi-LAT GI Proposal 2016

Other constraints from Fermi-LAT searches

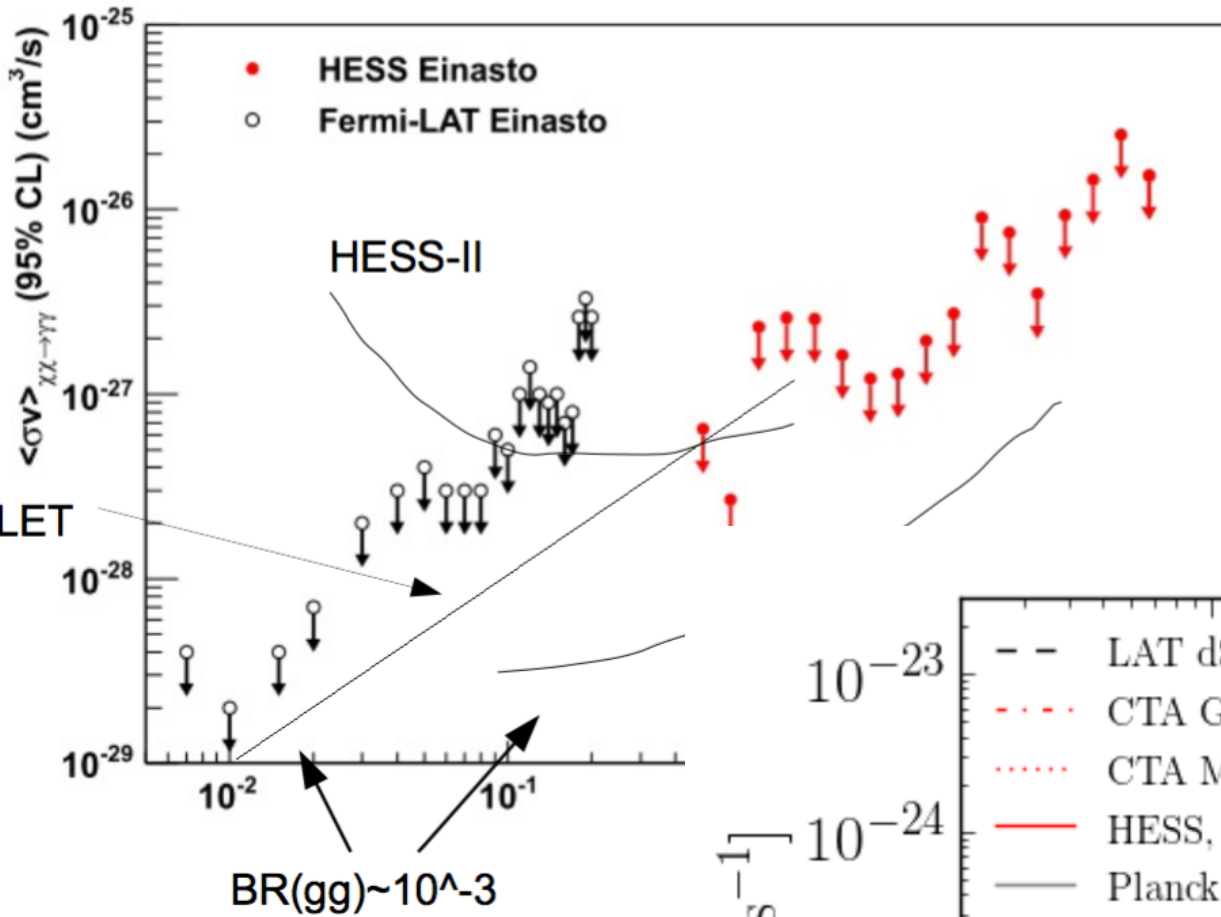


Future prospects



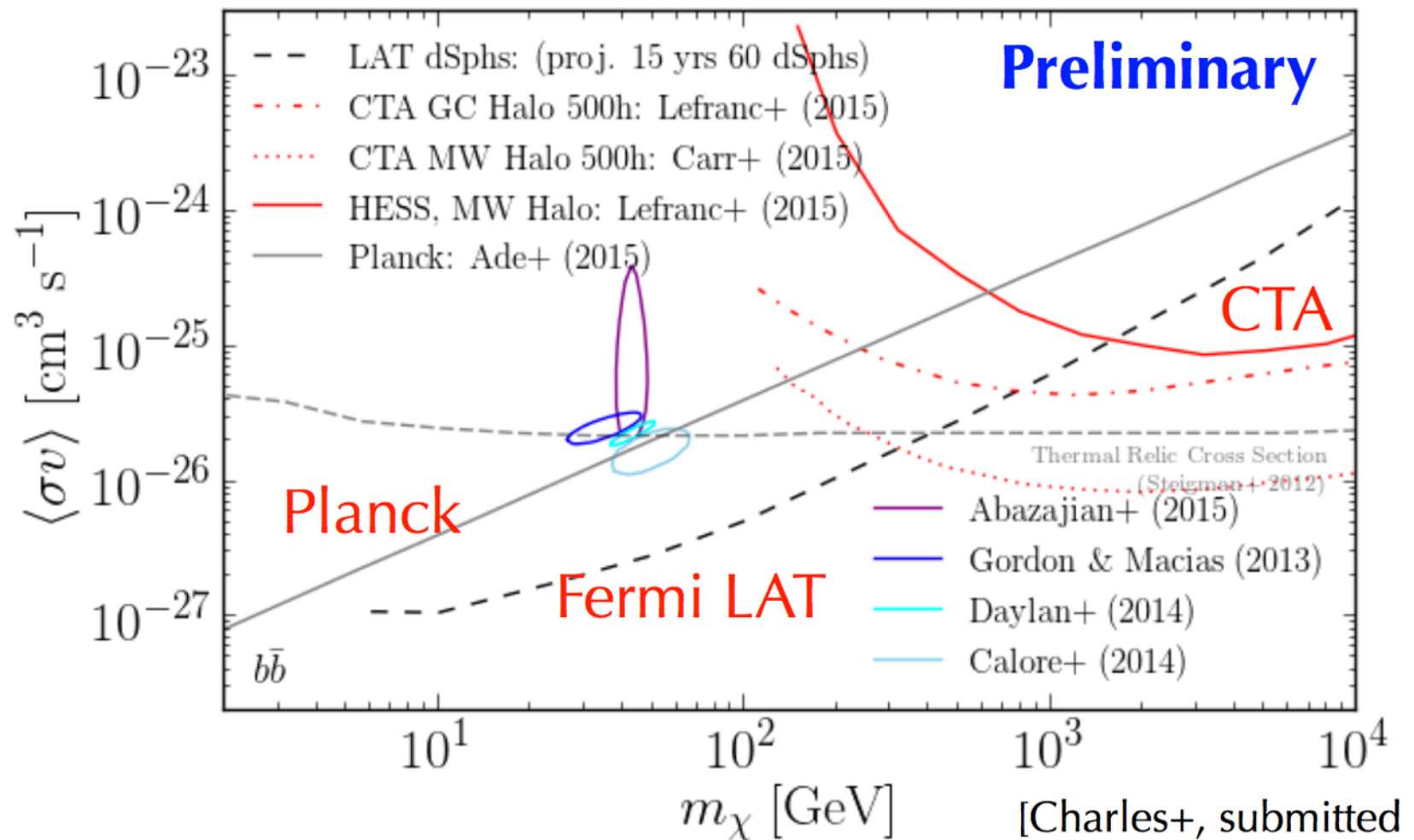
Line (spectral features)
searches

Future prospects



Line (spectral features) searches

Continuum gamma-ray targets



[Charles+, submitted to Physics Reports]

Searching for dark matter: Other messengers

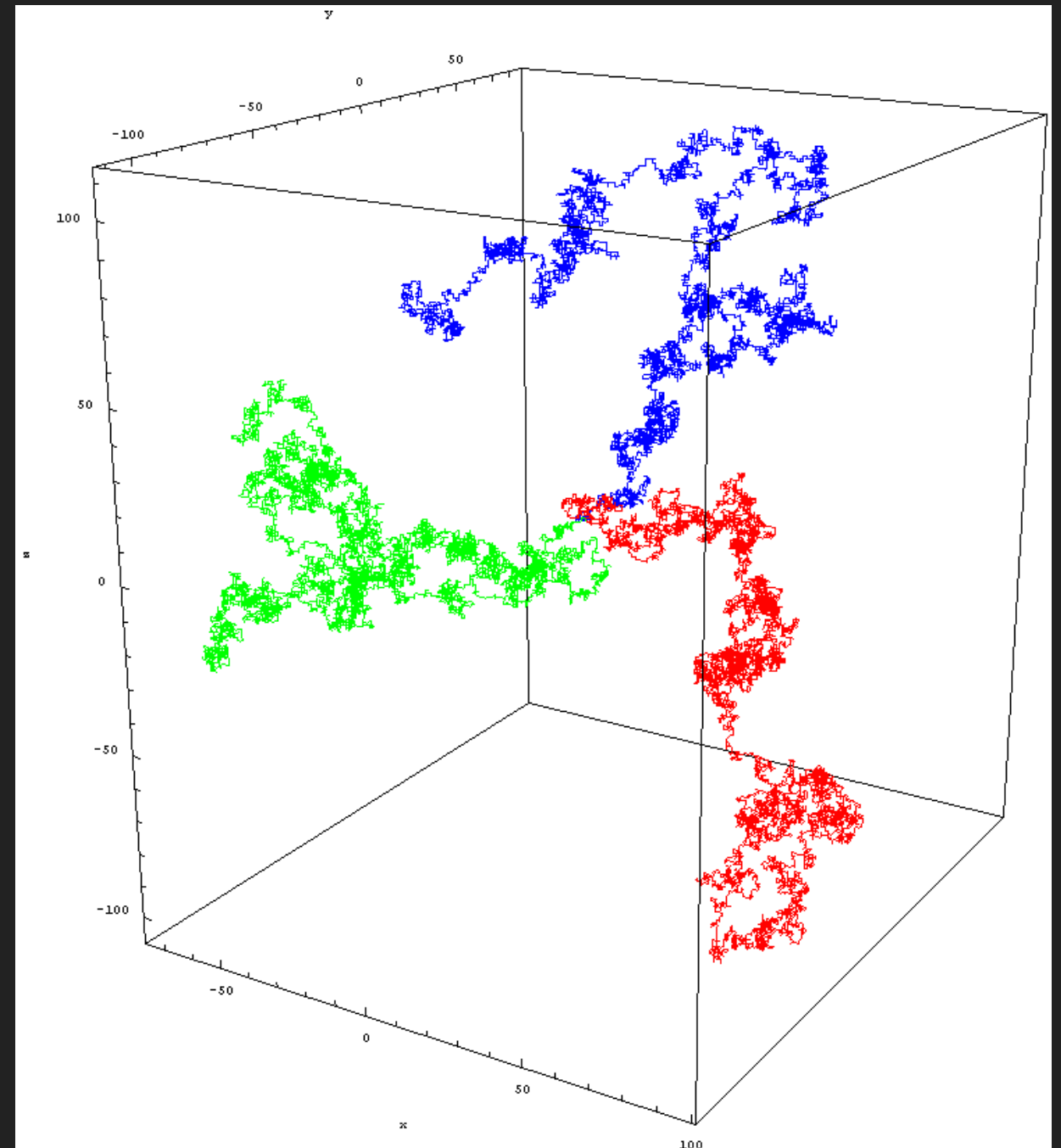
DOUBLY INDIRECT DETECTION

We can also think about the detection of electromagnetically interacting particles besides gamma-rays.

However these are either:

- 1.) Themselves charged
- 2.) Not promptly produced in the dark matter annihilation event.

In either case, we have to worry about the diffusion of energy from the dark matter annihilation event.



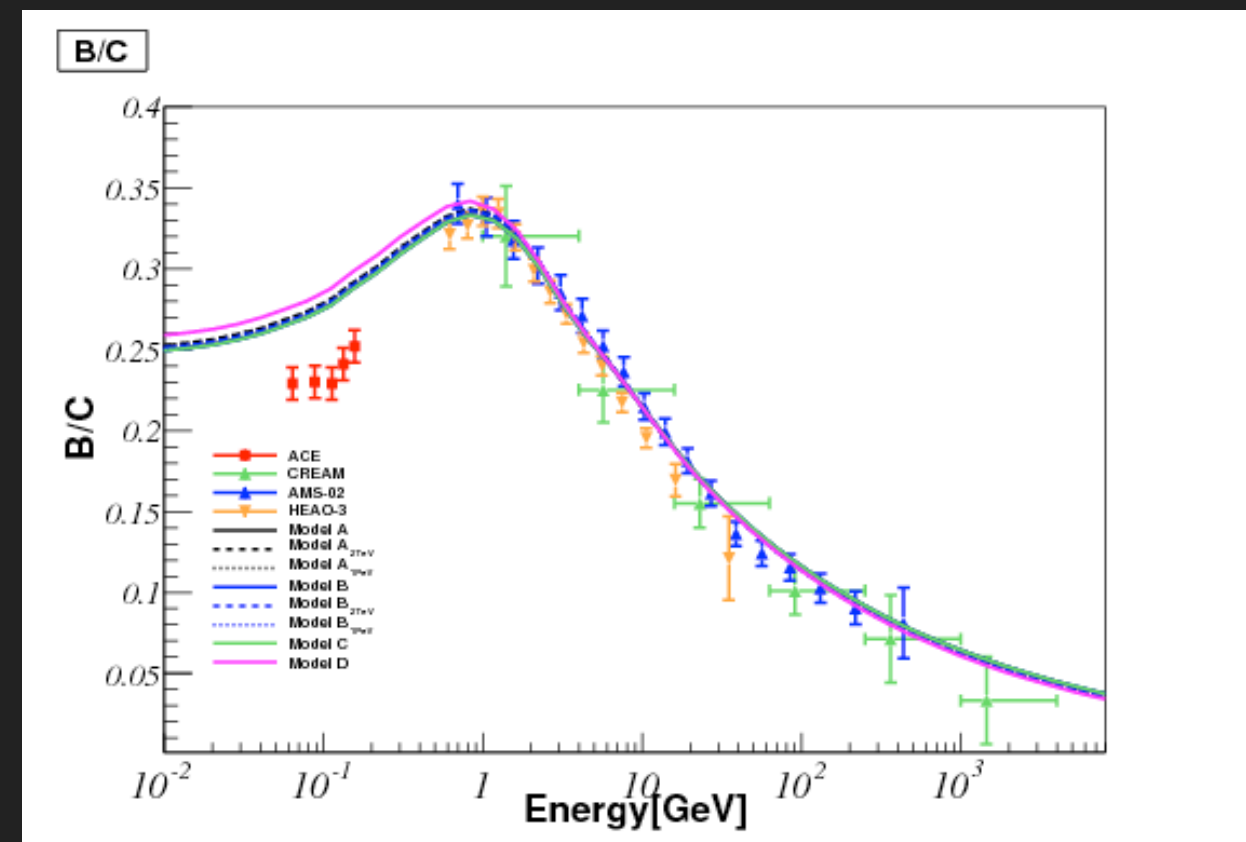
DOUBLY INDIRECT DETECTION

$$\frac{\partial f}{\partial t} = -V_{w,i} \frac{\partial f}{\partial x_i} + \frac{\partial}{\partial x_i} \kappa_{ij} \frac{\partial f}{\partial x_j} - V_{D,i} \frac{\partial f}{\partial x_i} + \frac{1}{3} \frac{\partial V_{w,i}}{\partial x_i} \frac{\partial f}{\partial \ln p} + Q$$

*advection**diffusion**drift**energy change*

Thus, we need to solve a diffusion equation in our galaxy. This is typically done with codes such as *Galprop*, or *Dragon*.

There are many free parameters in these codes, and we fix them by trying to solve for the ratio of cosmic-ray primary to secondary species in the Milky Way.

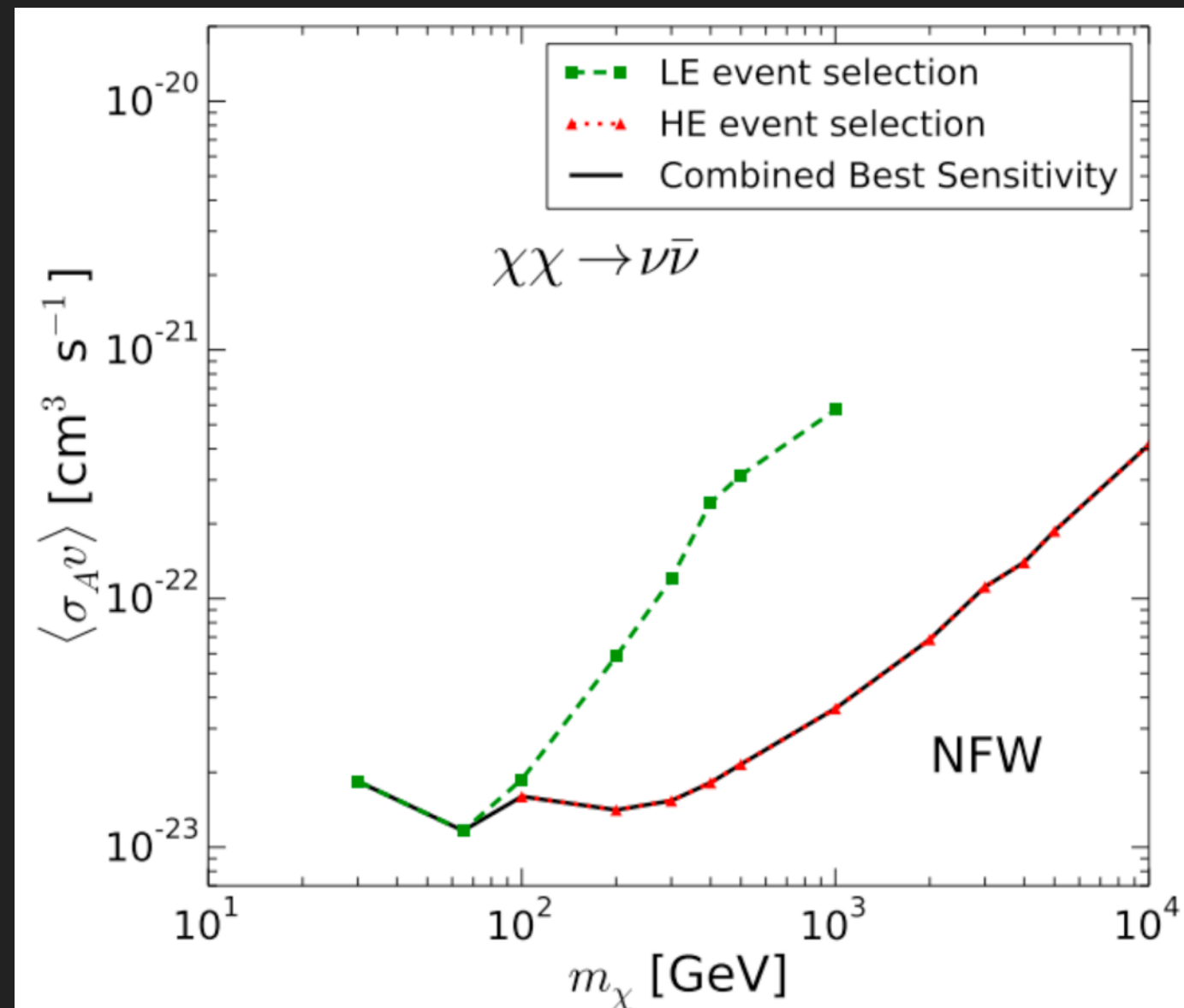


DOUBLY INDIRECT DETECTION

The mechanics of dark matter indirect detection with neutrinos are similar to those with gamma-rays.

IceCube observations take place at a much higher energy, and with a similar size instrument as Fermi ($\sim 1\text{m}^2$ effective area). Thus the constraints are significantly worse (compared to thermal).

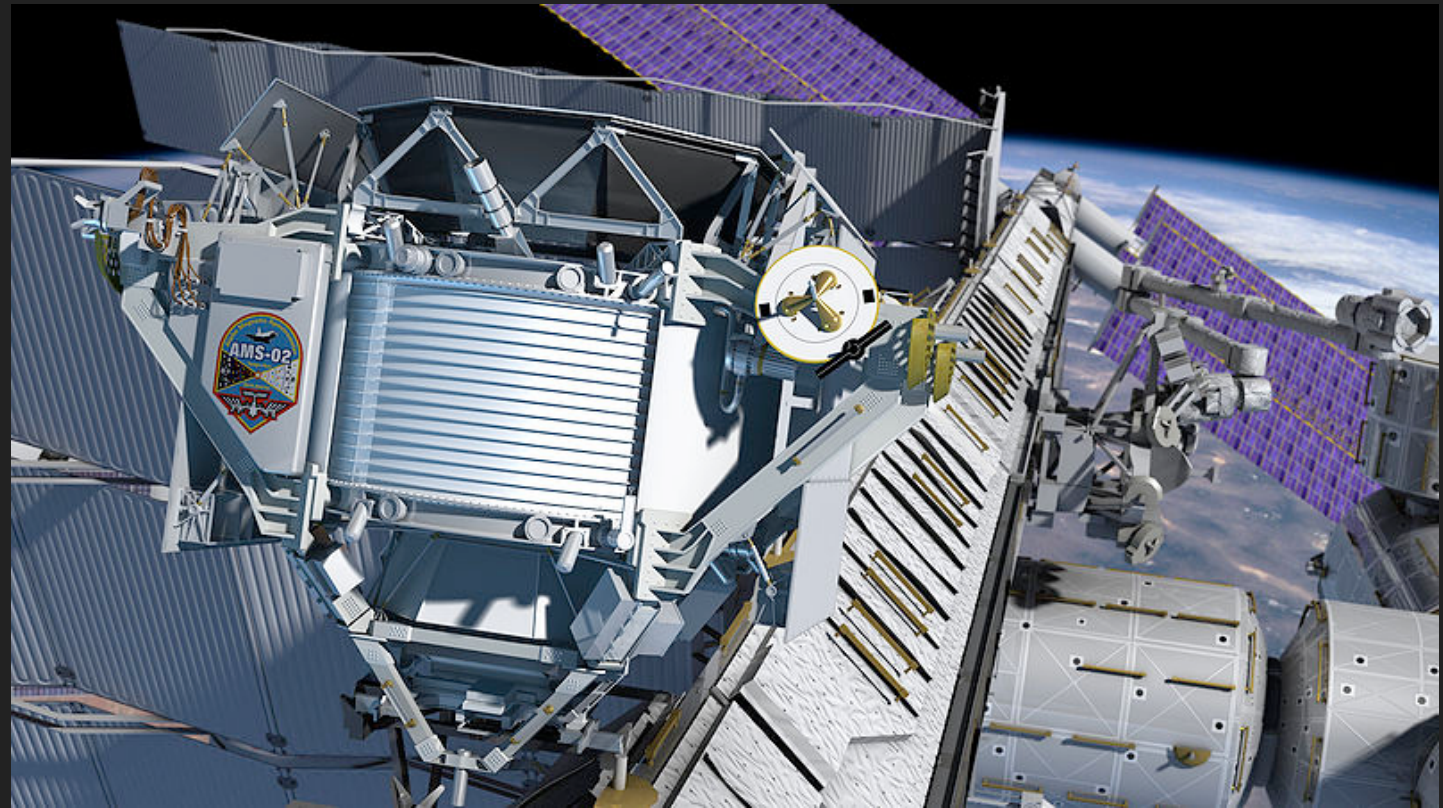
IceCube does provide competitive limits in the $XX \rightarrow \nu\bar{\nu}$ channel.



CHARGED COSMIC-RAYS



PAMELA
June 2006 –



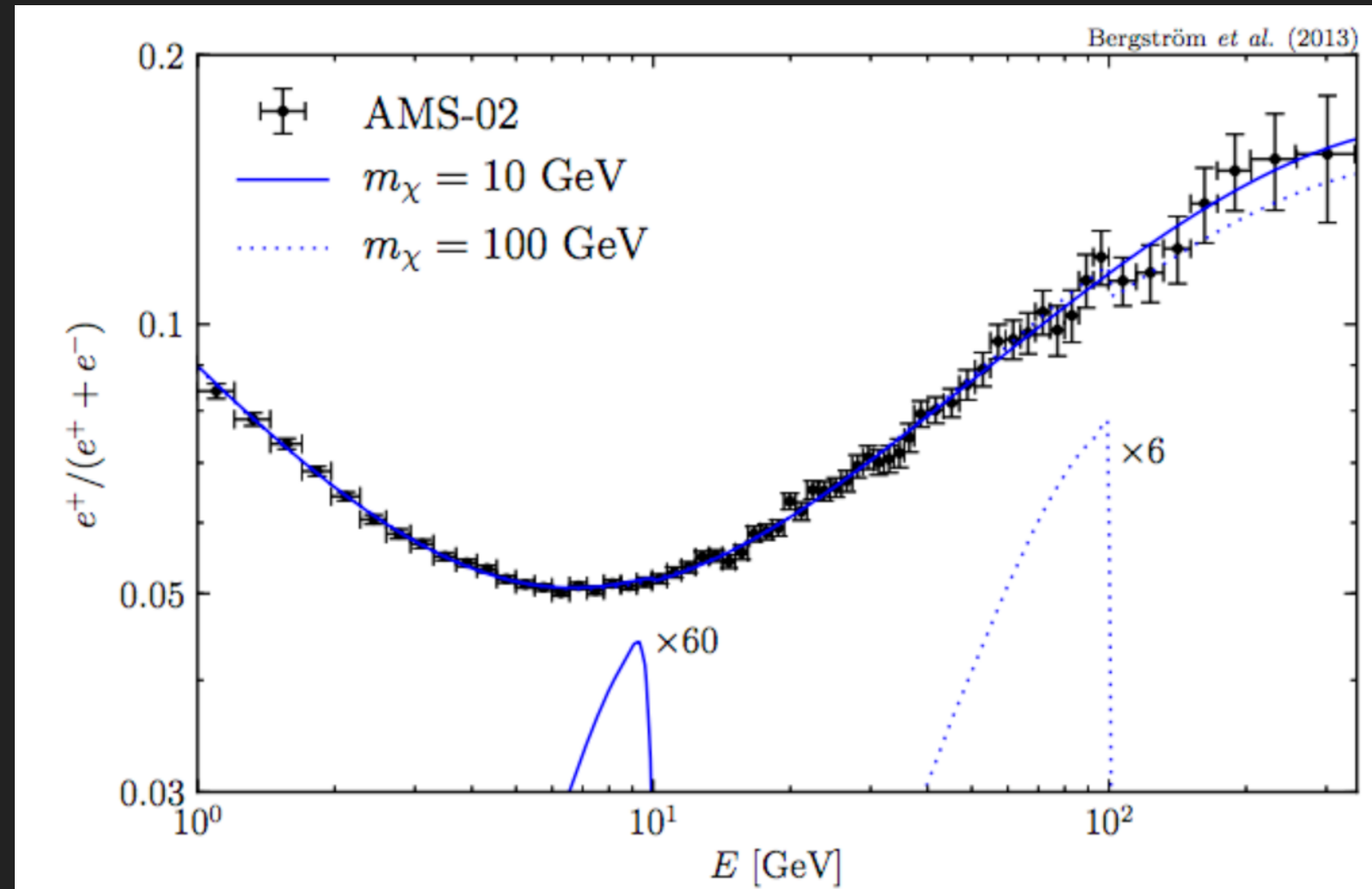
AMS-02
May 2011 –

COSMIC-RAY TARGETS

A particularly effective method is to look for bumps in the cosmic-ray particle/anti-particle ratio.

Astrophysical uncertainties can be constrained by using information from the energy sidebands.

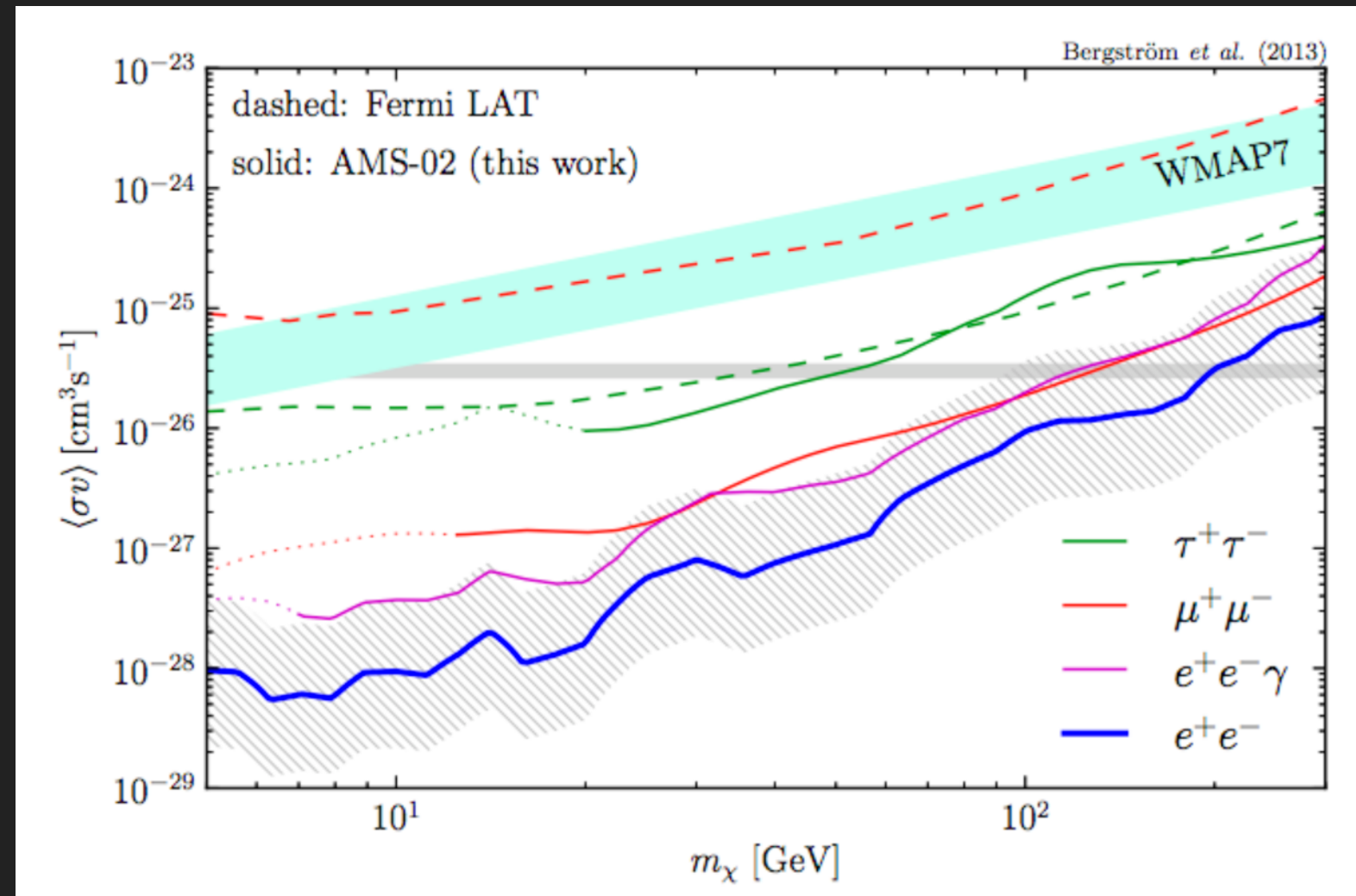
This is particularly effective for leptophilic dark matter candidates, since the electron energy is highly peaked. Also, results are most sensitive to electrons formed locally.



Bergstrom et al. (2013)

COSMIC-RAY TARGETS

For annihilation directly to electron/positron pairs, these constraints rule out dark matter at the thermal annihilation cross-section to masses ~ 200 GeV.



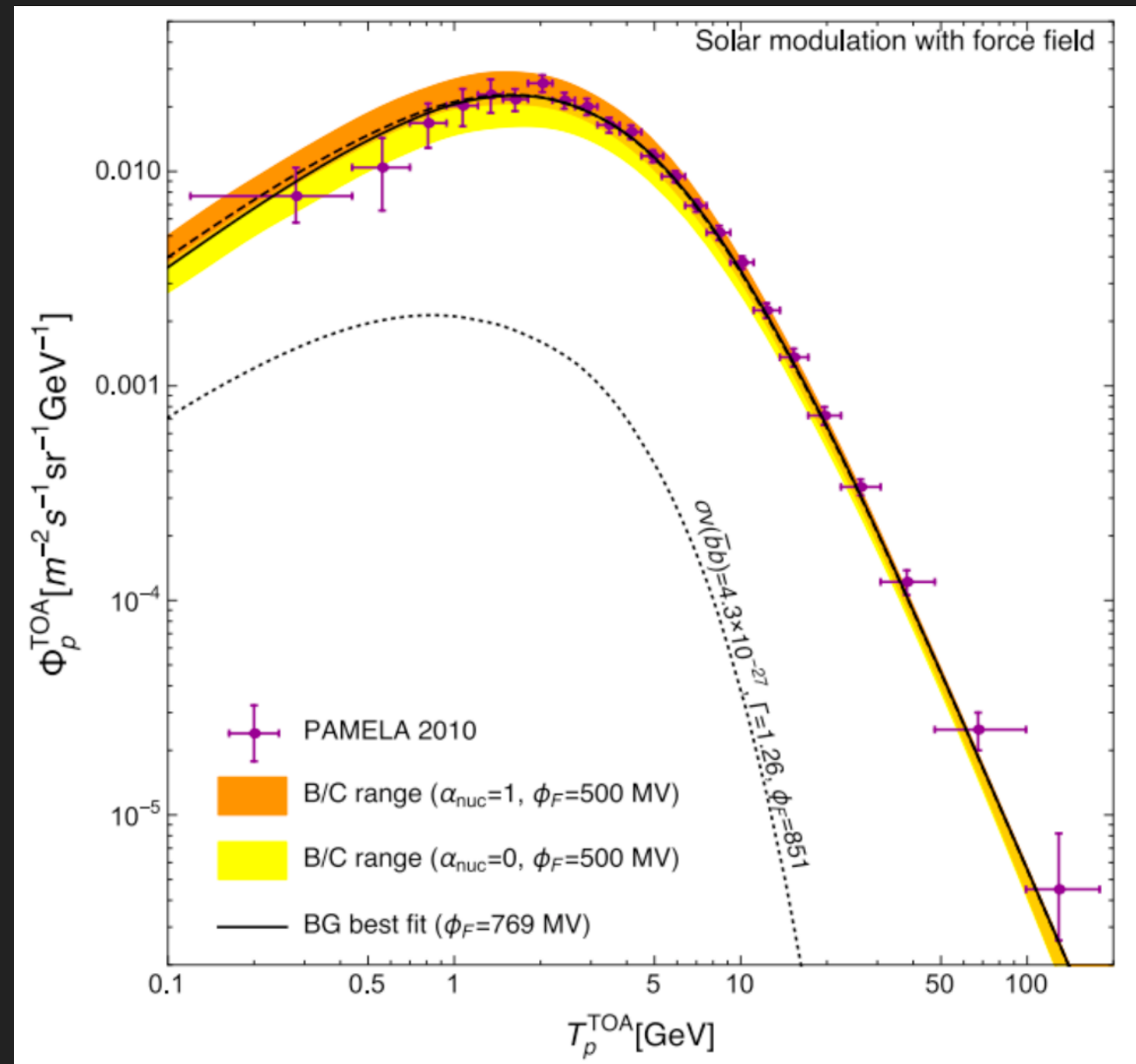
Bergstrom et al. (2013)

Constraints will continue to improve as AMS-02 data is collected (models hide in the statistical uncertainties in the positron fraction.)

COSMIC-RAY TARGETS

In the case of the antiproton flux, the bump is significantly wider, making the astrophysical background determination more important.

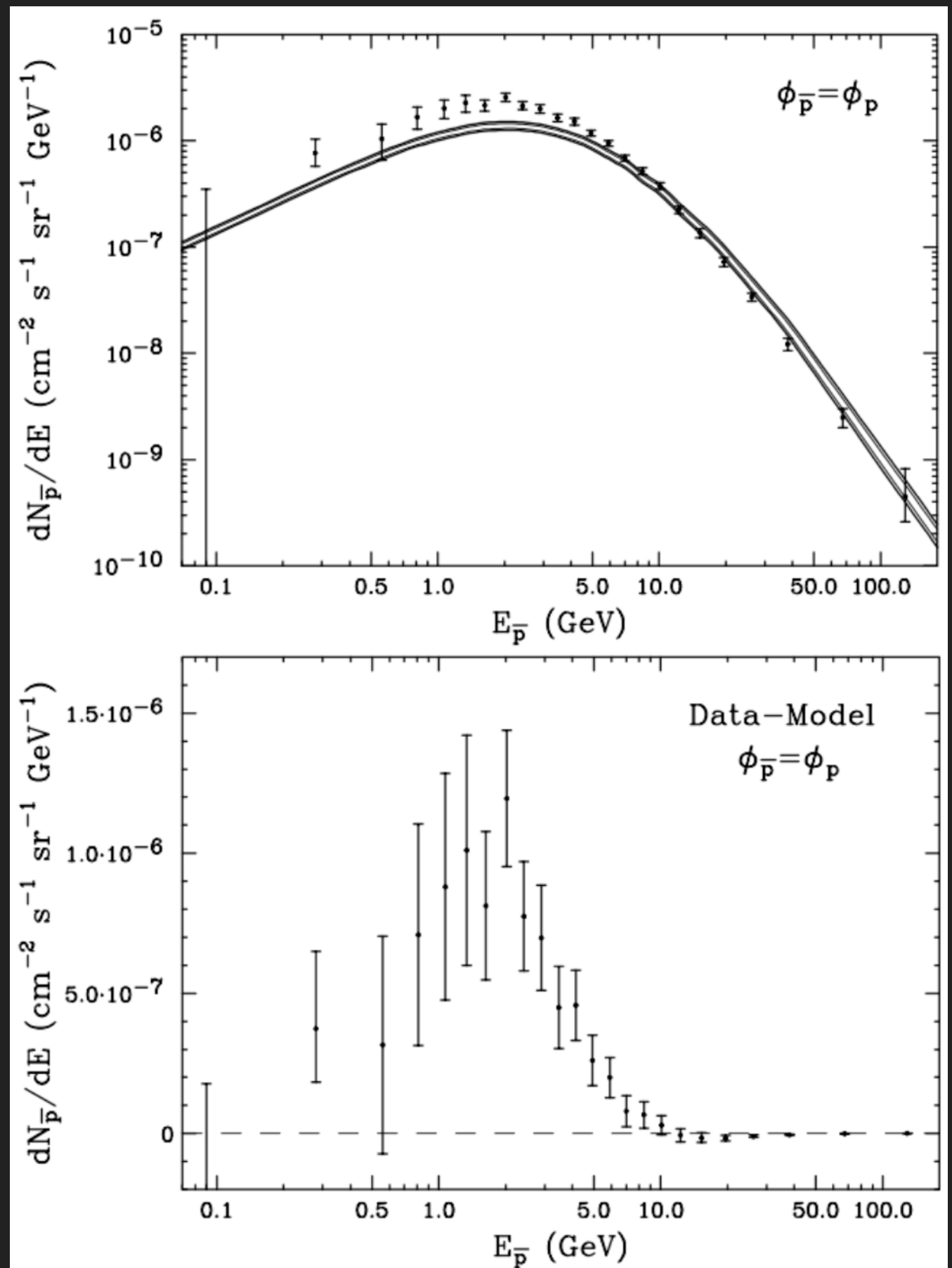
Moreover, because protons do not cool rapidly, models are sensitive to proton production and diffusion across the entire Galaxy.



COSMIC-RAY TARGETS

In the case of the antiproton flux, the bump is significantly wider, making the astrophysical background determination more important.

Moreover, because protons do not cool rapidly, models are sensitive to proton production and diffusion across the entire Galaxy.



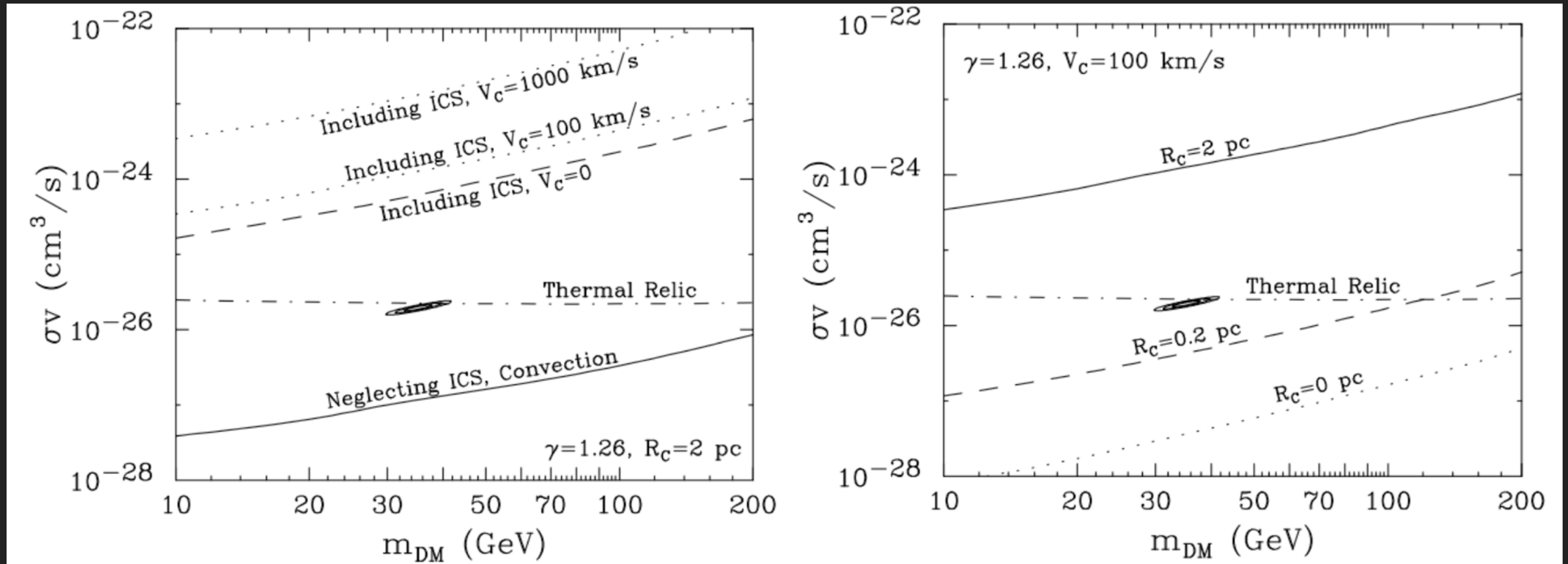
DOUBLY INDIRECT DETECTION

RADIO TARGETS



Galactic Center - Impressive Angular Resolution in Radio

RADIO TARGETS

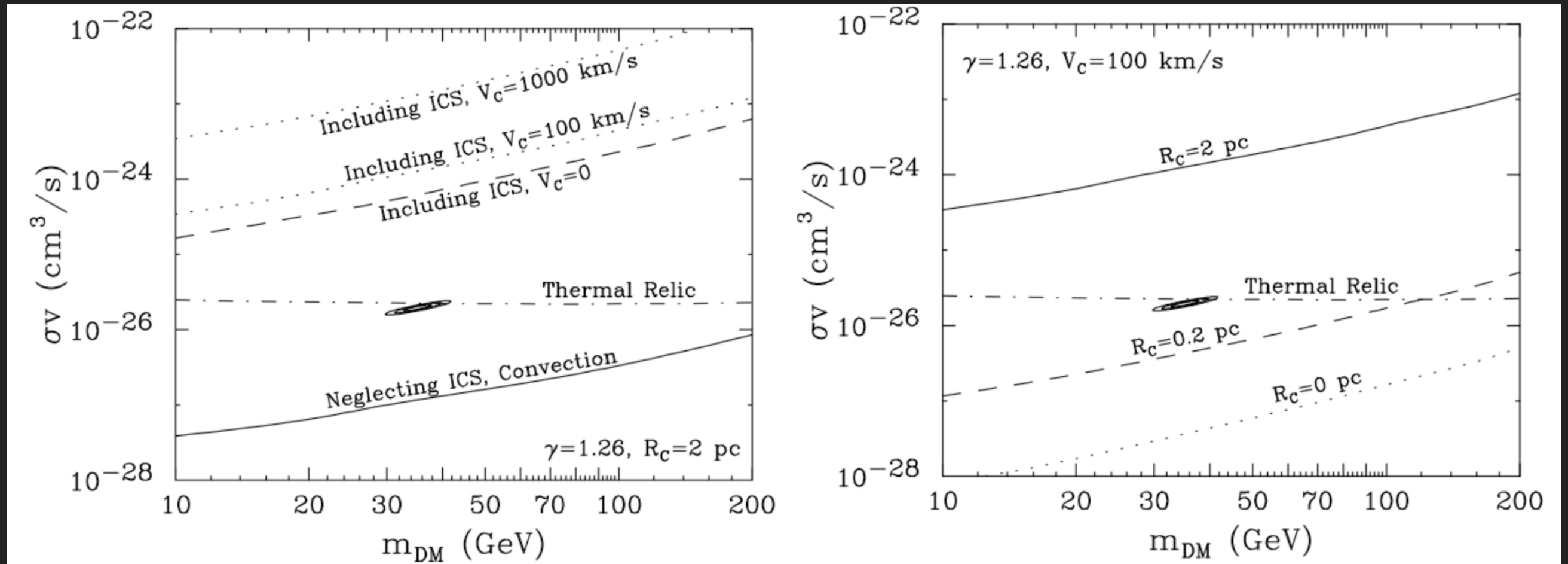


Cholis, Hooper, TL (2015)

Three Major Uncertainties:

- 1.) The ratio of the magnetic field and ISRF energy densities.
- 2.) The strength of the convective wind.
- 3.) The dark matter density profile.

RADIO TARGETS

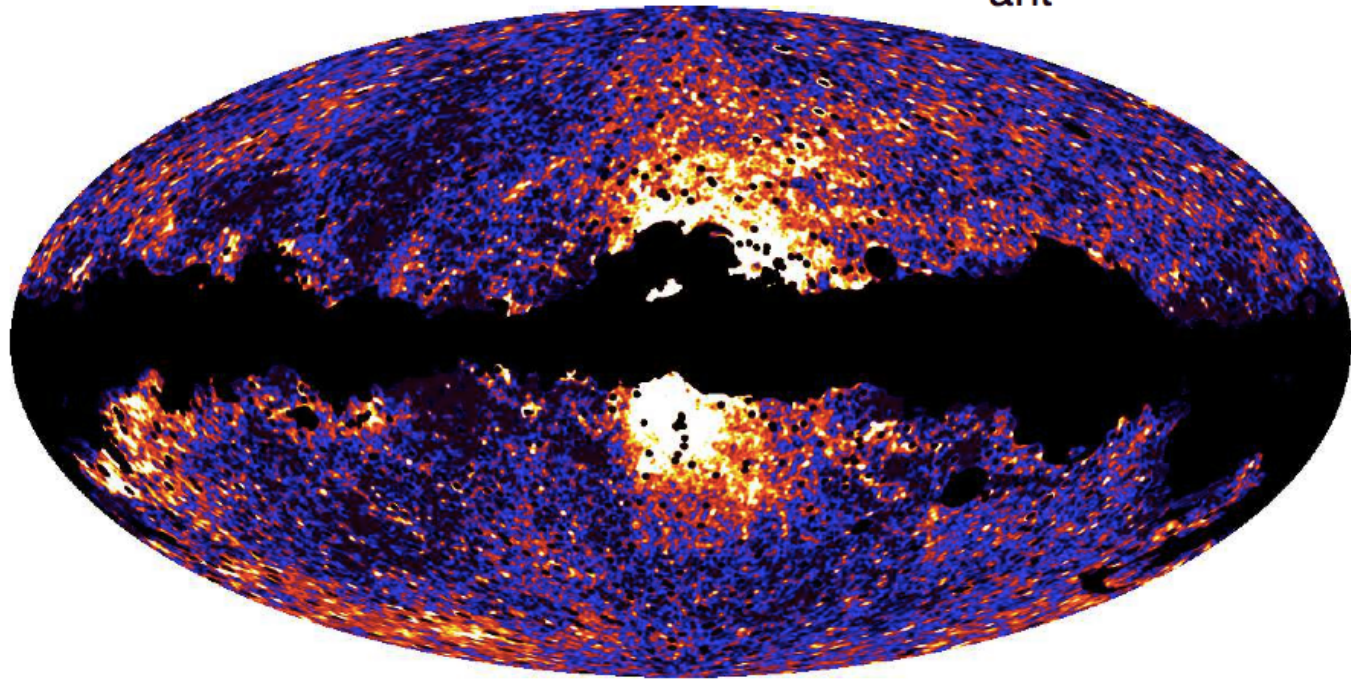


Cholis, Hooper, TL (2015)

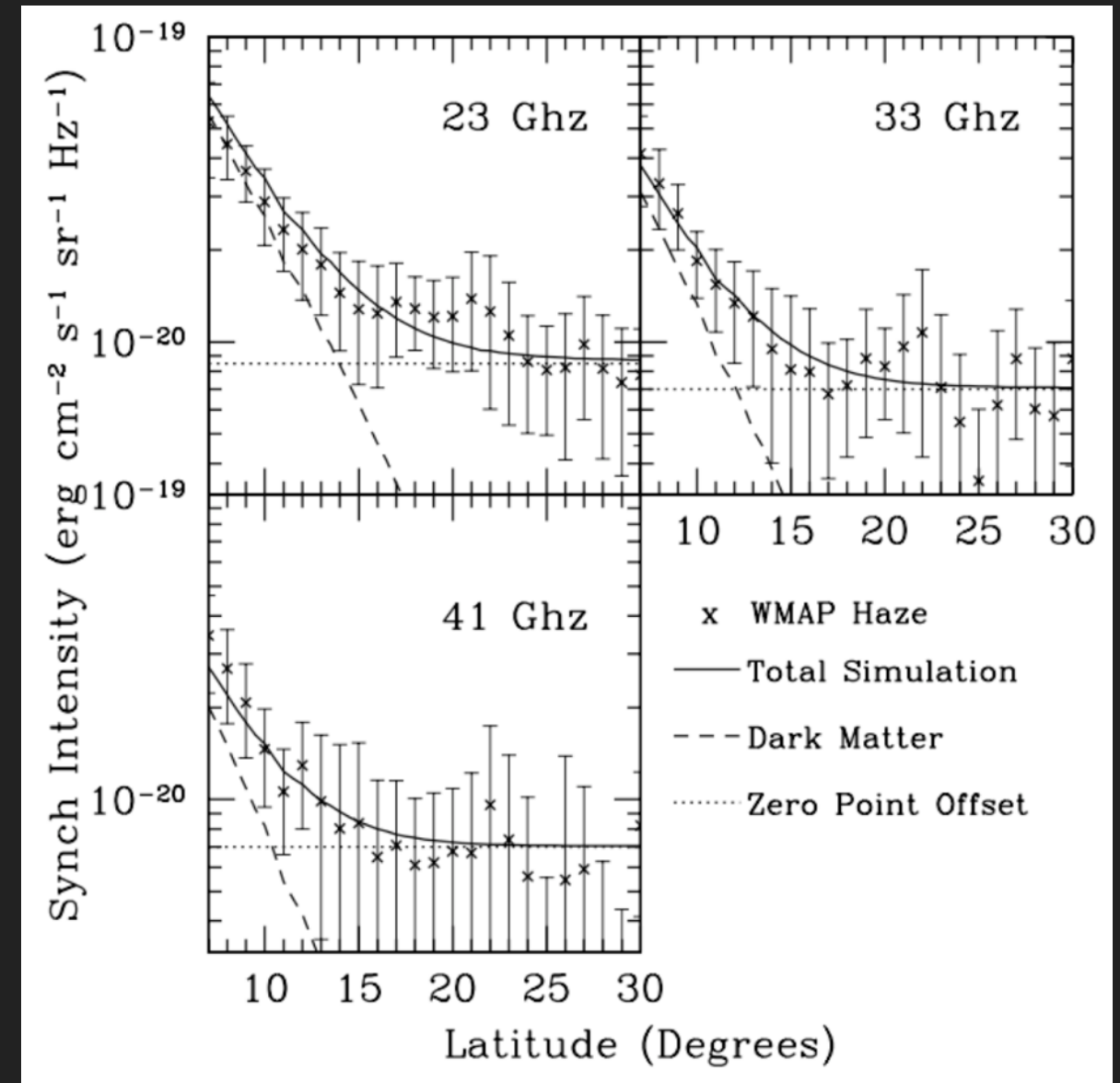
It is difficult to imagine that all of these uncertainties will be suitably controlled in the near future, to the extent that limits from dark matter induced synchrotron emission near the Galactic center will provide the most stringent limits.

RADIO TARGETS

WMAP K-band $T_{\text{ant}}^{\text{K}}$



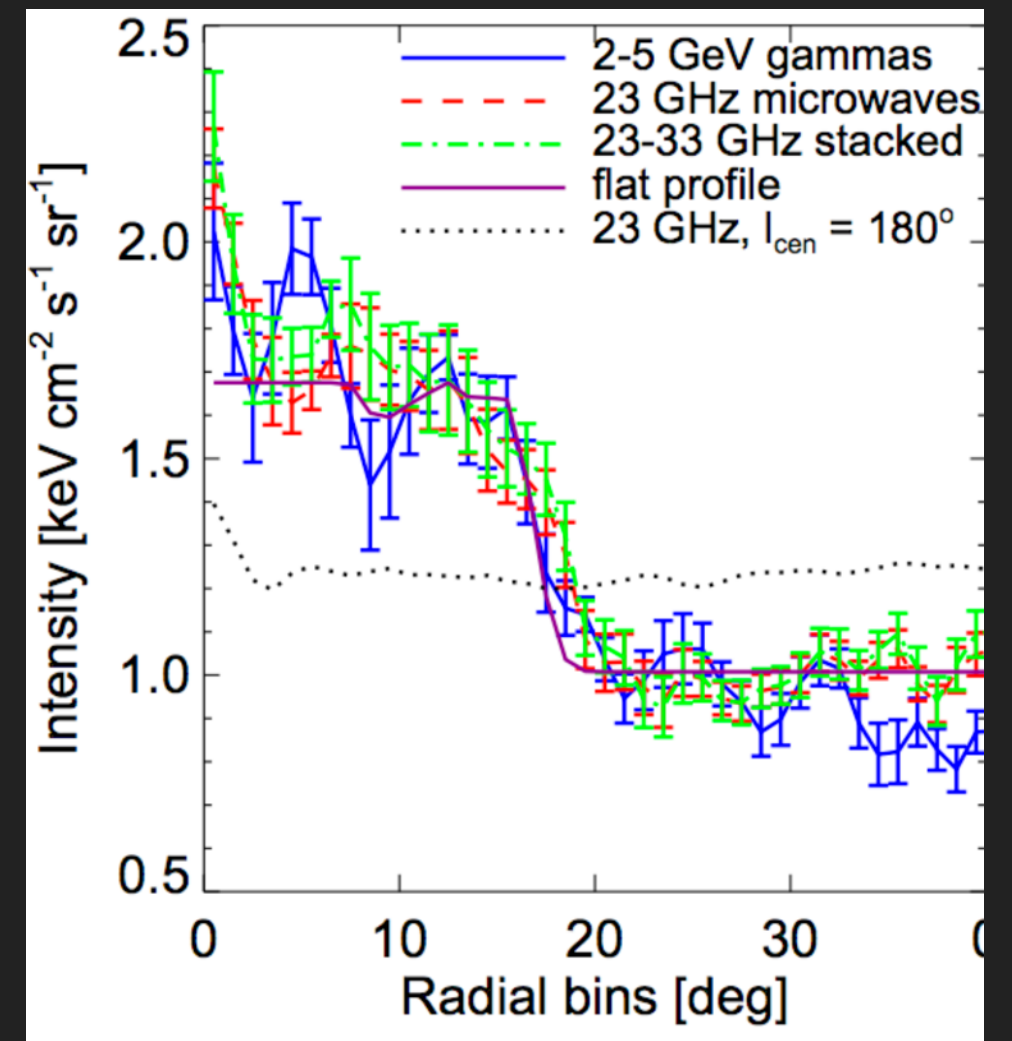
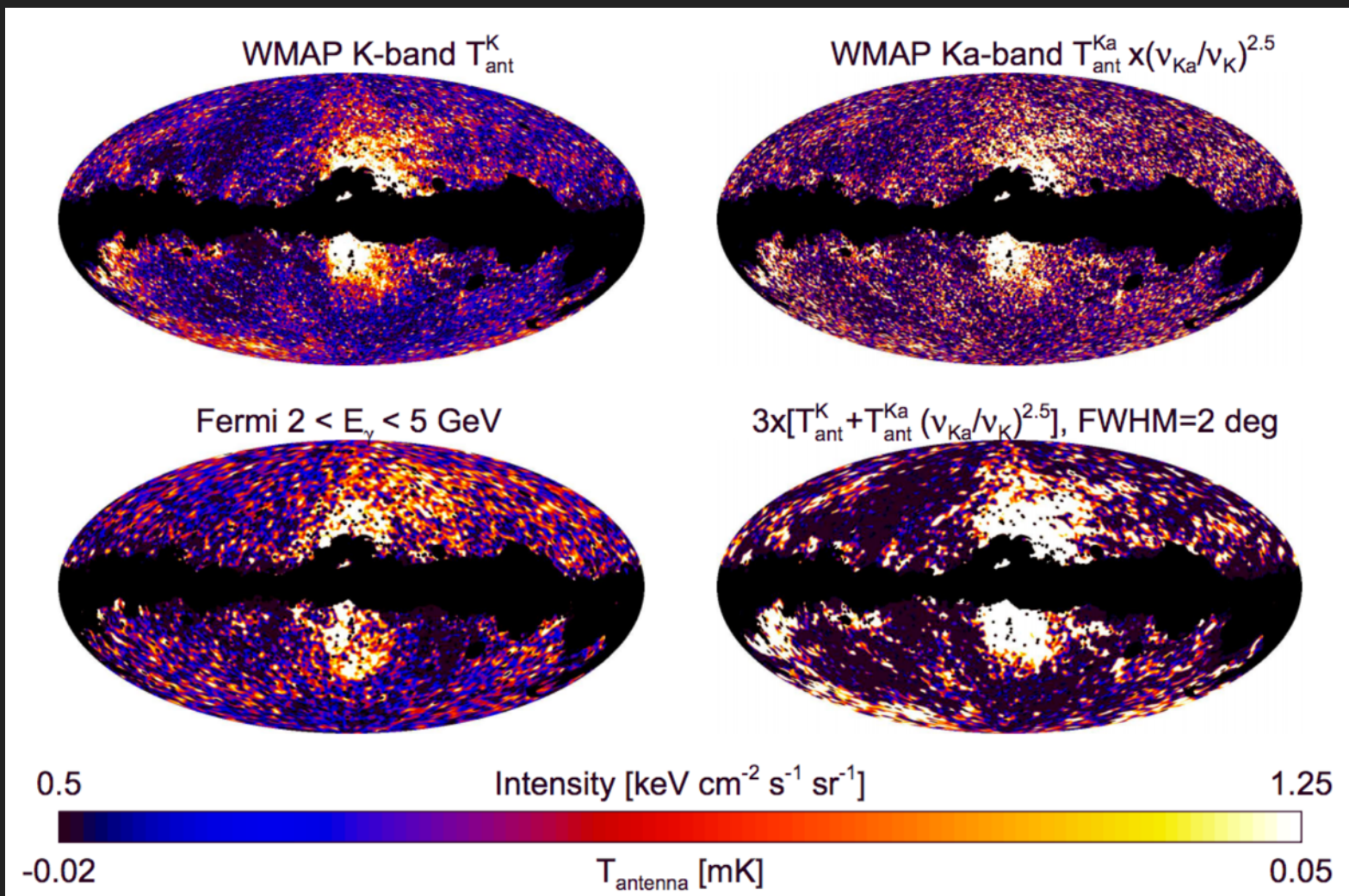
courtesy: Doug Finkbeiner



Hooper & Linden (2010)

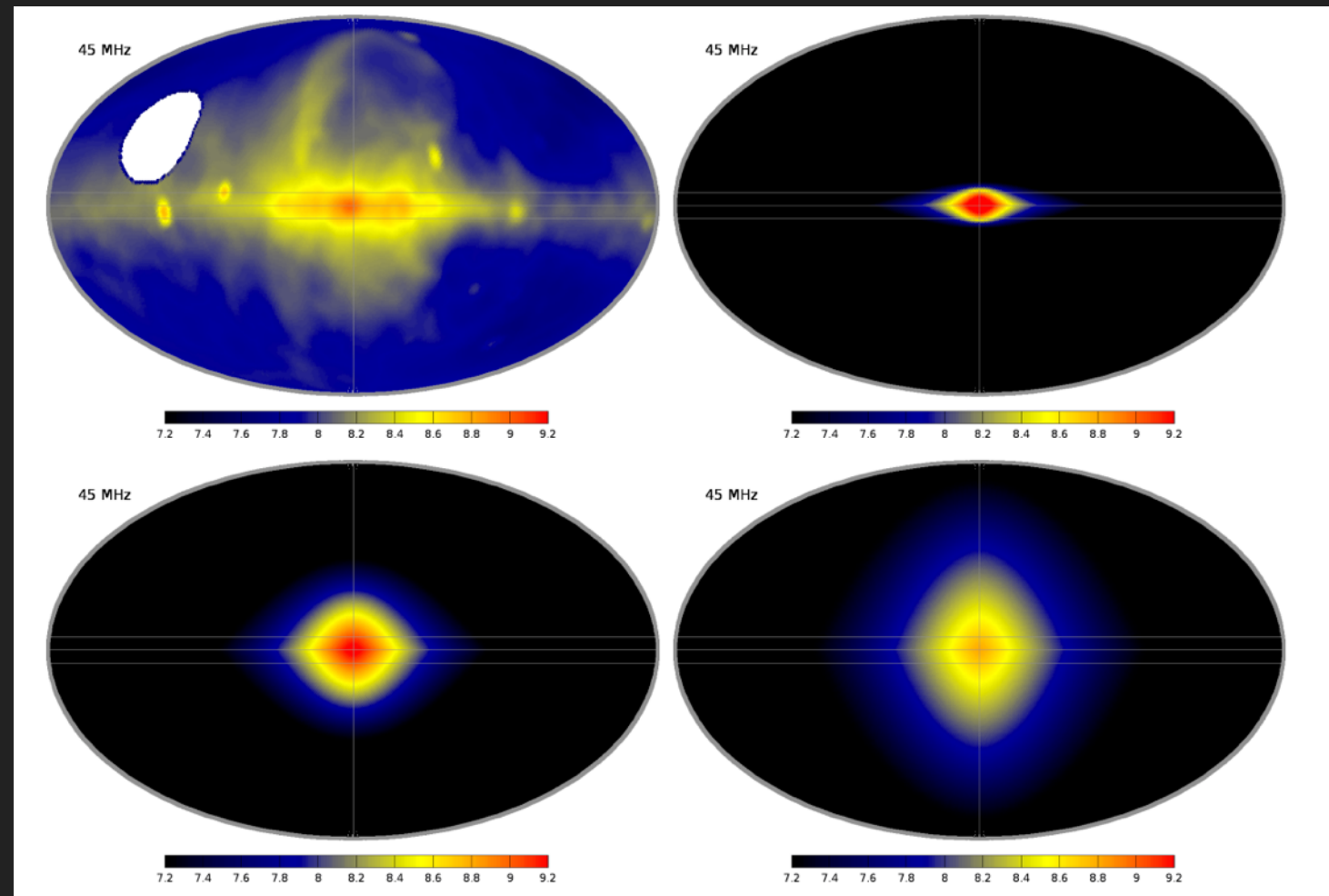
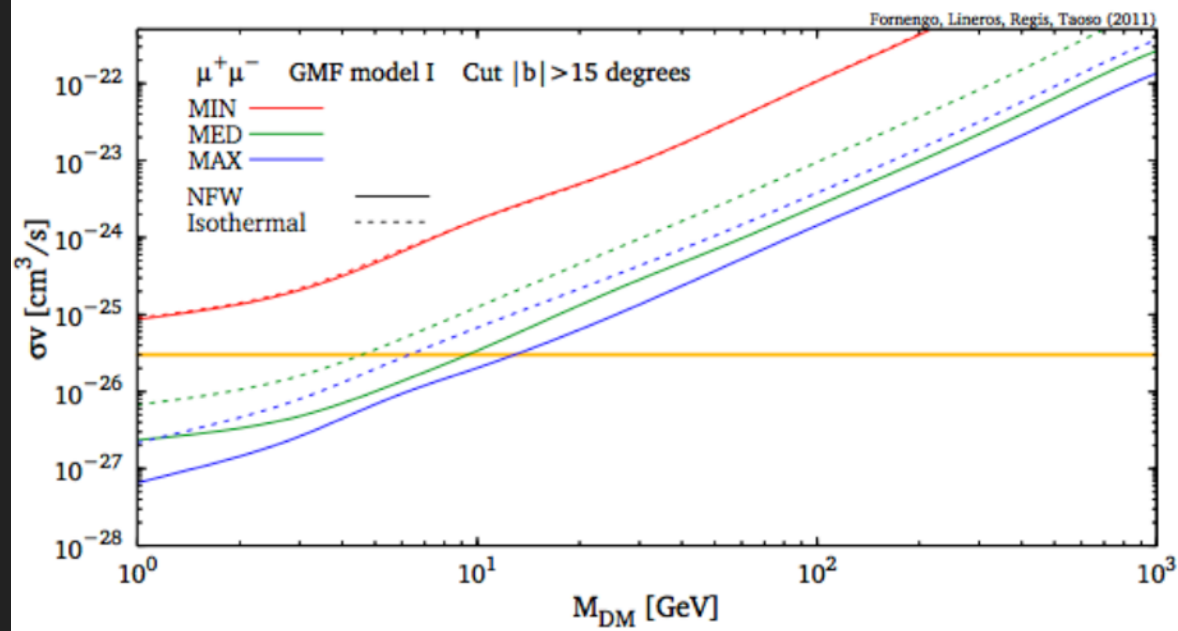
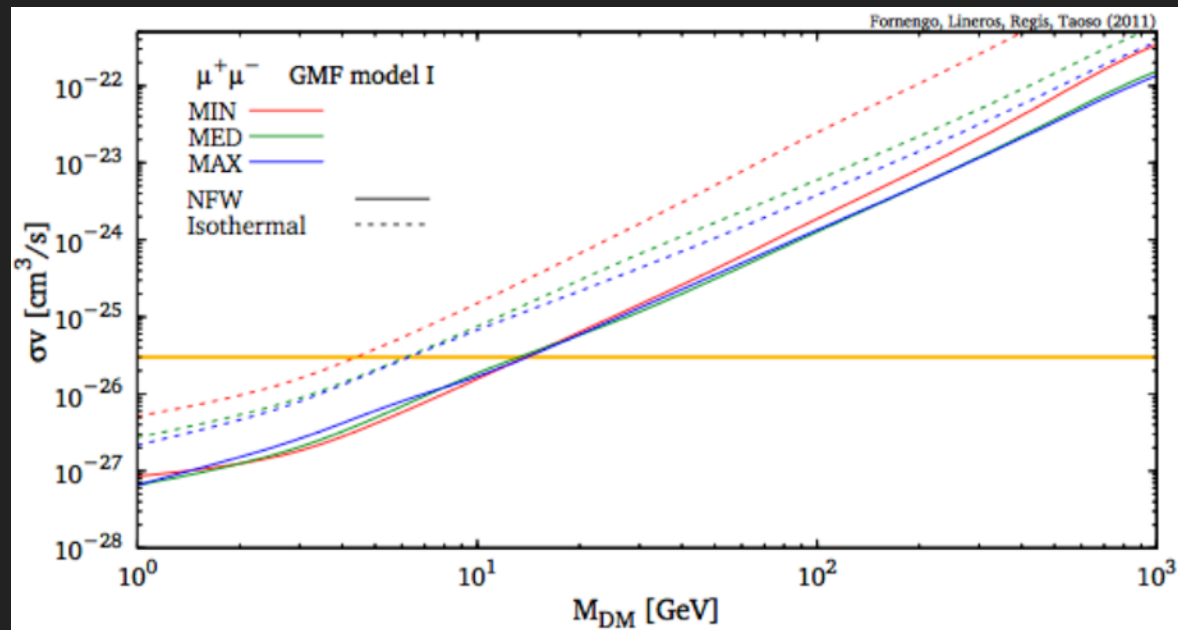
About 10 years ago, there was significant excitement that the synchrotron excess observed by WMAP (and later PLANCK) could be a sign of dark matter annihilation.

RADIO TARGETS



However, the WMAP residual has since been correlated with the Fermi bubbles. The sharp edges observed in both disfavor a dark matter interpretation.

RADIO TARGETS

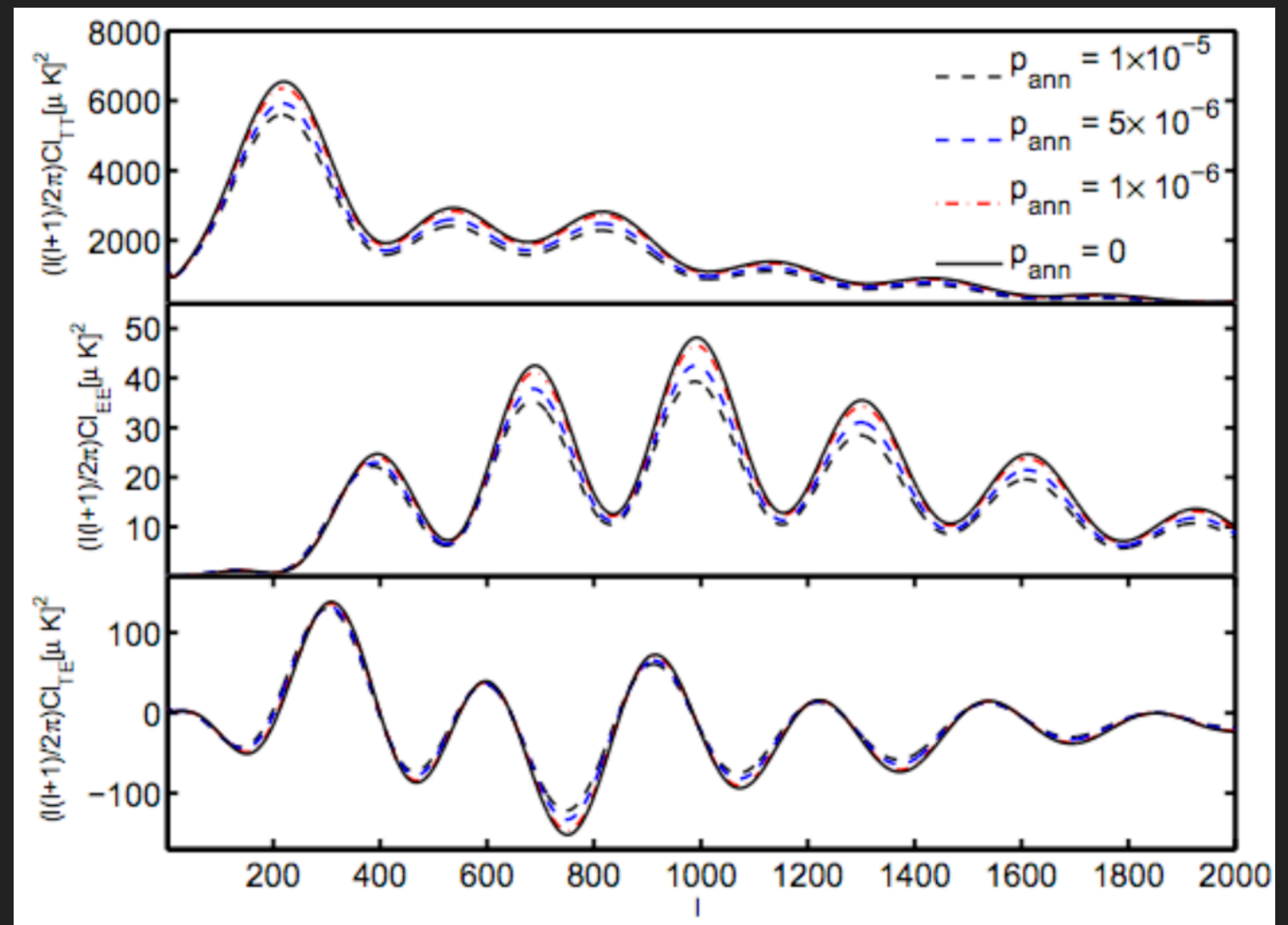


Can look for excesses above the level of the WMAP/PLANCK bubbles, setting constraints on dark matter signals.

CMB TARGETS

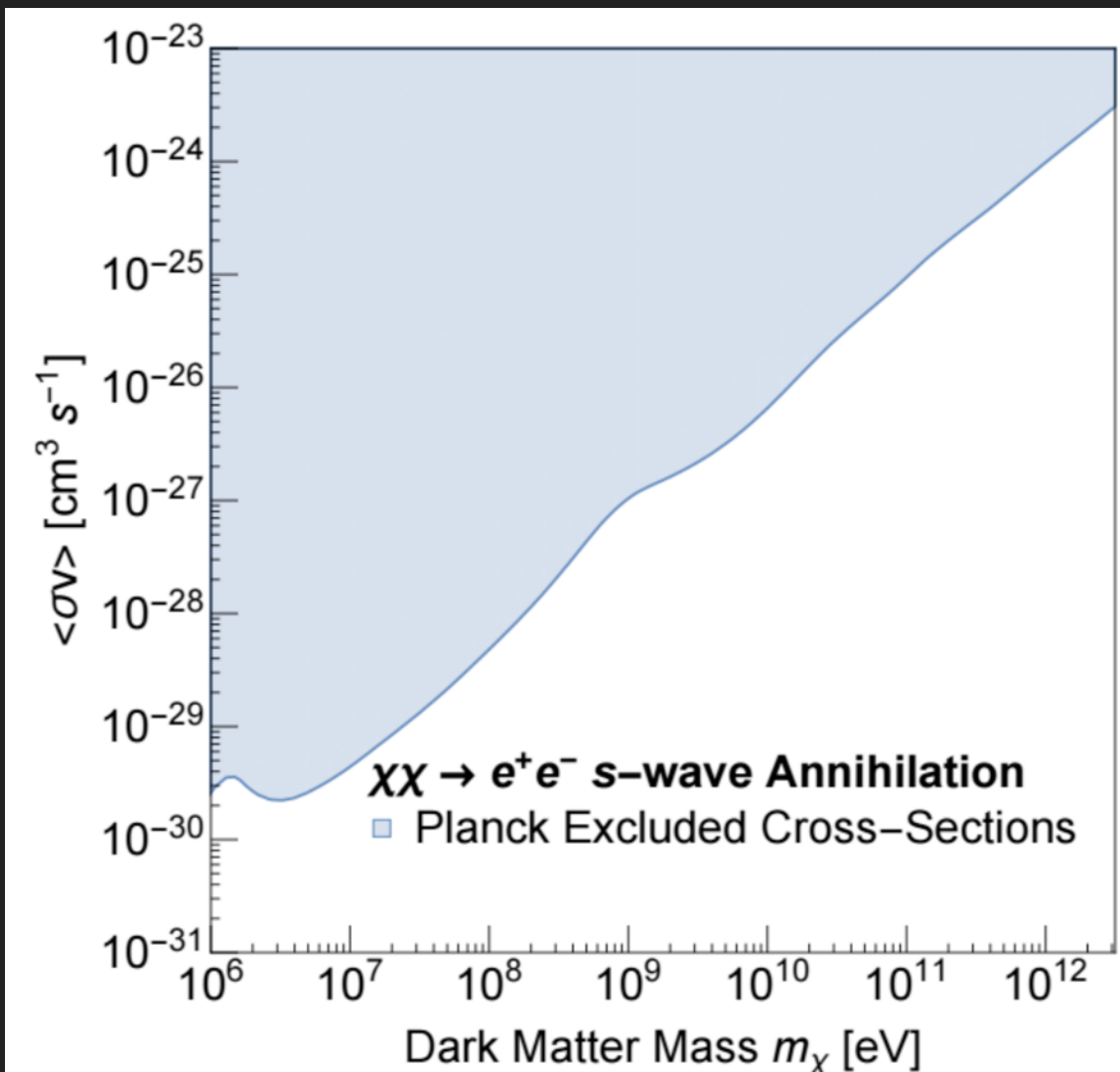
Going back to the beginning, remember that dark matter annihilations in the present day require dark matter annihilation in the Early universe.

Can study the fluctuations in the CMB imposed by the energy deposition of dark matter during the epoch of recombination.



CMB TARGETS

For annihilation directly to electron/positron pairs, these constraints rule out dark matter at the thermal annihilation cross-section to masses ~ 200 GeV.



| Channel | DM Mass (GeV) | f_{eff} | $f_{\text{eff,new}}$ |
|--|---------------|------------------|----------------------|
| Electrons | 1 | 0.85 | 0.45 |
| $\chi\chi \rightarrow e^+e^-$ | 10 | 0.77 | 0.67 |
| | 100 | 0.60 | 0.46 |
| | 700 | 0.58 | 0.45 |
| | 1000 | 0.58 | 0.45 |
| Muons | 1 | 0.30 | 0.21 |
| $\chi\chi \rightarrow \mu^+\mu^-$ | 10 | 0.29 | 0.23 |
| | 100 | 0.23 | 0.18 |
| | 250 | 0.21 | 0.16 |
| | 1000 | 0.20 | 0.16 |
| | 1500 | 0.20 | 0.16 |
| Taus | 200 | 0.19 | 0.15 |
| $\chi\chi \rightarrow \tau^+\tau^-$ | 1000 | 0.19 | 0.15 |
| XDM electrons | 1 | 0.85 | 0.52 |
| $\chi\chi \rightarrow \phi\phi$ | 10 | 0.81 | 0.67 |
| followed by | 100 | 0.64 | 0.49 |
| $\phi \rightarrow e^+e^-$ | 150 | 0.61 | 0.47 |
| | 1000 | 0.58 | 0.45 |
| XDM muons | 10 | 0.30 | 0.21 |
| $\chi\chi \rightarrow \phi\phi$ | 100 | 0.24 | 0.19 |
| followed by | 400 | 0.21 | 0.17 |
| $\phi \rightarrow \mu^+\mu^-$ | 1000 | 0.20 | 0.16 |
| | 2500 | 0.20 | 0.16 |
| XDM taus | 200 | 0.19 | 0.15 |
| $\chi\chi \rightarrow \phi\phi, \phi \rightarrow \tau^+\tau^-$ | 1000 | 0.18 | 0.14 |
| XDM pions | 100 | 0.20 | 0.16 |
| $\chi\chi \rightarrow \phi\phi$ | 200 | 0.18 | 0.14 |
| followed by | 1000 | 0.16 | 0.13 |
| $\phi \rightarrow \pi^+\pi^-$ | 1500 | 0.16 | 0.13 |
| | 2500 | 0.16 | 0.13 |
| W bosons | 200 | 0.26 | 0.19 |
| $\chi\chi \rightarrow W^+W^-$ | 300 | 0.25 | 0.19 |
| | 1000 | 0.24 | 0.19 |
| Z bosons | 200 | 0.24 | 0.18 |
| $\chi\chi \rightarrow ZZ$ | 1000 | 0.23 | 0.18 |
| Higgs bosons | 200 | 0.30 | 0.22 |
| $\chi\chi \rightarrow h\bar{h}$ | 1000 | 0.28 | 0.22 |
| b quarks | 200 | 0.31 | 0.23 |
| $\chi\chi \rightarrow b\bar{b}$ | 1000 | 0.28 | 0.22 |
| Light quarks | 200 | 0.29 | 0.22 |
| $\chi\chi \rightarrow u\bar{u}, d\bar{d}$ (50% each) | 1000 | 0.28 | 0.21 |

CMB TARGETS

Unfortunately, we are fast approaching the cosmic-variance limit of CMB observations (for an instrument with PLANCK-like angular resolution).

Currently, several observed excesses lie right at the threshold of the best possible CMB constraints.

